ROBUST COMPENSATION OF CONTINUOUS STIRRED TANK REACTOR: A 2-PERIODIC APPROACH

This thesis is submitted in the partial fulfilment of the requirements of the degree

MASTER IN CONTROL SYSTEM ENGINEERING

Submitted by

Ritam Halder

Examination Roll Number: M4CTL22019

Registration Number: 131362 of 2015–2016

Under the Guidance of

Dr. Sayantan Chakraborty

Department of Electrical Engineering

Faculty of Engineering and Technology

JADAVPUR UNIVERSITY

KOLKATA–700032

October, 2022

Faculty of Engineering and Technology

JADAVPUR UNIVERSITY

Kolkata-700032

Certificate of Recommendation

This is to certify that **Mr. Ritam Halder (002010804019)** has completed his dissertation entitled, "**Robust Compensation of Continuous Stirred Tank Reactor: A 2-Periodic Approach**", under the direct supervision and guidance of **Dr. Sayantan Chakraborty**, Department of Electrical Engineering, Jadavpur University. We are satisfied with his work, which is being presented for the partial fulfilment of the degree of **Master in Control System Engineering** of Jadavpur University, Kolkata-700032.

....

Dr. Sayantan Chakraborty

Assistant Professor,
Electrical Engineering Department
Jadavpur University, Kolkata-700032

....

Prof. Saswati Mazumdar

Head of the Department,
Electrical Engineering Department,
Jadavpur University, Kolkata-700032

....

Dr. Bhaskar Gupta

Dean,
Faculty of Engineering & Technology
Jadavpur University, Kolkata-700032

Faculty of Engineering and Technology

JADAVPUR UNIVERSITY

Kolkata-700032

Certificate of Approval

The foregoing thesis entitled "**Robust Compensation of Continuous Stirred Tank Reactor: A 2-Periodic Approach**" is hereby approved as a creditable study of an Engineering subject carried out and presented in a manner satisfactory to warrant its acceptance as a pre-requisite to the degree of Master in Control System Engineering for which it has been submitted. It is understood that, by this approval the undersigned does not necessarily endorse or approve any statement made, opinion expressed, or conclusion therein but approve this thesis only for the purpose for which it is submitted.

Final Examination for Evaluation of the Thesis

………………………………………………………

………………………………………………………

………………………………………………………

Signature of the Examiners

Declaration of Originality

I hereby declare that this thesis contains a literature survey and original research work by the undersigned candidate, as part of his Master in Control System engineering curriculum. All information in this document has been obtained and presented in accordance with academic rules and ethical conduct. I also declare that, as required by these rules and conduct, I have fully cited and referenced all material and results that are not original to this work.

Name: Ritam Halder

Examination Roll No.: M4CTL22019

Thesis Title: Robust Compensation of Continuous Stirred Tank Reactor: A 2-Periodic Approach

Signature with Date:

ACKNOWLEDGEMENT

I sincerely thank my supervisor, Dr. Sayantan Chakraborty, Department of Electrical Engineering, Jadavpur University, Kolkata, for his invaluable guidance, suggestions, encouragement, and constant support throughout my thesis work, which helped me in successfully completing it. It was a great honour for me to pursue my research under his supervision.

I would also like to thank all my classmate Rahul Kumar for his continuous help and support without which this would not have been possible.

I would like to express my gratitude towards all the staffs of control systems laboratory for providing constant encouragement throughout my thesis work.

Last but not the least, I extend my words of gratitude to my parents, Mr. Manas Halder and Mrs. Rikta Halder, for their endless love support to guide me through every thick and thin of life.

Ritam Halder

Jadavpur University,

Kolkata – 700032

ABSTRACT

The linear time invariant (LTI) controllers can be designed based on a plethora of methods that are available in the literature. However, LTI controllers have severe limitations in respect of compensation of SISO, LTI plant with Non-Minimum-Phase (NMP) zero(s). This is due to the fact that, although LTI controllers are capable of placing the closed-loop poles at desired locations, the loop-zeros in the closed loop transfer function remain unaltered, thus leading to unsatisfactory Gain Margin (GM).

On the other hand, a periodic controller, in addition to its pole-placement capability, can relocate all the loop zeros at any arbitrary locations increasing the system's stability margins. Unfortunately, it was seen that due to the periodic fluctuations in the controller settings, the response to a step input exhibits ripples even at the steady-state. In recent literatures, it has been demonstrated that in case of Discrete-Time Periodic Controllers if the loop transfer function satisfies certain conditions, then the steady-state ripples may be eliminated.

The present work employs the capabilities of 2-Periodic Controllers to mitigate the difficulties associated with the control of Continuous Stirred Tank Reactor (CSTR) which is very frequently used in the chemical industry to transform reactants into products. CSTRs are generally operated around a few specific equilibrium points that correlate to an ideal yield or an optimal productivity of the process in order to achieve high conversion and economic advantages. However, the control of CSTR provides a difficult task for process control experts owing to the very pronounced nonlinearity and variety of process dynamics, including inverse response and parameter uncertainties involved.

In order to address these issues, a 2-Periodic Controller is designed to improve the stability margin and robustness of a Van de Vusse CSTR. A comparative study of the proposed controllers with a discrete-time PID controller shows significant improvements in robustness in respect of parameter uncertainties and disturbances.

Keywords: CSTR, Periodic Control, Loop-Zero Placement.

CONTENTS

List of Abbreviations

SISO : Single Input Single Output
LTI : Linear Time Invariant
PID : Proportional, Integral and Derivative
LQR : Linear Quadratic Regulator
CSTR : Continuous Stirred Tank Reactor
CCF : Controller Canonical Form
MIMO : Multi Input Multi Output
ISE : Integral Square Error
SEOM : Statically Equivalent Output Map
RSOFC : Robust Static Output Feedback Control
DOF : Degree of Freedom
SMC : Sliding Mode Control
PSO : Particle Swarm Optimization

List of Figures

List of Tables

Chapter 1

Introduction & Literature Survey

1.1 History and Background

The main goal of any Control System is to ensure a desired output from any plant. We, the control engineers, must develop a controller that can meet the following fundamental conditions in order to achieve the control objective for a Single-Input-Single-Output (SISO), Linear-Time-Invariant (LTI) plant.

Stability The primary focus of the control systems is the stability of the given system. So, we must ensure that the given plant is stable and if found otherwise, it should be first stabilized with proper compensation. According to fundamental control theory, all the poles of the compensated system should be located within the unit circle on the z-plane for discrete-time systems or on the left half of the s-plane for continuous-time systems.

Pole Placement If necessary, the controller should be able to place the closed loop poles at any arbitrary desired locations in the s and/or z-plane.

Robustness The controller should be robust with respect to model and parameter uncertainties, i.e., it should ensure stability as well as performance under such conditions.

Disturbance Rejection The compensated system should be capable of handling external disturbances without affecting the performance significantly.

Several time-invariant/time-varying or linear/non-linear controllers have been employed in literature to meet these control challenges. P, PI, PD, PID, LQR controllers, Lead, Lag, Lead-Lag compensator, to name a few, and others have been frequently used in industrial applications.

The existence of the plant zeros in the closed-loop transfer function is a major barrier in the design of control systems for defined transient response. It would be conceivable to build the controller to cancel such zeros if they are stable (Sebakhy et al., 1988) [10]. To preserve internal stability in the closed-loop system, we normally avoid pole-zero cancellations when the plant is not in minimum phase. In this scenario, the closed-loop system that is created will have the same number of zeros as the plant. Therefore, using traditional techniques, it might not be feasible to get the desired closed-loop transfer function or *perfect model matching*. However, if the zeros can be suitably relocated then it may become possible to achieve perfect model matching and significant improvement in robust performance of the system. In this regard, periodic controllers with their zero placement capabilities has proved to be an viable option as reported in several literatures.

According to Wolovich [11] and Doyle *et al* [12], LTI controllers that has certain limitations in providing robust compensation to a class of LTI plants having NMP pole(s) and zero(s). The situation becomes even worse as the NMP pole(s) and zero(s) are in close vicinity of each other. In the later cases the maximum achievable GM for such plants using LTI controllers tends to 1 as the NMP pole and zero come closer to each other. However, periodic controllers have been shown to be able to overcome this limitation by means of their Loop-zero-placement capability, Lee et al. (1987)[13]-Das and Rajagopalan (1996)[3]. With a focus on discrete-time systems, Das and Rajagopalan [9] demonstrated that by positioning the loop zeros inside the unit circle, (discrete-time) 2-periodic controllers can provide better loop robustness. It should be noted that LTI controllers lack this feature of zero placement. However, the same reference does not address the issue of defining a organized approach to obtain the periodic controller parameters.

Further, Das [37] has demonstrated that 2-periodic controllers are capable of simultaneously stabilizing 2 LTI plants. However, it is to be noted that such simultaneous stabilization property of LTI controllers is restricted to a rather small class of plant pairs satisfying certain necessary conditions. More importantly, this reference also provides an effective technique for finding the 2- periodic controller parameters to achieve the simultaneous stabilization goal. In fact, the work of Das and Kar [38] extended this work to accomplish the simultaneous stabilization of M plants using an M-periodic controller.

In order to improve upon what can be accomplished with LTI compensation in terms of loop robustness, this thesis explores a 2-periodic controller, as in Das and Rajagopalan [9], to place not only the closed loop poles but also the loop-zeros of a discrete-time LTI plant at suitable locations.

1.2 Continuous Stirred Tank Reactor (CSTR)

All chemical process industries may be thought of as being centered around chemical reactors. They are typically difficult to regulate because of their complex behavior and potential safety issues. Batch reactors, Continuous Stirred Tank Reactors (CSTR), and plug-flow reactors are the traditional idealized forms of reactors. A CSTR consists of a vessel encircled by a jacket for heating or cooling, an agitator inside the vessel for (perfect) mixing, feed lines entering the vessel, and a liquid product stream leaving the vessel. The product stream's composition and temperature match those of the liquid that fills the whole vessel.

The Continuous Stirred Tank Reactor (CSTR), which is frequently used in the chemical industry to transform reactants into products, is crucial to the whole process. CSTRs are often operated around a few specific equilibrium points that correlate to an ideal yield or an optimal productivity of the process in order to achieve high conversion and economic advantages (Luyben, 1990) [48]. Arrhenius reaction rates would be included in a multi-dimensional system of linked nonlinear ordinary differential equations in a typical model for an exothermic reaction in a CSTR.

The CSTR, however, may exhibit a range of unusual behavior mainly due to the nonlinear relationships of the system parameters owing to the complexity of the internal sequential and secondary reactions. The control of CSTRs might provide a difficult task for process control experts due to the very pronounced nonlinearity and variety of process dynamics, including inverse response and parameter uncertainty. In a dynamic test, an inverse response occurs when the process's initial reaction is in the opposite direction of its ultimate response. It may be brought on by the conflicting impacts of two response dynamics in CSTRs. In the literature, a process with inverse response behavior is frequently referred to as a non-minimum phase process. Some recent advancements in the field of process control, as described by Garcia and Morari [41] and Bequette [47], depend implicitly or explicitly on an inverse of the process.

The process model is frequently divided into minimum phase and non-minimum phase sections when dealing with linear non-minimum phase processes, with the controller design inverting just the minimum phase element. The breakdown into minimum phase and non-minimum subsystems is quite challenging for nonlinear, non-minimum phase processes, such as many CSTRs.

1.3 Periodic Control

A unique class of linear controller called a periodic controller contains gains and coefficients that change on a regular basis throughout time. Therefore, it may be claimed that periodic control is a linear time varying control [1],[2],[3]. For example, the gains of a 2-periodic controller take on distinct values at even and odd instants. It has been shown in literature that by virtue of this time-varying nature of the controller parameters the periodic controllers are capable of relocating the loop-zeros of any system at arbitrary locations thus leading to improved robustness of the compensated system. It should be noted that LTI controllers cannot achieve such loop-zero-placement and as a result yields poor robustness for NMP systems. Next, let us discuss the definition of the loop-zeros and how 2-periodic controllers can be used to relocate them.

1.3.1 Definition of Loop-Zeros

From the perspective of the characteristic equation of a loop, the zeros may be thought of as the roots of the characteristic equation as the loop gain approaches infinity. On the other hand, as the loop gain tends to zero, the loop poles are the roots of the characteristic equation. [3] In light of the fact that the loop-gain approaches to ∞, the loop-zeros may be defined as the roots of the closed-loop characteristic equation. It is crucial to remember that the notion of the loop-zeros and the conventional zeros are entirely comparable for LTI compensated systems in this situation. However, the same is not true for periodic controllers, as will be discussed next.

1.3.2 Periodic Controller Configuration

A 2-periodic controller configuration with the highest degrees of freedom is shown in Fig. 1.1. All the feedback and feed forward gains involved may take on distinct values at the even and odd instants of time. Such a 2-periodic (often M-periodic) system may be analyzed using a number of different techniques. These techniques are:

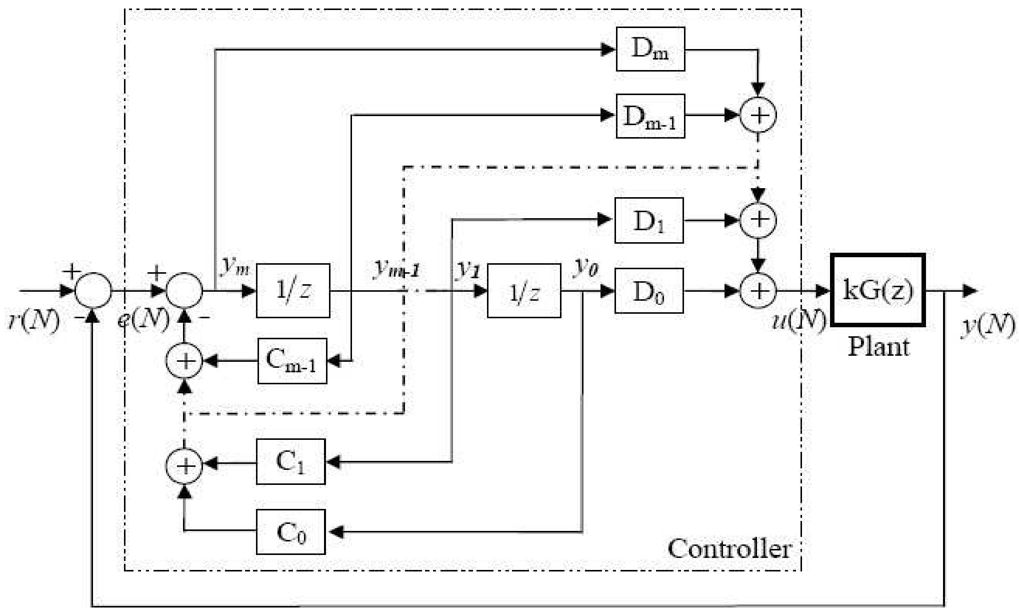

Fig. 1.1: The 2-Periodic controller in Controller Canonical Form (CCF) and the LTI plant [1]

i. **Time-lifted Reformulation:** The input and output can both be split into two sets, the even-instant and the odd-instant ones, in this instance for a 2-periodic example. The 2 × 2 transfer matrix connecting them thus acquires temporal invariance. The system may then be examined in the same way that a MIMO time-invariant system is examined.

ii. **Cyclic Reformulation:** It entails selecting one sample every period and moving it to a certain location on an enhanced vector. Now, as time passes, the location of the identical sample in the augmented vector successively changes in a modulo-M manner. The related transfer matrix regains temporal invariance if the input and output are so reformulated.

iii. **Frequency-lifted Reformulation:** A discrete Fourier series with M terms can be used to represent the input and output signals of an M-periodic system. They are connected via a transfer matrix that is also time-invariant.

iv. **Floquet Theory:** In Floquet theory, a solution $x(N)$ of a difference equation is x with M-periodic coefficients must occur in the form $x(N) = \gamma^N C(N)$, with $C(N) = C(N + M)$. Expressing $C(N)$ in a discrete Fourier Series, the characteristic roots γ can be obtained as the eigenvalues of a time-invariant characteristic matrix.

1.4 Literature Review

1.4.1 Control of CSTR

Significant advancements in the field of nonlinear process control have been made in recent years, and there has been an increase in interest in the creation of diversified control systems for the operation of CSTRs (Iyer and Farell, 1995; M'Saad et al., 1995; Lagerberg and Breitholtz, 1997; Ge et al., 1999; Alvarez-Ramirez and Morales, 2000; Camacho and Smith, 2000; Vielhaben et al; Gopaluni et al. (2003); Morimoto et al. (2002).

As mentioned by Kravaris et al. [18-22], the correction of the inverse response behavior is often one of the most challenging control difficulties caused by the functioning of the CSTR. Alternative strategies have been put up in the literature to deal with this challenging issue (Kravaris and Daoutidis, 1990; Wright and Kravaris, 1992; Kravaris et al., 1994; Aoyama et al., 1996).

Kravaris and Daoutidis (1990) [22] created a unique static state-feedback synthesis formula based on an ISE-optimal decomposition for dealing with second-order nonlinear non-minimum phase phenomena. By easing the ISE-optimality constraint and using the zero placement method, Kravaris et al. (1998) developed a way for creating a minimum-phase statically equivalent output for general nonlinear systems. Niemiec and Kravaris (2003) expanded on their earlier work to create statically identical outputs for multivariable nonlinear non-minimum phase processes with prescribed transmission zeros.

Wright and Kravaris (1992) [20] proposed a generalized Smith predictor for nonlinear processes within the context of input/output linearization, where a statically equivalent lowest phase output is calculated and controlled to the setpoint. Kravaris et al. (1994) [21] investigated a broader framework for the analysis and output feedback management of an open-loop stable nonlinear non-minimum phase process by introducing a Smith-type abstract operator structure.

Engell and Klatt [4] first developed a complex reaction system in a CSTR which leads to a nonlinear dynamic behaviour with unstable zero dynamics. Then one particular control problem for this system is analyzed and solved using a novel combination of gain scheduling and linear frequency domain design techniques.

An internal model-based neural network controller for nonlinear non-minimum phase processes with relative degree 1 was created by Aoyama et al. in 1996 [25]. They developed a comparable minimum-phase control affine neural model within a general Smith predictor framework as the core component of their strategy.

A rough stable/anti-stable factorization was put out by Allgöwer [14] for the nonlinear process with problematic zero dynamics. For the formulation of a feedback control rule for small non-minimum phase processes, Hauser et al. [27] used an approximation input-output linearization technique.

Chen and Lee (2002) suggested a single neural controller based learning control system for non-minimum phase nonlinear processes with implementation in a minimum phase predictor setup. In 2006, Chen and Peng [5] developed a novel sliding mode control scheme for continuous stirred tank reactors (CSTRs) in the simultaneous presence of the non-minimum phase behavior and process uncertainties. To circumvent the negative effect of the inverse response in the control scheme, they incorporated a statically equivalent output map (SEOM) based on a zero-placement method.

Jo et al. (1998) [18] studied the issue of robust stabilisation for a class of nonlinear systems with non-minimum phase behaviour and mismatched uncertainty based on the approximate input/output linearization and a particular state transformation. Shkolnikov and Shtessel (2002) [29] created a method for asymptotic output tracking control of a class of causal non-minimum phase uncertain nonlinear systems by applying the system centre approach together with certain linear algebraic techniques. With internal dynamics expressed in power series, their technique presents a nonlinear feedback linearizable plant model in normal form.

Bakosova et al. [30] presented the application of robust static output feedback control (RSOFC) to an exothermic CSTR with parametric uncertainties. Wonghong [31] presented a real-time PID controller tuning technique via unfalsified control for a continuous stirred tank reactor (CSTR) model with a non-minimum phase behaviour.

Nonlinear model predictive control based on online dynamic optimization has been proposed for non-minimum phase continuous stirred tank reactor (CSTR) to combine optimal operation and feedback control, coupled with a nonlinear gain-scheduled state estimator to provide output feedback by Idris [32].

Singh et al. [33] proposed optimization of a proportional-integrator-derivative (PID) controller aimed for the improvement of continuous-stirred tank reactor (CSTR) system using JAYA algorithm which minimizes the performance index, i.e., Integral Time-weighted Square Error (ITSE).

1.4.2 Periodic Compensation of LTI Systems

1.4.2.1 Continuous-time Periodic Control

Continuous time periodic control was conceived from the pioneering work by Lee et al. [8]. It was observed that the controller proposed by them was capable of placing zeros at desired location by varying the values of the controller parameters. However, significant ripples of order 1 i.e. $O(1)$ was present in the output response, along with $O(\omega^r)$ oscillations (where, ω is the frequency of patameter variation and r is the relative order of the plant) in the controller output i.e. the plant input. As a consequence, the performance of overall control system was found to be poor.

Hence, Periodic controllers therefore remained only as theoretical constructs till Das and Dey (2007) [40] proposed a new periodic controller (2-DOF) that causes the plant input to have oscillations of only $O(1)$ and the plant output of $O({}^{1}/_{\omega^r})$ order of complexities. Averaging principle was used as a tool to synthesize the periodic controller in [41].

Practical systems have been compensated using the continuous time periodic controller [40–44]. [41] describes the use of a continuous time periodic controller to correct an inverted cart pendulum system. It has been demonstrated that when utilized to adjust a system with non-minimum phase zero, periodic controller performs better than LQR controller. Because of the high amplitude of signals at certain of the controller's intermediate points, the [40] architecture could not be implemented effectively. The authors compare Sliding Mode Control (SMC) with periodic control in [43] and demonstrate that periodic control provides greater stability margins.

1.4.2.2 Discrete-time Periodic Control

Similar to continuous-time periodic controllers, discrete time periodic controllers can move the loop-zeros, enhancing the system's loop robustness and gain margin. On discrete time periodic control, several studies have been done. The modified z-transform approach, the lifting technique, and the Floquet theory are only a few of the methods for creating discrete time periodic controllers that have been demonstrated in the literature. In [2, 6, 42], compensation of a SISO LTI plant using a 2-periodic controller was demonstrated.

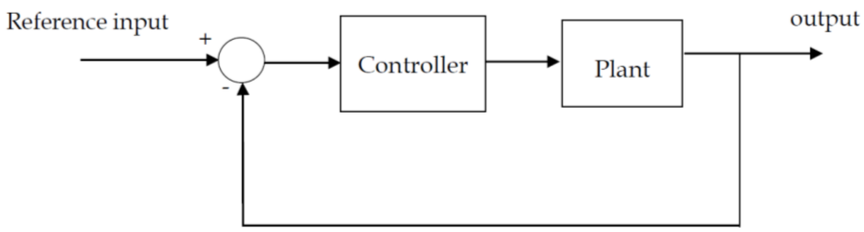

Fig. 1.2: 1-DOF control topology

The discrete time periodic controller is available in 1-DOF and 2-DOF models. Poles and loop zeros can be positioned at specific places using 1-DOF periodic controllers [1-2],[6]. In [1], a 2-periodic controller with controller order $m \geq n$ (where n is the plant order) has been developed. The controller could improve stability margins and place poles and loop zeros where they were needed. Regrettably, there was a significant degree of ripple in the output. The architecture for 1-DOF control is shown in Figure 1.2.

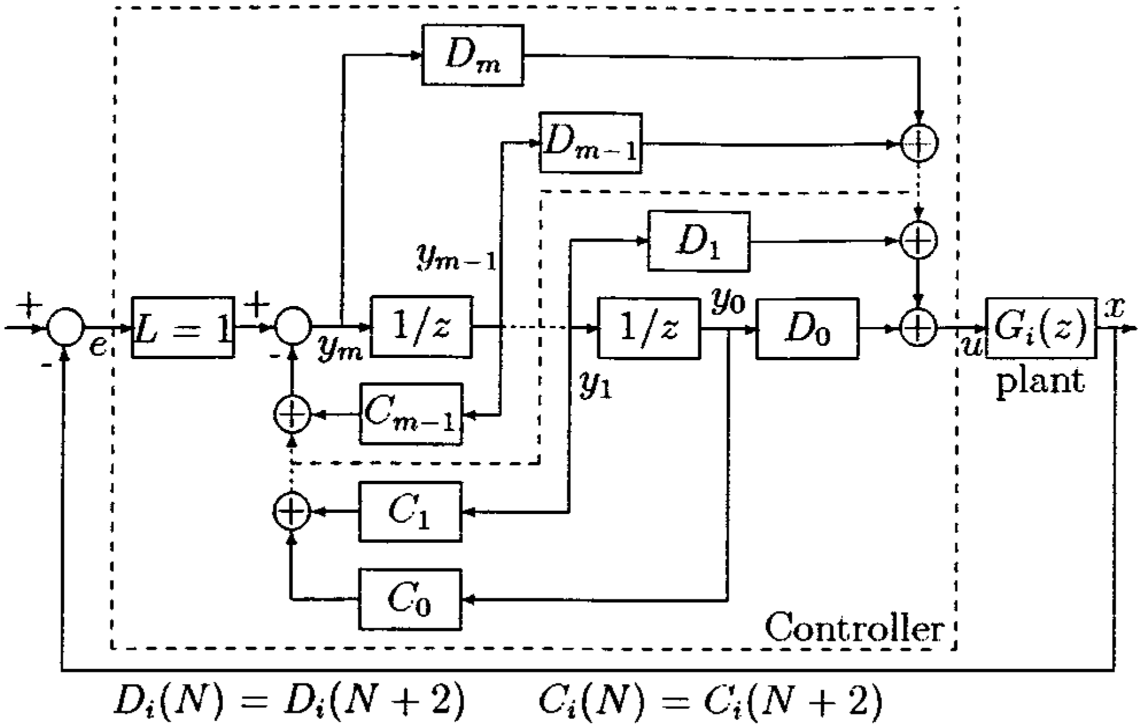

Figure 1.3: 1-DOF 2-periodic discrete time controller [3]

Figure 1.3 depicts the 2-periodic discrete time controller's 1-DOF setup [3]. It has been noted that the steady-state response to a step input exhibits ripples when there is periodic fluctuation in the controller settings [2,6]. It has been demonstrated in the literature that if the loop transfer function has a zero at -1 or a pole at 1, these ripples may be removed in the discrete-time domain [1].

A 2-DOF, 2-periodic discrete time controller is shown schematically in Figure 1.4. (taken from [7]). The controller was created using $m \geq n$ in [7] where, n is the plant order and m is the controller order. It has been demonstrated by authors that the existence of feedforward gain K_i causes a few poles to cancel out, lowering the order of the entire system. A two-step technique has been used for controller synthesis. By multiplying the input with a periodic gain, output ripples have been avoided.

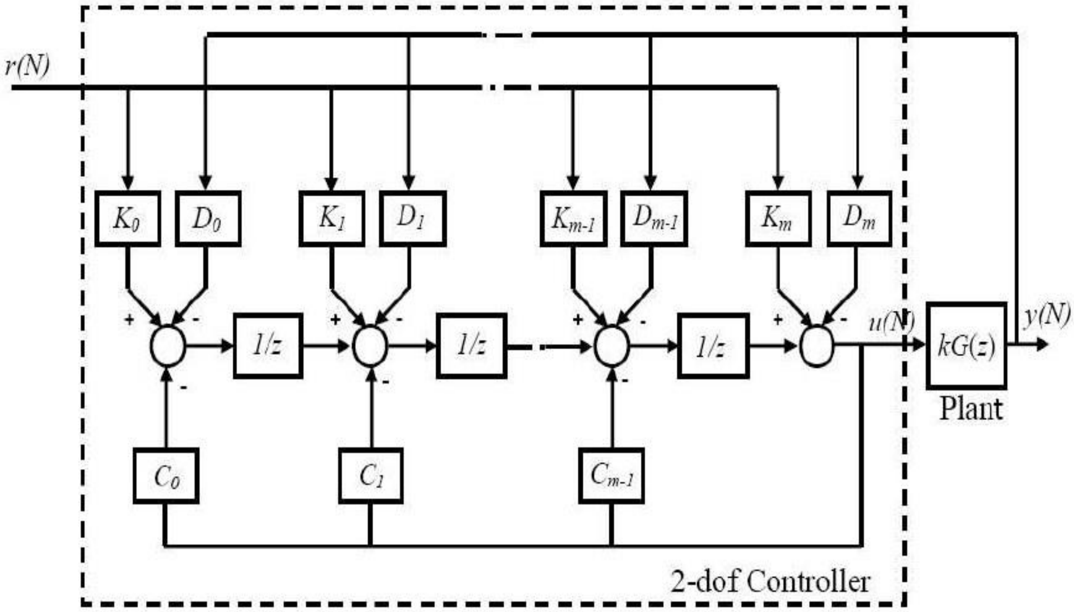

Figure 1.4: 2-DOF 2-periodic discrete time controller [7]

In 2020, Saha et al. proposed a PSO (Particle Swarm Optimization) based tuning rule for 2-rate controllers for the stabilization of cart-inverted pendulum system. They deployed a PSO based approach where, a group of particles in the solution space searches to find out the optimal locations of the controller poles and loop-zeros that yield satisfactory loop robustness.

1.5 Motivation and Thesis Outline

The regulation of CSTRs with the simultaneous existence of the nonlinearities, uncertainties, and inverse response behavior has only rarely been addressed (Jo et al., 1998; Shkolnikov and Shtessel, 2002, Chen et al., 2006), despite the notable advances and remarkable interest in nonlinear, non-minimum phase processes. This is due to the possibility that the mathematical model for CSTRs may be unreliable due to the presence of unmodeled side reaction dynamics, unknown internal or external disturbances, environmental impacts, etc. The presence of model uncertainties can make it more challenging to determine the process's inverse, which can lead to many existing approaches failing to manage the nonlinear uncertain CSTRs. Hence, we shall apply the ever so evolving method of periodic control into the CSTR scenario. Our main motive will be to improve the stability margins with satisfactory transient and steady-state response. Apart from that, however, we shall check the robustness of the same against parameter variations and disturbance rejection.

In this thesis, **Chapter 1** includes the introduction to the basic control objectives and the concept of periodic control. It points out the limitations of LTI controllers and discusses how periodic controllers can overcome them. Then basics of Continuous Stirred Tank Reactor (CSTR) has been discussed followed by literature survey for both periodic control and CSTR.

Chapter 2 revisits the compensation of LDTI plants by 1-DOF 2-periodic controllers. In this regard, the chapter presents the controller synthesis for a synthetic LDTI plant with several iterations of control designs and a comparative study of the results is carried out. Also, further improvement for ripple free steady state response has been discussed with example.

Chapter 3 discusses about the development of mathematical model followed by State-Space model for the chemical reaction occurring in a CSTR. Thereafter, its transfer function has been developed and uncontrolled response has been presented for both continuous-time and discrete-time.

In **Chapter 4**, first the drawback from LTI control is shown and then the 2-periodic controller for CSTR considering each of the possible controller configurations has been designed and simulated for responses. Thereafter, the augmentations for ripple-free steady-state responses are applied and new controller are designed and simulated. Among these, the best possible configuration is considered and robustness analysis is done in terms of plant parameter variations and disturbance rejection. Finally, the results are compared with the results from a Discrete LTI PID controller applied in the same scenarios.

Chapter 5 concludes the contributions of the thesis and points out the scope of future work.

Chapter 2

2-Periodic Controller Design for SISO LDTI Plant

2.1 Introduction

We know from control theory that SISO LTI systems are stable when all of their poles are located in the left side of the s-plane. However, it is clear from the literature that utilizing LTI controllers, it is very challenging to robustly stabilize a single-input, single-output (SISO), linear-time-invariant (LTI) plant with unstable poles and non-minimum phase (NMP) zeros. This is due to the fact that LTI controllers can not to shift the plant zeros, which remains intact in the closed loop as well as loop transfer functions. If the plant contains unstable poles and NMP zeros in close proximity then the maximum possible gain margin (GM) achievable by LTI controllers is constrained to an upper bound, which tends to unity as the NMP pole and zero comes near each other. Due to their capability to relocate the loop zeros, periodic controllers are a common treatment that can enhance the loop robustness of such plants.

However, it's crucial to remember that LTI controllers lack this feature for zero placement. For discrete-time plants utilizing periodic controllers, a practical technique for loop-zero placement has just been created. This only applies to a portion of all conceivable controllers, though.

In order to increase the loop robustness of a discrete-time LTI plant, a 2-periodic controller has been taken into consideration to put the loop-zeros as well as the closed loop poles. After that, a methodical technique is presented to assess the controller settings generally, allowing one to investigate all potential subsets of such 2-periodic controllers.

2.2 M-Periodic Parameters

In contrast to the LDTI scenario, the form in which periodic controllers should be sought out is not well-standardized, so we will need to make an appropriate decision in that regard. Now, bearing in mind that the controller (i) should be realizable and (ii) should have the greatest number of degrees of freedom feasible in order to achieve minimal order designs, we choose the following m^{th} order M-periodic:

$$\left.\begin{aligned} y_i(N+1) &= y_{i+1}(N), \quad i = 0,1,\dots,(m-1) \\ y_m(N) &= L(N)e(N) - \sum_{i=0}^{m-1} C_i(N)y_i(N) \\ u(N) &= \sum_{i=0}^{m} D_i(N)y_i(N) \end{aligned}\right\} \tag{2.1}$$

Where, the M-periodic gains for the feedback and feedforward are $C_i(N)$ and $D_i(N)$, respectively, and $e(N)$ and $u(N)$ are the input and output of the controller, respectively. Be aware that in order to specify C_i or D_i, one must provide their values at the time instants $N = 0,1,\dots,(M-1)$; alternatively, they may be expressed as discrete Fourier series as:

$$\left.\begin{aligned} C_i(N) = C_i(N+M) &= \sum_{k=0}^{M-1} \alpha^{kN} c_{i,k}\,, \quad i = 0,1,\dots,(m-1) \\ D_i(N) = D_i(N+M) &= \sum_{k=0}^{M-1} \alpha^{kN} d_{i,k}\,, \quad i = 0,1,\dots,m \end{aligned}\right\} \tag{2.2}$$

Where, $\alpha = e^{j2\pi/M}$

By design, the aforementioned controller is causal and realizable. It may also be considered to have the most degrees of freedom imaginable since any extra M-periodic gain introduced at any point in it can be absorbed in the C_i's and D_i's.

For the 2-periodic case, $M = 2$. Putting it in equation (2.2); we get

$$\left.\begin{aligned} D_i(N) &= d_{i,0} + (-1)^N d_{i,1} \quad , i = 0,1, \dots, m \\ C_i(N) &= c_{i,0} + (-1)^N c_{i,1} \quad , i = 0,1, \dots, (m-1) \end{aligned}\right\}$$

(2.3)

2.3 System Definition

Let us consider, an n^{th} order, with r < n, Single Input Single Output (SISO), Discrete LTI Plant with a transfer function, $G(z) = \frac{b(z)}{a(z)}$ as shown in Fig. 2.1. The numerator (zero) and the denominator (pole) polynomials are expressed as:

$$\left.\begin{aligned} a(z) &= z^n + a_{n-1}z^{n-1} + \cdots + a_1 z + a_0 \\ b(z) &= b_r z^r + b_{n-1}z^{n-1} + \cdots + b_1 z + b_0 \end{aligned}\right\}$$

(2.4)

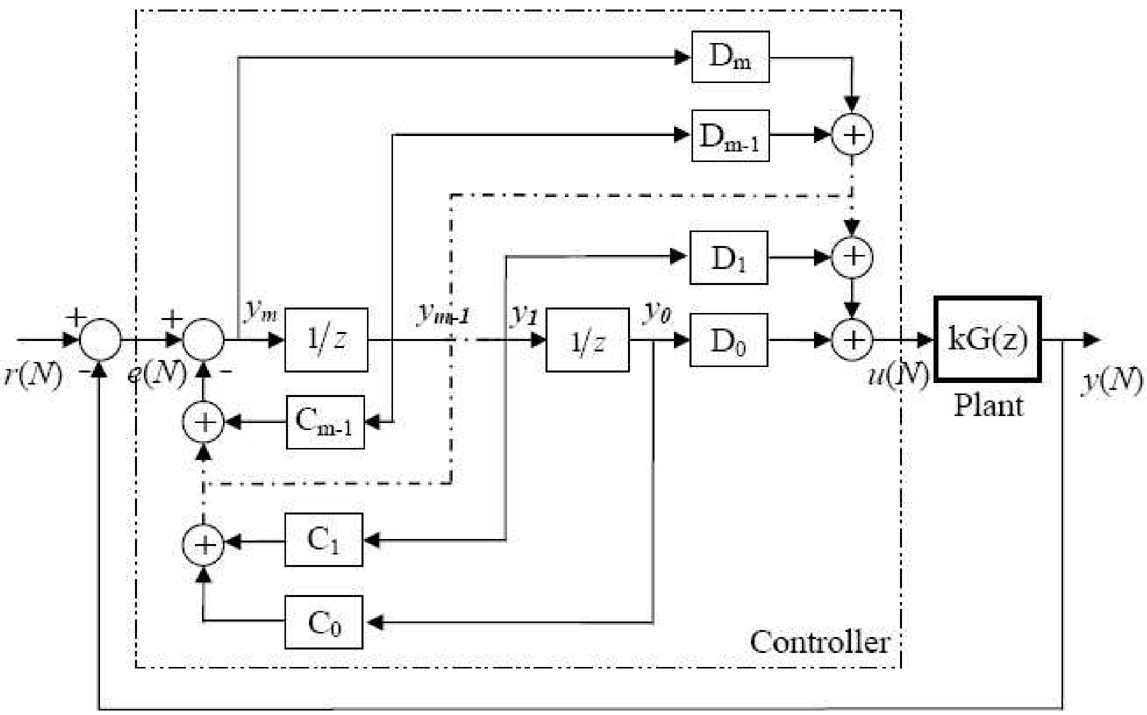

Fig. 2.1: The Periodic controller in Controller Canonical Form (CCF) and the LTI plant [1]

The 2-periodic, m^{th} order controller shown in Fig. 2.1, where D_i and C_i are 2-periodically time varying gains, which can be described as, following [2],

$$D_i(N) = d_{i,0} + (-1)^N d_{i,1} \quad , i = 0,1, \dots, m$$

$$C_i(N) = c_{i,0} + (-1)^N c_{i,1} \quad , i = 0,1, \dots, (m-1)$$

Where, $N = 0,1, ...$ are the time instants.
And d, c are Discrete Fourier Series coefficients of controller parameters.

The equivalent periodic coefficient transfer function corresponding to the controller is

$$C(z,N) = [D_m z^m + D_{m-1} z^{m-1} + \cdots + D_0][z^m + C_{m-1} z^{m-1} + \cdots + C_0]^{-1}$$

Or, $$C(z,N) \triangleq [Q(z,N)][P(z,N)]^{-1} \quad (2.5)$$

Now, putting the periodic gains in terms of Fourier Series Coefficients, we get,

$$\begin{aligned} C(z,N) = {} & \left[\left\{d_{m,0} + (-1)^N d_{m,1}\right\} z^m + \left\{d_{(m-1),0} + (-1)^N d_{(m-1),1}\right\} z^{m-1} + \cdots \right. \\ & \left. + \left\{d_{0,0} + (-1)^N d_{0,1}\right\}\right]\left[z^m + \{c_{(m-1),0} + (-1)^N c_{(m-1),1}\} z^{m-1} + \cdots \right. \\ & \left. + \{c_{0,0} + (-1)^N c_{0,1}\}\right]^{-1} \end{aligned}$$

Rearranging the terms,

$$\begin{aligned} Q(z,N) = {} & \left[d_{m,0} z^m + d_{(m-1),0} z^{m-1} + \cdots + d_{0,0}\right] \\ & + (-1)^N \left[d_{m,1} z^m + d_{(m-1),1} z^{m-1} + \cdots + d_{0,1}\right] \end{aligned}$$

Or, $$Q(z,N) \triangleq Q_0(z) + (-1)^N Q_1(z) \quad (2.6)$$

$$\begin{aligned} P(z,N) = {} & \left[z^m + c_{(m-1),0} z^{m-1} + c_{(m-2),1} z^{m-2} \ldots + c_{0,0}\right] \\ & + (-1)^N \left[c_{(m-1),1} z^{m-1} + c_{(m-2),1} z^{m-2} \ldots + c_{0,1}\right] \end{aligned}$$

Or, $$P(z,N) \triangleq P_0(z) + (-1)^N P_1(z) \quad (2.7)$$

2.4 Time Domain Lifting Method

We shall analyze this time-varying system following the Time Domain Lifting Method, described in [2], that lifts a SISO 2-periodic map f to an 2-input 2-output time invariant form which can be represented as an LTI 2×2 transform domain matrix $\bar{F}(z^2)$ that satisfies the causality condition of $\bar{F}(\infty)$ being lower triangular.

Consider the input output relation,

$$y(N) = [q_0 + (-1)^N q_1]x(N)$$

Splitting the even and odd parts of q_0 and q_1 as follows –

$$q_{0,e}(z^2) = (q_0^+ + q_0^-)/2 \text{ and } z^{-1}q_{0,o}(z^2) = (q_0^+ - q_0^-)/2$$

And $$q_{1,e}(z^2) = (q_1^+ + q_1^-)/2 \text{ and } z^{-1}q_{1,o}(z^2) = (q_1^+ - q_1^-)/2$$

Where, $q^+ = \mathrm{q(z)}$ and $q^- = \mathrm{q(-z)}$.

The input and output sequence x(N) and y(N) can also be split into odd even terms in Z- transform domain as follows –

$$X(z) = X_e(z^2) + z^{-1}X_o(z^2)$$
$$\mathrm{Y}(z) = Y_e(z^2) + z^{-1}Y_o(z^2)$$

Therefore, from the odd even decomposition, the following relation can be achieved:

$$Y_e(z^2) = \left({}^1\!/_2\right)[q_0^+ + q_0^- + q_1^+ + q_1^-]X_e(z^2) + \left({}^1\!/_2\right)[q_0^+ - q_0^- + q_1^+ - q_1^-]z^{-1}X_o(z^2)$$

and

$$Y_o(z^2) = \left({}^1\!/_2\right)[q_0^+ - q_0^- - q_1^+ + q_1^-]zX_e(z^2) + \left({}^1\!/_2\right)[q_0^+ + q_0^- - q_1^+ - q_1^-]\, X_o(z^2)$$

Hence, we can write the above equations in matrix form as-

$$\begin{bmatrix} Y_e(z^2) \\ Y_o(z^2) \end{bmatrix} = \bar{G} \begin{bmatrix} X_e(z^2) \\ X_o(z^2) \end{bmatrix}$$

Where, $$\bar{G} = \frac{1}{2}\begin{bmatrix} G_{11} & z^{-1}G_{12} \\ zG_{21} & G_{22} \end{bmatrix}$$

And
$$G_{11} = q_0^+ + q_0^- + q_1^+ + q_1^- \qquad G_{21} = q_0^+ - q_0^- - q_1^+ + q_1^-$$
$$G_{12} = q_0^+ - q_0^- + q_1^+ - q_1^- \qquad G_{22} = q_0^+ + q_0^- - q_1^+ - q_1^-$$

Thus, the time variant system is lifted to a 2-input 2-output time invariant form which is represented as an LTI 2×2 transform domain matrix. In the following section, we shall apply the time-domain lifting method to 2-periodic controller as well as to a discrete linear time-invariant plant.

2.4.1 Time-lifted 2-Periodic Controller

Using the derivation shown in the previous section, we can represent the $Q(z,N)$ and $P(z,N)$ from equation (2.6) and (2.7) as LTI 2×2 transform domain matrices as follows:

$$\bar{Q}(z^2) = \frac{1}{2}\begin{bmatrix} Q_{11} & z^{-1}Q_{12} \\ zQ_{21} & Q_{22} \end{bmatrix}$$

With,

$$Q_{11} = Q_0^+ + Q_0^- + Q_1^+ + Q_1^-$$
$$Q_{12} = Q_0^+ - Q_0^- + Q_1^+ - Q_1^-$$
$$Q_{21} = Q_0^+ - Q_0^- - Q_1^+ + Q_1^-$$
$$Q_{22} = Q_0^+ + Q_0^- - Q_1^+ - Q_1^-$$

(2.8)

And,

$$\bar{P}(z^2) = \frac{1}{2}\begin{bmatrix} P_{11} & z^{-1}P_{12} \\ zP_{21} & P_{22} \end{bmatrix}$$

With,

$$P_{11} = P_0^+ + P_0^- + P_1^+ + P_1^-$$
$$P_{12} = P_0^+ - P_0^- + P_1^+ - P_1^-$$
$$P_{21} = P_0^+ - P_0^- - P_1^+ + P_1^-$$
$$P_{22} = P_0^+ + P_0^- - P_1^+ - P_1^-$$

(2.9)

Therefore, from equation (2.5), the time lifted representation of the 2-periodic controller becomes-

$$\bar{C}(z^2) = [\bar{Q}(z^2)][\bar{P}(z^2)]^{-1} \triangleq \frac{1}{\Delta_C}\begin{bmatrix} C_{11} & z^{-1}C_{12} \\ zC_{21} & C_{22} \end{bmatrix}$$

Where,

$$C_{11} = Q_{11}P_{22} - Q_{12}P_{21}$$
$$C_{12} = -Q_{11}P_{12} + Q_{12}P_{11}$$
$$C_{21} = Q_{21}P_{22} - Q_{22}P_{21}$$
$$C_{11} = -Q_{21}P_{12} + Q_{22}P_{11}$$
$$\Delta_C = 4(P_0^+P_0^- - P_1^+P_1^-)$$

(2.10)

2.4.2 Time-lifted LDTI Plant

The LDTI plant $G(z) = \frac{b(z)}{a(z)}$, in consideration, can also be lifted to LTI 2×2 transform domain form. For the LTI plant, there will be no time-varying terms. Therefore, all the q_1 (corresponding to time varying gains of the plant) terms will be zero in the lifted matrix form.

Therefore, following section 1.3, analogically replacing the 'Q' and 'P' terms by 'b' and 'a' terms for the plant, we can write the lifted LTI 2×2 transform domain matrix as:

$$\bar{G}(z^2) = \begin{bmatrix} G_{11} & z^{-1}G_{12} \\ zG_{21} & G_{22} \end{bmatrix}$$

Where, $G_{11} = G_{22} = (b^+a^- + b^-a^+)/2a^+a^-$

And $G_{12} = G_{21} = (b^+a^- - b^-a+)/2a^+a^-$

(2.11)

2.5 Closed-Loop Characteristic Equation

Now that we have developed the lifted LTI transform matrices for both the controller and the plant, we can write the closed loop characteristic equation of the system shown in Fig. 2.1 as –

$$\det[I + k\bar{G}\bar{C}] = 0$$

Putting the expressions for $\bar{G}$ and $\bar{C}$ as obtained earlier, the characteristic equation of the closed loop system can be obtained as

$$\boldsymbol{a^+a^-[P_0^+P_0^- - P_1^+P_1^-] + k[a^-b^+\{Q_0^+P_0^- - Q_1^-P_1^+\} + a^+b^-\{Q_0^-P_0^+ - Q_1^+P_1^-\}]}$$
$$\boldsymbol{+ k^2b^+b^-[Q_0^+Q_0^- - Q_1^+Q_1^-] = 0}$$

(2.12)

This is a quadratic equation in k. By choosing suitable values of the coefficients of the quadratic, we can perform pole placement as well as zero placement for the closed loop system. However, there are certain constraints to choose the coefficient values which shall be discussed next.

2.6 Loop-Zero Placement

2.6.1 Necessary Condition for Zero Placement

The loop-zeros of a system can be understood to be the roots of the characteristic equation with the loop gain tending to ∞. Then the loop-zeros of (2.12) would be given by the coefficient of the k^2-term present in it. However, this term contains the factor b^+b^- which stands for the plant zeros. On the other hand, note that the k-term does not contain any such factor. In fact, the roots of this coefficient are fully assignable. Therefore, to make the loop zeros independent of plant zeros, the k^2 -term must be made zero.

From equation (2.12), it is evident that, the coefficient of k^2 can be made zero by choosing any of the following four conditions:

$$\boldsymbol{Q}_{\boldsymbol{0}}^{+} = \pm\boldsymbol{Q}_{\boldsymbol{1}}^{\pm} \tag{2.13}$$

Thus, the characteristic equation becomes –

$$\hat{A}(z^2)\hat{P}(z^2) + \widehat{kZ}(z^2) = \hat{\Delta}(z^2) = \check{\Delta}(z^2)\breve{D}(z^2) = 0 \tag{2.14}$$

where,

- $\hat{A}(z^2) = \boldsymbol{a}^{+}\boldsymbol{a}^{-}$ = Plant poles polynomial
- $\hat{P}(z^2) = \boldsymbol{P}_{\boldsymbol{0}}^{+}\boldsymbol{P}_{\boldsymbol{0}}^{-} - \boldsymbol{P}_{\boldsymbol{1}}^{+}\boldsymbol{P}_{\boldsymbol{1}}^{-} \triangleq \hat{p}_0 + \hat{p}_2 z^2 + \hat{p}_4 z^4 + \cdots + (-1)^m z^{2m}$

  = Controller poles polynomial (2.15)
- $\hat{Z}(z^2) = \boldsymbol{a}^{-}\boldsymbol{b}^{+}\{\boldsymbol{Q}_{\boldsymbol{0}}^{+}\boldsymbol{P}_{\boldsymbol{0}}^{-} - \boldsymbol{Q}_{\boldsymbol{1}}^{-}\boldsymbol{P}_{\boldsymbol{1}}^{+}\}\} + \boldsymbol{a}^{+}\boldsymbol{b}^{-}\{\boldsymbol{Q}_{\boldsymbol{0}}^{-}\boldsymbol{P}_{\boldsymbol{0}}^{+} - \boldsymbol{Q}_{\boldsymbol{1}}^{+}\boldsymbol{P}_{\boldsymbol{1}}^{-}\} \triangleq r_0 + r_2 z^2 + \cdots + r_{2(m+n-1)} z^{2(m+n-1)}$

  = Loop zero polynomial for the overall system (2.16)
- $\check{\Delta}(z^2)$ = Desired closed loop poles
- $\breve{D}(z^2)$ = Additional closed loop poles introduced by the controller dynamics

The point to be noted is that here, not only the controller pole polynomial $\hat{P}(z^2)$, but the loop-zero polynomial $\hat{Z}(z^2)$ is assignable as well. This loop zero placement capability of a periodic controller is what provides a designer with much more freedom in controller design than a LTI controller.

The four subsets of the proposed controller that correspond to each of the four choices mentioned above are discussed next.

2.6.2 Proposed 2-Periodic Controllers

Depending on the four conditions mentioned above, we can obtain four different types of controllers. Each will lead to different set of controller parameters. These four types of controllers can be synthesized as follows-

2.6.2.1 Case I: $\boldsymbol{Q_0^+ = Q_1^+}$

Putting this condition in the expression of $\bar{Q}(z^2)$ from equation (2.8), it follows that,

$$\bar{Q}(z^2) = \frac{1}{2}\begin{bmatrix} Q_0^+ + Q_0^- + Q_1^+ + Q_1^- & z^{-1}(Q_0^+ - Q_0^- + Q_1^+ - Q_1^-) \\ z(Q_0^+ - Q_0^- - Q_1^+ + Q_1^-) & Q_0^+ + Q_0^- - Q_1^+ - Q_1^- \end{bmatrix}$$

$$= \frac{1}{2}\begin{bmatrix} Q_0^+ + Q_0^- + Q_1^+ + Q_1^- & z^{-1}(Q_0^+ - Q_0^- + Q_1^+ - Q_1^-) \\ 0 & 0 \end{bmatrix}$$

$$= \begin{bmatrix} Q^+ + Q^- & z^{-1}(Q^+ - Q^-) \\ 0 & 0 \end{bmatrix},$$

where, $Q^+ = Q_0^+ = Q_1^+$ and $Q^- = Q_0^- = Q_1^-$

$$\triangleq \begin{bmatrix} Q_{11} & z^{-1}Q_{12} \\ 0 & 0 \end{bmatrix}$$

Therefore, following equation (2.10), the lifted controller matrix becomes –

$$\bar{C}(z^2) = [\bar{Q}(z^2)][\bar{P}(z^2)]^{-1} = \frac{1}{\Delta_C}\begin{bmatrix} C_{11} & z^{-1}C_{12} \\ 0 & 0 \end{bmatrix}$$

Where,

$$C_{11} = Q_{11}P_{22} - Q_{12}P_{21}$$

$$C_{12} = -Q_{11}P_{12} + Q_{12}P_{11}$$

$$\Delta_C = 4(P_0^+P_0^- - P_1^+P_1^-)$$

Such a controller is termed as **Even Output Controller**, as it provides outputs at even instants of time only. It is to be noted that such a controller may also be implemented as a composite system consisting of a time invariant unit ${}^{2Q(z)}\!/_{P(z)}$ followed by an even instant 2T-sampler.

2.6.2.2 Case II: $\boldsymbol{Q_0^+ = -Q_1^+}$

Putting this condition in the expression of $\bar{Q}(z^2)$ from equation (2.8), it follows that,

$$\bar{Q}(z^2) = \frac{1}{2}\begin{bmatrix} Q_0^+ + Q_0^- + Q_1^+ + Q_1^- & z^{-1}(Q_0^+ - Q_0^- + Q_1^+ - Q_1^-) \\ z(Q_0^+ - Q_0^- - Q_1^+ + Q_1^-) & Q_0^+ + Q_0^- - Q_1^+ - Q_1^- \end{bmatrix}$$

$$= \frac{1}{2}\begin{bmatrix} Q_0^+ + Q_0^- + Q_1^+ + Q_1^- & z^{-1}(Q_0^+ - Q_0^- + Q_1^+ - Q_1^-) \\ 0 & 0 \end{bmatrix}$$

$$= \begin{bmatrix} 0 & 0 \\ z(Q^+ - Q^-) & Q^+ + Q^- \end{bmatrix} \quad ,$$

where, $Q^+ = Q_0^+ = Q_1^+$ and $Q^- = Q_0^- = Q_1^-$

$$\triangleq \begin{bmatrix} 0 & 0 \\ zQ_{21} & Q_{22} \end{bmatrix}$$

Therefore, following equation (7), the lifted controller matrix becomes –

$$\bar{C}(z^2) = [\bar{Q}(z^2)][\bar{P}(z^2)]^{-1} = \frac{1}{\Delta_C}\begin{bmatrix} 0 & 0 \\ zC_{21} & C_{22} \end{bmatrix}$$

Where,

$$C_{21} = Q_{21}P_{22} - Q_{22}P_{21}$$
$$C_{22} = -Q_{21}P_{12} + Q_{22}P_{11}$$
$$\Delta_C = 4(P_0^+P_0^- - P_1^+P_1^-)$$

Such a controller is termed as **Odd Output Controller**, as it provides outputs at odd instants of time only. It is to be noted that such a controller may also be implemented as a composite system consisting of a time invariant unit $2Q(z)/P(z)$ followed by an odd instant 2T-sampler.

2.6.2.3 Case III: $\boldsymbol{Q_0^+ = Q_1^-}$

Putting this condition in the expression of $\bar{Q}(z^2)$ from equation (2.8), it follows that –

$$\bar{Q}(z^2) = \frac{1}{2}\begin{bmatrix} Q_0^+ + Q_0^- + Q_1^+ + Q_1^- & z^{-1}(Q_0^+ - Q_0^- + Q_1^+ - Q_1^-) \\ z(Q_0^+ - Q_0^- - Q_1^+ + Q_1^-) & Q_0^+ + Q_0^- - Q_1^+ - Q_1^- \end{bmatrix}$$

$$= \begin{bmatrix} Q^+ + Q^- & 0 \\ z(Q^+ - Q^-) & 0 \end{bmatrix} \quad ,$$

where, $Q^+ = Q_0^+ = Q_1^+$ and $Q^- = Q_0^- = Q_1^-$

$$\triangleq \begin{bmatrix} Q_{11} & 0 \\ zQ_{21} & 0 \end{bmatrix}$$

Therefore, following equation (2.10), the lifted controller matrix becomes –

$$\bar{C}(z^2) = [\bar{Q}(z^2)][\bar{P}(z^2)]^{-1} = \frac{1}{\Delta_C}\begin{bmatrix} C_{11} & z^{-1}C_{12} \\ zC_{21} & C_{22} \end{bmatrix}$$

where,

$C_{11} = Q_{11}P_{22}, \qquad C_{12} = -Q_{11}P_{12}, \qquad C_{21} = Q_{21}P_{22}, \qquad C_{22} = -Q_{21}P_{12}$

$$\Delta_C = 4(P_0^+P_0^- - P_1^+P_1^-)$$

Further if the controller is assumed to satisfy the condition –

$$P_0^+ = (-1)^m P_0^-$$

Then, for even and odd values of m, the following controller transfer matrices are obtained –

i. **For m = even**

$P_0^+ = P_0^-$.
Therefore, from equation (6), $P_{12} = P_0^+ - P_0^- + P_1^+ - P_1^- = 0$.
Thus, the controller reduces to -

$$\bar{C}(z^2) = \frac{1}{\Delta_C}\begin{bmatrix} C_{11} & 0 \\ zC_{21} & 0 \end{bmatrix}$$

This is termed as **Even Input Controller** because it takes inputs only at even instants of time. It is to be noted that such a controller may be implemented as a composite system consisting of a time invariant unit $2Q(z)/P(z)$ preceded by an even instant 2T-sampler.

ii. **For m = odd**

$P_0^+ = -P_0^-$.

Therefore, from equation (6), $P_{22} = P_0^+ + P_0^- - P_1^+ - P_1^- = 0$.
Thus, the controller reduces to –

$$\bar{C}(z^2) = \frac{1}{\Delta_C}\begin{bmatrix} 0 & z^{-1}C_{12} \\ 0 & C_{22} \end{bmatrix}$$

This is termed as **Odd Input Controller** because it takes inputs only at odd instants of time. It is to be noted that such a controller may be implemented as a composite system consisting of a time invariant unit $2Q(z)/P(z)$ preceded by an odd instant 2T-sampler.

2.6.2.4 Case IV: $\boldsymbol{Q_0^+ = -Q_1^-}$

Putting this condition in the expression of $\bar{Q}(z^2)$ from equation (2.8), it follows that,

$$\bar{Q}(z^2) = \frac{1}{2}\begin{bmatrix} Q_0^+ + Q_0^- + Q_1^+ + Q_1^- & z^{-1}(Q_0^+ - Q_0^- + Q_1^+ - Q_1^-) \\ z(Q_0^+ - Q_0^- - Q_1^+ + Q_1^-) & Q_0^+ + Q_0^- - Q_1^+ - Q_1^- \end{bmatrix}$$

$$= \begin{bmatrix} 0 & z^{-1}(Q^+ - Q^-) \\ 0 & Q^+ + Q^- \end{bmatrix} \quad ,$$

where, $Q^+ = Q_0^+ = Q_1^+$ and $Q^- = Q_0^- = Q_1^-$

$$\triangleq \begin{bmatrix} 0 & z^{-1}Q_{12} \\ 0 & Q_{22} \end{bmatrix}$$

Therefore, following equation (2.10), the lifted controller matrix becomes –

$$\bar{C}(z^2) = [\bar{Q}(z^2)][\bar{P}(z^2)]^{-1} = \frac{1}{\Delta_C}\begin{bmatrix} C_{11} & z^{-1}C_{12} \\ zC_{21} & C_{22} \end{bmatrix}$$

Where,

$C_{11} = -Q_{12}P_{21}$, $\quad C_{12} = Q_{12}P_{11}$, $\quad C_{21} = -Q_{22}P_{21}$, $\quad C_{22} = Q_{22}P_{11}$

$$\Delta_C = 4(P_0^+P_0^- - P_1^+P_1^-)$$

Further if the controller is assumed to satisfy the condition –

$$P_0^+ = (-1)^m P_0^-$$

Then, for even and odd values of m, the following controller transfer matrices are obtained –

i. For m = odd

$P_0^+ = -P_0^-$.
Therefore, from equation (2.9), $P_{11} = P_0^+ + P_0^- + P_1^+ + P_1^- = 0$.
Thus, the controller reduces to -

$$\bar{C}(z^2) = \frac{1}{\Delta_C}\begin{bmatrix} C_{11} & 0 \\ zC_{21} & 0 \end{bmatrix}$$

This is termed as **Even Input Controller** because it takes inputs only at even instants of time. It is to be noted that such a controller may be implemented as a composite system consisting of a time invariant unit $2Q(z)/P(z)$ preceded by an even instant 2T-sampler.

ii. For m = even

$P_0^+ = P_0^-$.
Therefore, from equation (2.9), $P_{21} = P_0^+ - P_0^- - P_1^+ + P_1^- = 0$.
Thus, the controller reduces to –

$$\bar{C}(z^2) = \frac{1}{\Delta_C}\begin{bmatrix} 0 & z^{-1}C_{12} \\ 0 & C_{22} \end{bmatrix}$$

This is termed as **Odd Input Controller** because it takes inputs only at odd instants of time. It is to be noted that such a controller may be implemented as a composite system consisting of a time invariant unit $2Q(z)/P(z)$ preceded by an odd instant 2T-sampler.

Thus, considering the necessary condition for loop-zero placement, we have obtained four subset of 2-periodic controllers. Next, we shall discuss the algorithm to design the controller for suitable pole-zero placement.

2.7 Relocatable Zeros and Order of the Controller

It is easy to see from (2.16) that the loop-zero polynomial $\hat{Z}(z^2)$ is of degree

$$\theta = m + \eta \text{ with } \eta = n - I^+\{(n-r)/2\}$$

Where, the integer (ceiling) operator I^{+} is used. This means that the assignable plant zeros and the m controller zeros, which depend on the relative order of the plant, will provide the total number of relocatable loop-zeros.

The controller has (*2m + m*) assignable coefficients to position the *m* controller poles and the $m+\eta$ loop zeros, as is evident from (2.6), (2.7) and (2.16). This suggests that one must have

$$m \geq \eta = n - I^{+}\{(n-r)/2\} \tag{2.17}$$

It is noteworthy that, for plants with relative order $(n-r) = 1\ or\ 2$, the controller order is, $m \geq n-1$.

2.8 Determination of Controller Parameters for Pole and Zero Placement

Here we shall discuss a two-stage algorithm involving only linear algebraic steps for evaluating the 2-periodic controller parameters to achieve controller-pole as well as loop-zero placement. In the first stage, given a desired $\hat{Z}(z^2)$, some intermediate polynomial $\hat{L}(z)$ is found, and then, in the second stage, the controller polynomials $P_0(z)$, $P_1(z)$, $Q_0(z)$ and $Q_1(z)$ are derived in terms of this $\hat{L}(z)$ and a chosen $\hat{P}(z^2)$.

First, we need to define the following:

$$\begin{aligned}
\hat{B}(z) &\triangleq \boldsymbol{a}^{+}\boldsymbol{b}^{-} \\
&= \left[\hat{b}_0 + \hat{b}_2 z^2 + \cdots + \hat{b}_{2(n-1)} z^{2(n-1)}\right] + z[\hat{b}_1 + \hat{b}_3 z^2 + \cdots \\
&\quad + \hat{b}_{2n-1} z^{2(n-1)}] \\
&= B_e(z^2) + zB_d(z^2)
\end{aligned} \tag{2.18}$$

$$\begin{aligned}
\hat{L}(z) &\triangleq \boldsymbol{Q_0^{-}P_0^{+}} - \boldsymbol{Q_1^{+}P_1^{-}} \\
&= \left[\hat{l}_0 + \hat{l}_2 z^2 + \cdots + \hat{l}_{2m} z^{2m}\right] + z\left[\hat{l}_1 + \hat{l}_3 z^2 + \cdots + \hat{l}_{2m-1} z^{2(m-1)}\right] \\
&= L_e(z^2) + zL_d(z^2)
\end{aligned} \tag{2.19}$$

2.8.1 Design Stage – I : Intermediate Polynomial

From equation (2.16), (2.18) and (2.19), we can write,

$$\hat{Z}(z^2) = \hat{B}^+\hat{L}^+ + \hat{B}^-\hat{L}^- = 2B_e(z^2)L_e(z^2) + 2z^2B_d(z^2)L_d(z^2) \tag{2.20}$$

Since, $\hat{Z}(z^2)$ is a polynomial of order $(m+n-1)$, it has $(m+n)$ coefficients, which are to be assigned by suitable choices of the $(2m+1)$ independent coefficients of the $\hat{L}(z)$ polynomial. Therefore, one must have $m \geq (n-1)$ for satisfactory controller design.

Now, equating like powers of z^2 on both sides of (2.20), using (2.16), we obtain the Sylvester Matrix like equation that links the coefficients of $\hat{Z}(z^2)$ to that of $\hat{L}(z)$ as follows–

$$\begin{bmatrix} r_0 \\ r_2 \\ r_4 \\ \vdots \\ r_{2(m+n-1)} \end{bmatrix} = \begin{bmatrix} \hat{b}_0 & 0 & \dots & 0 & 0 & \dots & 0 \\ \hat{b}_2 & \hat{b}_0 & \dots & \begin{matrix} 0 \\ 0 \end{matrix} & \hat{b}_1 & \dots & 0 \\ \hat{b}_4 & \hat{b}_2 & \dots & \vdots & \hat{b}_3 & \dots & 0 \\ \vdots & \vdots & \ddots & \vdots & \vdots & \ddots & \vdots \\ 0 & 0 & \dots & \hat{b}_{2(n-1)} & 0 & \dots & \hat{b}_{2n-1} \end{bmatrix} \begin{bmatrix} \hat{l}_0 \\ \vdots \\ \hat{l}_{2m} \\ \hat{l}_1 \\ \vdots \\ \hat{l}_{2m-1} \end{bmatrix} \Rightarrow \hat{r} = \bar{B}\hat{l} \tag{2.21}$$

It is assumed that, for a desired controller design for a particular plant, $\hat{Z}(z^2)$ as well as $\hat{B}(z)$ are known. Putting their coefficients into the matrix equation (2.21), we can calculate the coefficients of $\hat{L}(z)$.

Now, it can be inferred that, the following requirements in the selection of the loop-zeros must be met for (2.21) to be a consistent system of equations (such that a solution exists):

- The loop-zero polynomial must have a root at p^2, if the plant has a pole-zero cancellation at p, which means that the effective loop transfer function would also have a pole-zero cancellation at p^2. (Obviously, the plant shouldn't have any unstable pole-zero cancellation at p, |p| > 1, for internal stability.)

- The loop-zero polynomial must include the same factor as the plant denominator because if the plant denominator had an even factor $(z^2 + c)$, the loop transfer function would likewise have a pole-zero cancellation at c. (Again, one needs $|c| < 1$ to have internal stability.)

- The loop-zero polynomial must include the same factor as the plant numerator if the plant numerator has an even factor $(z^2 + c)$.

The following assumes that (2.21) can be solved to obtain $\hat{L}(z)$using an appropriate numerical instrument. Additionally, it should be noted that the $\bar{B}$ matrix may become single in the following circumstances:

- If the plant has a pole (or a zero) at the beginning;
- If the denominator and numerator both include only even elements;
- If the plant has a pole-zero cancellation at origin.

All of these scenarios will result in certain all-zero identities, making the set of linear equations in (2.21) underdetermined but consistent and yielding non-unique solutions for the coefficients of the $\hat{L}(z)$ polynomial owing to the singular matrix $\bar{B}$.

2.8.2 Design Stage – II

It is clear from the previous discussions that, one has to obtain the controller parameters in terms of-

i. The coefficients of $\hat{\boldsymbol{L}}(\boldsymbol{z})$ obtained above and

ii. The coefficients of the controller pole polynomial, $\widehat{\boldsymbol{P}}(\boldsymbol{z}^{\mathbf{2}})$.

The coefficients of the controller pole polynomial $\widehat{\boldsymbol{P}}(\boldsymbol{z}^{\mathbf{2}})$ are chosen such as satisfactory closed-loop behavior is achieved. Methods to achieve the same are next presented corresponding to each of the four cases of controller constraints noted in (2.13).

2.8.2.1 Case I: $\boldsymbol{Q}_{\mathbf{0}}^{+} = \boldsymbol{Q}_{\mathbf{1}}^{-}$

It follows from equation (2.19),

$$\hat{L}(z) \triangleq Q_0^- P_0^+ - Q_1^+ P_1^- = Q_0^- (P_0^+ - P_1^-).$$

Now, following [3], we can find $\boldsymbol{Q}_{\mathbf{0}}^{-}$ and $(\boldsymbol{P}_{\mathbf{0}}^{+} - \boldsymbol{P}_{\mathbf{1}}^{-})$ by grouping the roots of $\hat{L}(z)$ into two equal halves such that,

i. Both the halves are real polynomials (i.e., a complex root and its conjugate are present in the same half.

ii. At least one of the halves has no even factor.

If the factor that satisfies the 2nd condition is, in addition, monic, then the same is chosen as $(\boldsymbol{P}_{\mathbf{0}}^{+} - \boldsymbol{P}_{\mathbf{1}}^{-})$ and the rest would constitute $\boldsymbol{Q}_{\mathbf{0}}^{-}$. Once the segregation is done, we can find the 2-periodic controller coefficients $\boldsymbol{d}_{i,\mathbf{0}}$ and $\boldsymbol{d}_{i,\mathbf{1}}$ for $i = 0,1,\dots,m$ directly from $\boldsymbol{Q}_{\mathbf{0}}^{-}$ using the equation (2.6). Thus, the controller polynomials $Q_0(z)$ and $Q_1(z)$ are derived.

However, to get $\boldsymbol{c_{i,0}}$ and $\boldsymbol{c_{i,1}}$ the following additional steps are necessary. Let us assume,

$$(P_0^+ - P_1^-) \triangleq \Gamma(z) = \gamma_0 + \gamma_1 z + \ldots + \gamma_m z^m \tag{2.22}$$

Eliminating P_1^+ and P_1^- from (2.15) and (2.22), we get the following relation,

$$P_0^+ \Gamma^- + P_0^- \Gamma^+ = \hat{P}(z^2) + \Gamma^+ \Gamma^- \tag{2.23}$$

Equating the like powers of z^2 on both sides of (2.23), we shall obtain another Sylvester Matrix equation, from which $\boldsymbol{c_{i,0}}$ for $i = 0,1, \ldots, (m-1)$ are calculated as follows [5]-

$$2\begin{bmatrix} \gamma_0 & 0 & 0 & 0 & \cdots & 0 & 0 \\ \gamma_2 & -\gamma_1 & \gamma_0 & 0 & \cdots & 0 & 0 \\ \gamma_4 & -\gamma_3 & \gamma_2 & -\gamma_1 & \cdots & 0 & 0 \\ \vdots & \vdots & \vdots & \vdots & \ddots & \vdots & \vdots \\ 0 & 0 & 0 & 0 & \cdots & (-1)^{m-1}\gamma_{m-1} & (-1)^m \gamma_{m-2} \\ 0 & 0 & 0 & 0 & \cdots & 0 & (-1)^m \gamma_m \end{bmatrix} \begin{bmatrix} c_{0,0} \\ c_{1,0} \\ c_{2,0} \\ c_{3,0} \\ \vdots \\ c_{(m-1),0} \\ 1 \end{bmatrix} = \begin{bmatrix} \hat{p}_0 + \gamma_0^2 \\ \hat{p}_2 + 2\gamma_0\gamma_2 - \gamma_1^2 \\ \hat{p}_4 + \gamma_0\gamma_4 - 2\gamma_1\gamma_3 + \gamma_2^2 \\ \vdots \\ \hat{p}_{2(m-1)} + (-1)^m 2\gamma_m\gamma_{m-2} - (-1)^m \gamma_{m-1}^2 \\ (-1)^m + (-1)^m \gamma_m^2 \end{bmatrix} \tag{2.24}$$

Solving this, we get the coefficients of $P_0(z)$ i.e., $\boldsymbol{c_{i,0}}$ for $i = 0,1, \ldots, (m-1)$.

Finally, using equation (2.22), we can get the coefficients of $P_1(z)$ i.e., $\boldsymbol{c_{i,1}}$ as –

$$\boldsymbol{c_{i,1}} = (-1)^i (\boldsymbol{c_{i,0}} - \gamma_i), \qquad \text{for } i = 0,1, \ldots, (m-1) \tag{2.25}$$

This completes the evaluation of the 2-periodic controller feedback and feed-forward gains.

2.8.2.2 Case II: $\boldsymbol{Q_0^+ = -Q_1^-}$

It follows from equation (2.19),

$$\hat{L}(z) \triangleq Q_0^- P_0^+ - Q_1^+ P_1^- = Q_0^- (P_0^+ + P_1^-).$$

Like the previous case, we shall segregate the roots of $\hat{L}(z)$ into $\boldsymbol{Q_0^-}$ and $(\boldsymbol{P_0^+} + \boldsymbol{P_1^-})$ and assume,

$$(P_0^+ + P_1^-) \triangleq \Gamma(z).$$

Proceeding in the similar manner as discussed earlier, we can easily calculate the controller polynomials $Q_0(z)$ and $Q_1(z)$ from the expression of $\boldsymbol{Q_0^-}$.

To obtain the polynomial $P_0(z)$, we shall construct and solve a similar Sylvester Matrix equation as discussed above. Finally, the coefficients of the controller polynomial $P_1(z)$ are calculated as follows –

$$\boldsymbol{c_{i,1}} = (-1)^i(\gamma_i - \boldsymbol{c_{i,0}}), \quad \text{for } i = 0,1, \dots, (m-1) \tag{2.26}$$

2.8.2.3 Case III: $\boldsymbol{Q_0^+} = \boldsymbol{Q_1^+}$

In this case, it is evident from equation (2.19), in order to be able to extract the factor Q_0 from the $\hat{L}(z)$ polynomial, one must satisfy the following relation:

$$\boldsymbol{Q_i^+} = (-\boldsymbol{1})^{\boldsymbol{m}}\boldsymbol{Q_i^-}, \quad \text{for } i = 0,1 \tag{2.27}$$

Therefore, equation (2.19) becomes,

$$\hat{L}(z) \triangleq Q_0^- P_0^+ - Q_1^+ P_1^- = Q_0^- (P_0^+ - (-1)^m P_1^-)$$

Where, m = order of the controller

Now, Depending on the controller order *m*, two scenarios may arise –

i. **m = even**
Here, the calculation for evaluation of controller parameters should be proceeded as describes in Case I.

ii. **m = odd**
Here, the calculation for evaluation of controller parameters should be proceeded as describes in Case II.

2.8.2.4 Case IV: $\boldsymbol{Q_0^+} = -\boldsymbol{Q_1^+}$

In this case, it is evident from equation (2.19), in order to be able to extract the factor Q_0 from the $\hat{L}(z)$ polynomial, one must satisfy the following relation:

$$\boldsymbol{Q_i^+} = (-\mathbf{1})^{\boldsymbol{m}} \boldsymbol{Q_i^-}, \quad \text{for } i = 0,1$$

Therefore, equation (2.19) becomes,

$$\hat{L}(z) \triangleq Q_0^- P_0^+ - Q_1^+ P_1^- = Q_0^- (P_0^+ + (-1)^m P_1^-)$$

Where, m= order of the controller
Now, Depending on the controller order 'm', two scenarios may arise –

i. **m = odd**
Here, the calculation for evaluation of controller parameters should be proceeded as describes in **Case I**.

ii. **m = even**
Here, the calculation for evaluation of controller parameters should be proceeded as describes in **Case II**.

2.9 Ensuring Ripple-Free Response in Steady-State

If or whether one can remove the 2-periodic ripples that would typically be present in the transient as well as steady-state output of such a compensated system determines whether utilizing a 2-periodic controller in a real application is feasible. This section aims to obtain the situations where the steady state ripples as produced by 2-periodic controllers can be eliminated so that it becomes physically applicable.

Following (2.10) and (2.11), the lifted transform domain relation between the reference input $r(N)$ and error $e(N)$ (see Fig. 1.1) may be found as –

$$\begin{bmatrix} E_e(z^2) \\ E_o(z^2) \end{bmatrix} = [I + k\bar{G}\bar{C}]^{-1} \begin{bmatrix} R_e(z^2) \\ R_o(z^2) \end{bmatrix}$$

Applying Odd-Even decomposition to the input step signal $r(N)$, we get –

$$\begin{bmatrix} R_e(z^2) \\ R_o(z^2) \end{bmatrix} = \frac{z^2}{z^2 - 1} \begin{bmatrix} 1 \\ 1 \end{bmatrix}$$

Thereafter, from these two relations, after simplification, we yield

$$\begin{bmatrix} E_e(z^2) \\ E_o(z^2) \end{bmatrix} = \frac{1}{\Delta} \begin{bmatrix} \Delta_c d - z^{-1}(n_1 - n_2)C_{12} + (n_1 - z^{-2}n_2)C_{22} \\ \Delta_c d + (n_1 - n_2)C_{11} - z(n_1 - z^{-2}n_2)C_{21} \end{bmatrix} \frac{z^2}{z^2 - 1} \tag{2.28}$$

Where,

$$\Delta = \Delta_c d + n_1(C_{11} + C_{22}) + z^{-1} n_2 (C_{12} + C_{21}) + b^+ b^-$$

$$n_1 = b^+ a^- + a^+ b^- \;, \qquad n_2 = z(b^+ a^- - a^+ b^-) \qquad \text{and} \qquad d = a^+ a^-$$

The final value theorem may be used to determine the equivalent steady-state errors at the even and odd instants, which would then be –

$$\begin{bmatrix} E_{e,ss} \\ E_{o,ss} \end{bmatrix} = \lim_{z^2 \to 1} \left\{ \frac{z^2}{\Delta} \begin{bmatrix} \Delta_c d - z^{-1}(n_1 - n_2)C_{12} + (n_1 - z^{-2} n_2)C_{22} \\ \Delta_c d + (n_1 - n_2)C_{11} - z(n_1 - z^{-2} n_2)C_{21} \end{bmatrix} \right\}$$

It is evident therefrom that for $E_{e,ss}$ and $E_{o,ss}$ to be identical both the terms $(n_1 - n_2)$ and $(n_1 - z^{-2} n_2)$ should be zero when $(z^2 \to 1)$, which requires that they should contain the factor $(z^2 - 1)$.

From (2.27), it follows that,

$$(n_1 - n_2) = b^+ a^- (1 - z) + a^+ b^- (1 + z)$$
$$(n_1 - z^{-2} n_2) = z^{-1}[b^+ a^- (z - 1) + a^+ b^- (z + 1)]$$

It is now clear that the steady-state response won't have any ripples if the plant has a denominator factor of $(z - 1)$ or a numerator factor of $(z + 1)$, that is, either a pole at 1 or a zero at -1. However, if the plant is missing one of them, one must supplement it, as illustrated in Fig. 2.2, before developing the 2-periodic controller.

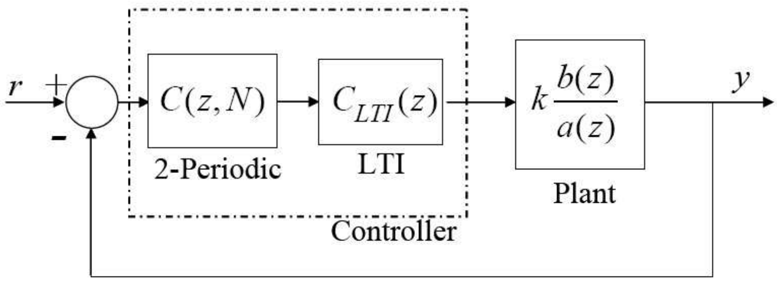

Figure 2.2: The augmented controller [1]

2.10 Numerical Example

2.10.1 General 2-Periodic Control

Let's consider the unstable as well as Non-Minimum-Phase (NMP) plant

$$G(z) = \frac{b(z)}{a(z)} = \frac{(z - 1.2)}{(z - 0.5)(z - 1.5)} \tag{2.29}$$

The primary problem in treating such plants is to provide adequate loop robustness, which can be evaluated by the gain margin (GM). The maximum GM for this plant under LTI control is determined to be 2.778 employing The Nevanlinna-Pick (NP) Matrix Method, as shown in [2]. The responses to these limiting controllers, however, are completely oscillatory (having very small damping).

On the other side, LTI dead-beat control might be used if settling time is the main issue. In actuality, this plant's deadbeat controller is

$$C(z) = \frac{11.43(z - 0.5156)}{(z - 9.429)}$$

However, given that the comparable GM is only 1.08, as shown in [13], the same might not be acceptable.

The corresponding step response of the closed loop system is shown below:

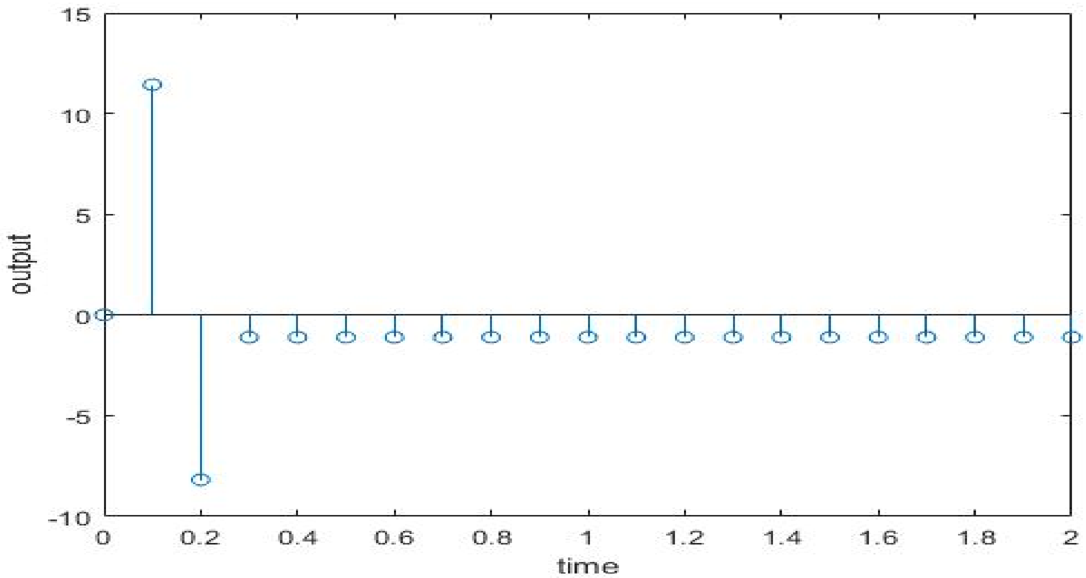

Fig. 2.3: Step response of LTI deadbeat controlled plant of example 2.10

The gain margin in this case is 1.08, which is unsatisfactory even if the system converges within three sampling instants. Additionally, it exhibits some steady-state inaccuracy. Furthermore, the controller is basically unrealizable due to the fact that its pole is located quite distant from the origin.

Next, we'll develop a 2-periodic controller with order $m = n - 1 = 1$ that has the shape of Fig. 2.1. There would be 3 closed loop poles and 2 loop zeros according to the characteristic equation (2.14). In order to increase the loop's robustness, we would also like to move the loop zeros near the origin, if that is possible. While making these decisions, it would be practical to get as many stable pole-zero cancellations as feasible.

In order to guarantee that one of the closed loop poles remains at origin, we first choose one of the loop zeros and the one controller pole at the origin. The other loop zero then would have to be placed at 0.225 such that the two plant poles also end up at the origin in closed loop.

Then the corresponding pole and zero polynomials become:

$$\hat{A}(z^2) = a^+a^- = (z^2 - 0.25)(z^2 - 2.25)$$
$$\hat{P}(z^2) = -z^2$$
$$\hat{Z}(z^2) = z^2(z^2 - 0.225) \tag{2.30}$$

Consequently, the effective loop transfer function becomes:

$$L(z) = \frac{-k(z^2 - 0.225)}{(z^2 - 2.25)(z^2 - 0.25)}$$

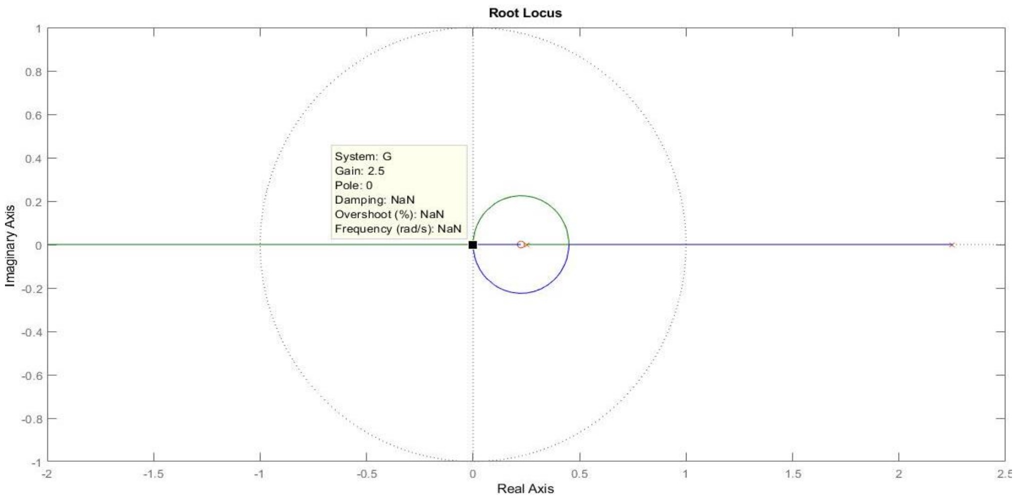

Fig. 2.4: Root Locus for Dead-Beat 2-periodic controller for example 2.10

From the root locus, it follows that, a loop-gain of $k = 2.5$ would yield the closed loop characteristic equation as:

$$\Delta_{CL} = -z^6 = 0$$

Now it is simple to determine that the 2-periodically adjusted system's loop gain margin would be 2.74, which is significantly better than the LTI design. The intermediate polynomial is found as,

$$\hat{L}(z) = 0.857z + 1.6964z^2 = 1.6964z(z + 0.5053) \tag{2.31}$$

Therefore, the 2-periodic controller gains are calculated for case-I, as follows:

$d_{1,0} = -1.6964$	$d_{1,1} = 1.6964$	$c_{0,0} = 0.2526$	$c_{0,1} = -0.2526$
$d_{0,0} = 0$	$d_{0,1} = 0$		

Table 2.1: 2-Periodic controller parameters (Case-I) for example 2.10

The step response for the same is obtained as:

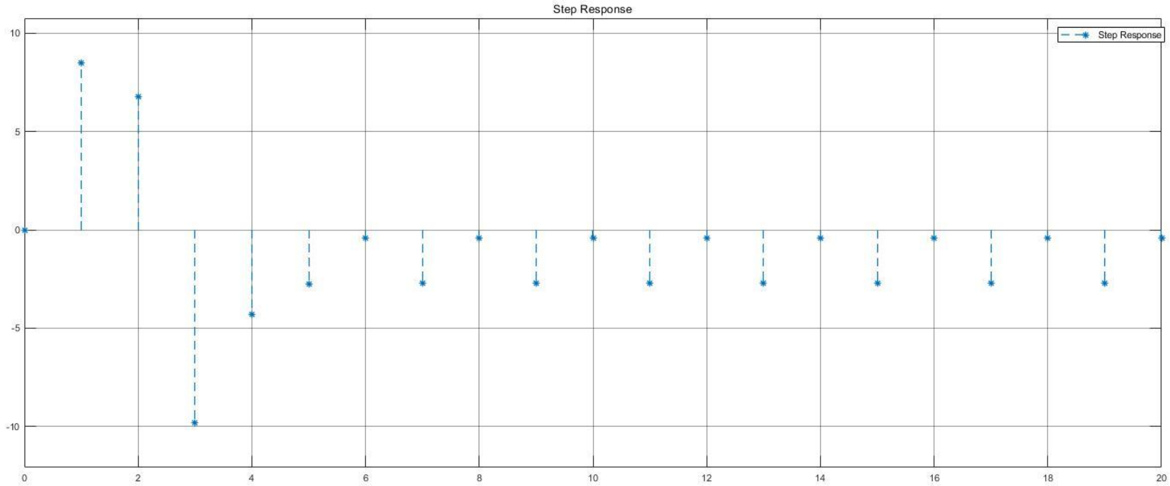

Fig. 2.5: Step response of 2-periodic compensated plant of example 2.10 (Case-I)

Similarly, from (2.31), the 2-periodic controller gains are calculated for case-II, as follows:

$d_{1,0} = -1.6964$	$d_{1,1} = -1.6964$	$c_{0,0} = 0.2526$	$c_{0,1} = 0.2526$
$d_{0,0} = 0$	$d_{0,1} = 0$		

Table 2.2: 2-Periodic controller parameters (Case-II) for example 2.10

The step response for the same is obtained as:

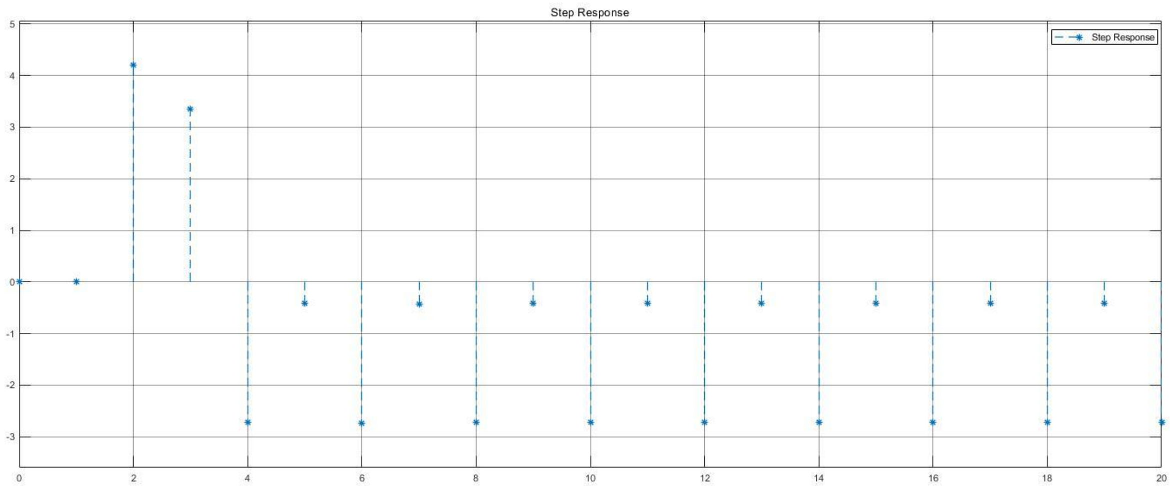

Fig. 2.6: Step response of 2-periodic compensated plant of example 2.10 (Case-II)

For cases III and IV, we can easily find that, the step responses are same as shown in the above cases. Here, we can clearly see from Fig. 2.5 and 2.6 that, the steady-state step response has constant ripples for odd and even instants of time. Therefore we need to apply the ripple reduction method as explained in section 2.9 for the above system.

2.10.2 Ripple-Free 2-Periodic Control

2.10.2.1 With Augmentation $\frac{(z+1)}{z}$

With this augmentation, the plant transfer function becomes –

$$G(z) = \frac{b(z)}{a(z)} = \frac{(z-1.2)(z+1)}{z(z-0.5)(z-1.5)}$$

The corresponding 2-periodic controller order will then become $m = n - 1 = 2$. Then the corresponding pole and zero polynomials become and assumed to be:

$$\hat{A}(z^2) = a^+a^- = -z^2(z^2 - 0.25)(z^2 - 2.25)$$
$$\hat{P}(z^2) = z^2(z^2 - 0.322)$$
$$\hat{Z}(z^2) = -0.8696(z^2)^3(z^2 - 0.25)$$

The root locus of the system is obtained as:

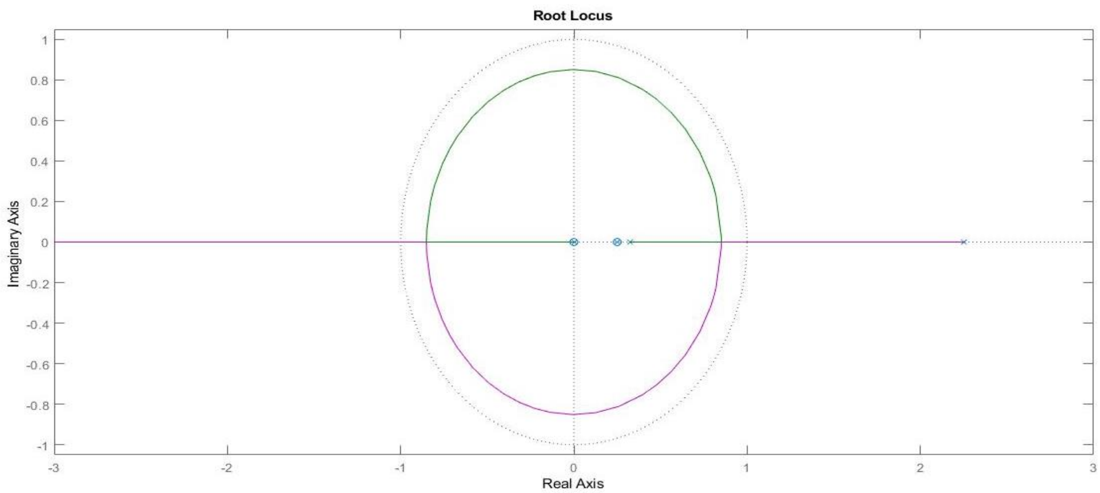

Fig. 2.7: Root locus of 2-Periodic controller with augmentation $(z+1)/z$

Here, we can find the loop GM of the system to be 4.296. The corresponding controller parameters, considering Case-I ($Q_0^+ = Q_1^-$), are listed below:

$d_{2,0} = 4.3483$	$d_{2,1} = 4.3483$	$c_{1,0} = 1.1212$	$c_{1,1} = 0.5788$
$d_{1,0} = 0$	$d_{1,1} = 0$	$c_{0,0} = 0.3$	$c_{0,1} = -0.3$
$d_{0,0} = 0$	$d_{0,1} = 0$		

Table 2.3: 2-Periodic controller parameters (Case-I) for augmentation $(z+1)/z$

The step response (normalized) of the 2-periodic compensated system for case-I is as shown:

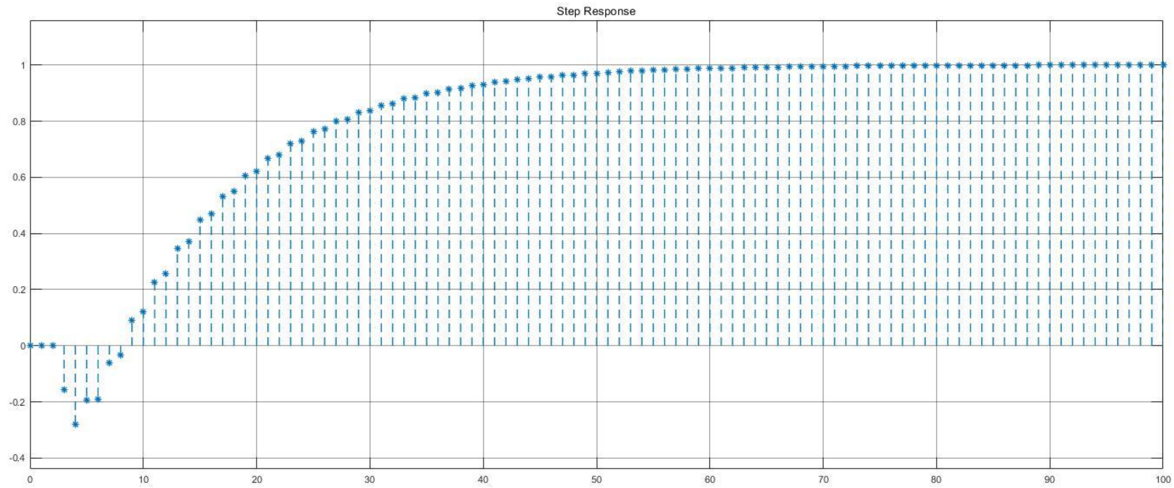

Fig. 2.8: Step response (normalized) of 2-Periodic controller for case-I with augmentation $(z+1)/z$

Similarly, the controller parameters and the step response for Case-II ($Q_0^+ = -Q_1^-$) are as follows:

$d_{2,0} = 4.3483$	$d_{2,1} = -4.3483$	$c_{1,0} = 1.1212$	$c_{1,1} = -0.5788$
$d_{1,0} = 0$	$d_{1,1} = 0$	$c_{0,0} = 0.3$	$c_{0,1} = 0.3$
$d_{0,0} = 0$	$d_{0,1} = 0$		

Table 2.4: 2-Periodic controller parameters (Case-II) for augmentation $(z+1)/z$

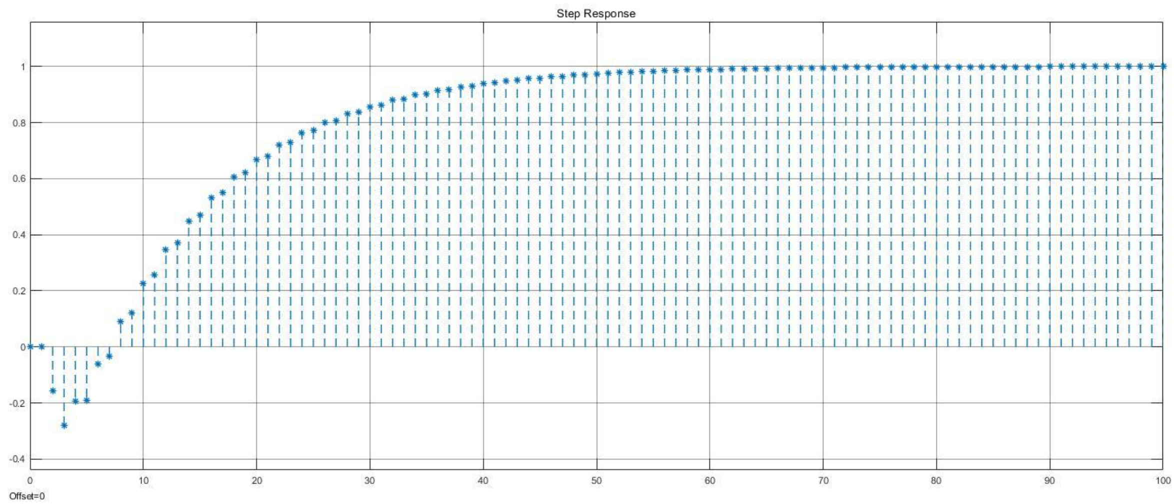

Fig. 2.9: Step response (normalized) of 2-Periodic controller for case-II with augmentation $(z+1)/z$

2.10.2.2 With Augmentation $\frac{z}{(z-1)}$

With this augmentation, the plant transfer function becomes –

$$G(z) = \frac{b(z)}{a(z)} = \frac{z(z-1.2)}{(z-1)(z-0.5)(z-1.5)}$$

The corresponding 2-periodic controller order will then become $m = n - 1 = 2$. Then the corresponding pole and zero polynomials become and assumed to be:

$$\hat{A}(z^2) = a^+a^- = -(z^2-1)(z^2-0.25)(z^2-2.25)$$
$$\hat{P}(z^2) = (z^2)^2$$
$$\hat{Z}(z^2) = -2.0497(z^2)^2(z^2-0.25)(z^2-0.922)$$

The root locus of the system is obtained as:

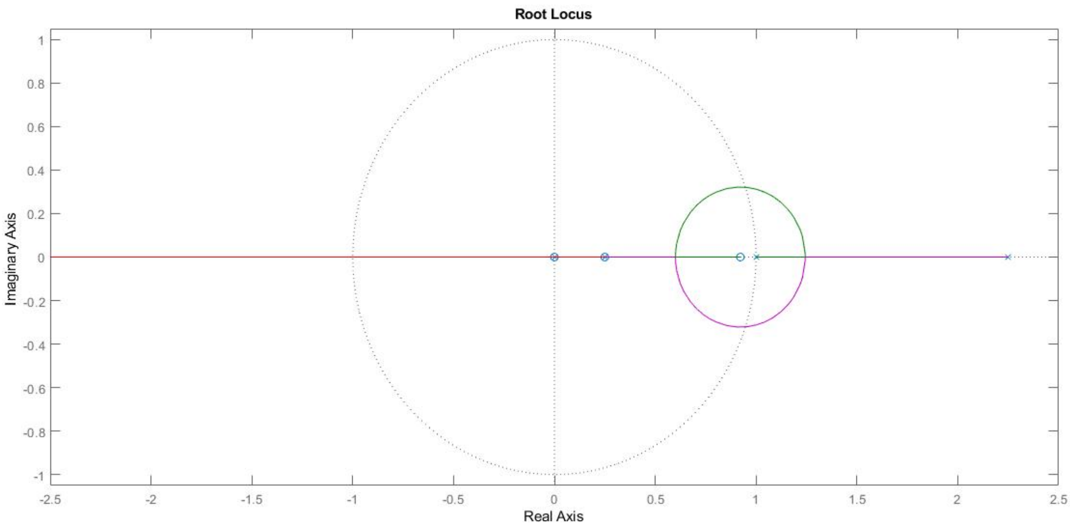

Fig. 2.10: Root locus of 2-Periodic controller with augmentation $z/(z-1)$

Here, we can find the loop GM of the system to be 3.381. The corresponding controller parameters, considering Case-I ($Q_0^+ = Q_1^-$), are listed below:

$d_{2,0} = 3.9491$	$d_{2,1} = 3.9491$	$c_{1,0} = 0.5202$	$c_{1,1} = 0.5202$
$d_{1,0} = -1.9745$	$d_{1,1} = 1.9745$	$c_{0,0} = 0$	$c_{0,1} = 0$
$d_{0,0} = 0$	$d_{0,1} = 0$		

Table 2.5: 2-Periodic controller parameters (Case-I) for augmentation $z/(z-1)$

The step response of the 2-periodic compensated system for case-I is shown below:

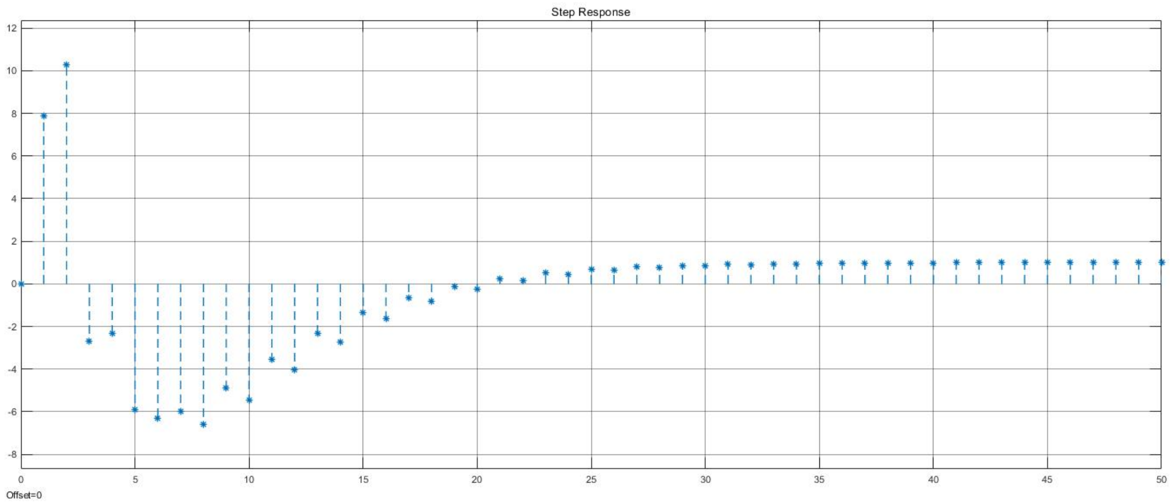

Fig. 2.11 Step response (normalized) of 2-Periodic controller for case-I with augmentation $z/(z-1)$

Similarly, the controller parameters and the step response for Case-II ($Q_0^+ = -Q_1^-$) are as follows:

$d_{2,0} = 3.9491$	$d_{2,1} = -3.9491$	$c_{1,0} = 0.5202$	$c_{1,1} = -0.5202$
$d_{1,0} = -1.9745$	$d_{1,1} = -1.9745$	$c_{0,0} = 0$	$c_{0,1} = 0$
$d_{0,0} = 0$	$d_{0,1} = 0$		

Table 2.6: 2-Periodic controller parameters (Case-II) for augmentation $z/(z-1)$

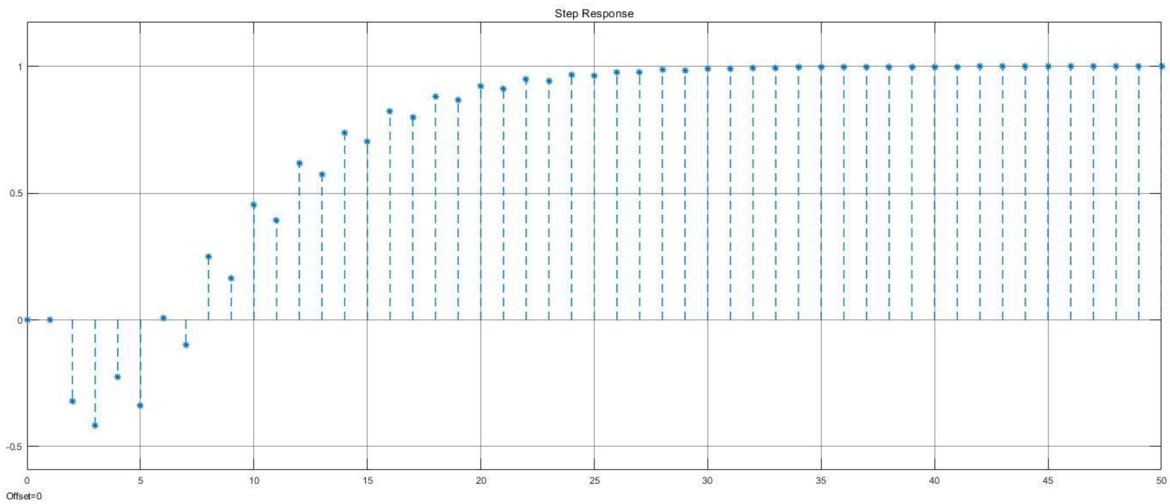

Fig. 2.12: Step response (normalized) of 2-Periodic controller for case-II with augmentation $z/(z-1)$

Chapter 3

Continuous Stirred Tank Reactor (CSTR) Modelling

3.1 Introduction

Units known as stirred tank reactors are often employed in industry, particularly in the chemical and biological sectors. Because the input flow of the reactant or cooling liquid may be readily adjusted, continuous stirred tank reactors (CSTR) are frequently used for control. CSTR belongs to the category of nonlinear systems with continuous distributed parameters from the perspective of system engineering. These reactors' mathematical models consist of a series of nonlinear ordinary differential equations (ODEs). Currently, computer simulation is utilized a lot because it provides benefits over experiments on actual systems, which are occasionally impractical, risky, or expensive to do.

The primary reaction that results in the desired product is frequently followed by subsequent and parallel reactions that result in undesirable by-products. Kantor in [24] discussed the application of extended linearization techniques to the control of reactions in a non-isothermal Van de Vusse continuous stirred tank reactors with an example for a broad reaction scheme of this sort. The reaction mechanism considered by Engell and Klatt (1993) can be written as –

$$A \xrightarrow{k_1} B \xrightarrow{k_2} C$$

$$2A \xrightarrow{k_3} D$$

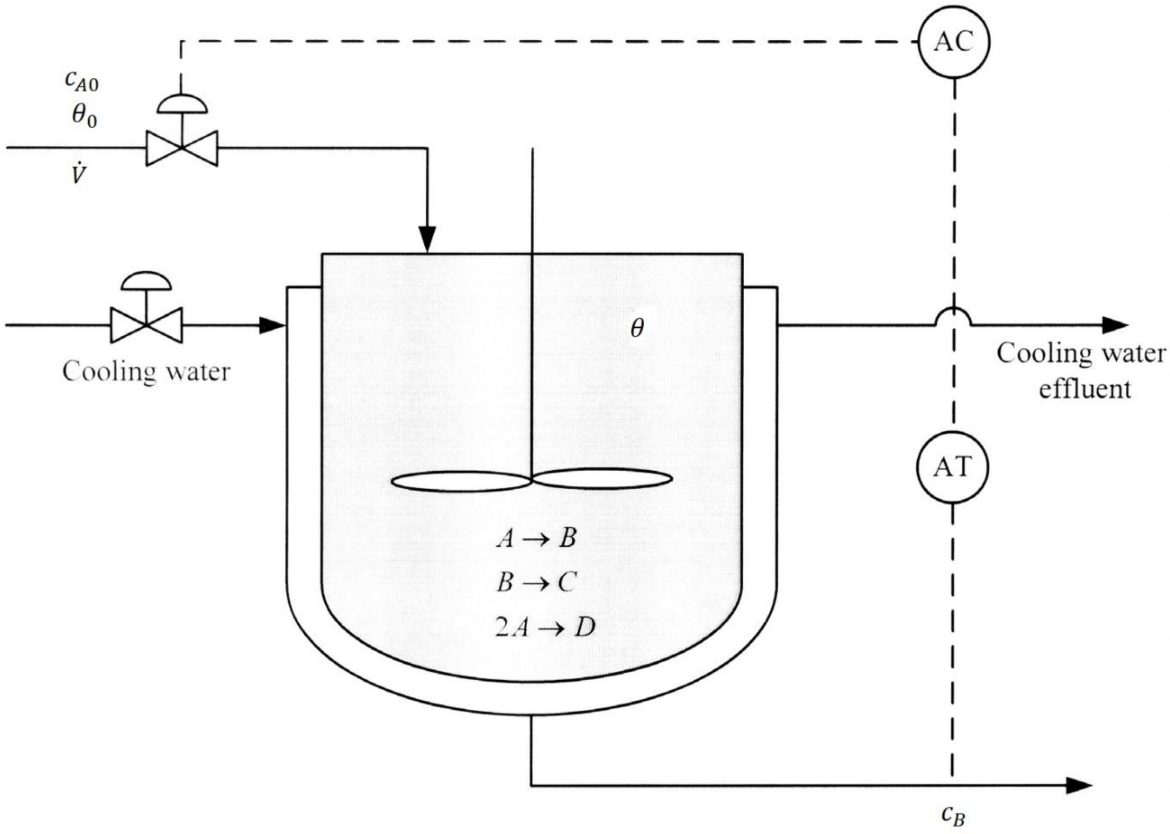

Fig. 3.1: Schematic diagram of the CSTR control system [5]

Where, A (cyclopentadiene) is the educt, B (Cyclopentenol) the desired product, C (Cyclopentanediol) and D (Dicyclopentadiene) the unwanted by-products. The procedure that we are thinking about is the electrophilic addition of water in diluted solution, catalyzed by an acid, to produce Cyclopetenol (B) from Cycloetadiene (A). Dicyclopentadiene (D) is formed by the Diels-Alder reaction as a side product due to the strong reactivity of the educt and the product, and Cyclopentanediol (C) is produced as a subsequent by adding another water molecule. The complete reaction scheme is –

$$\underset{\text{cyclopentadiene}}{C_5H_6} \xrightarrow{H_2O/H^+} \underset{\text{cyclopentenol}}{C_5H_7OH} \xrightarrow{H_2O/H^+} \underset{\text{cyclopentanediol}}{C_5H_8(OH)_2}$$

$$2\left(\underset{\text{cyclopentadiene}}{C_5H_6}\right) \longrightarrow \underset{\text{dicyclopentadiene}}{C_{10}H_{12}}$$

A fourth order nonlinear dynamical MIMO system that may be used to model this process has unstable zero dynamics and cannot be controlled by the well-known piecewise linearization and decoupling approaches (Isidori 1989) [35].

3.2 Mathematical Modelling of CSTR

Only cyclopentadiene at very low concentration c_{A0}, is present in the educt flow. The balance equations for the pertinent concentrations of cyclopentadiene and the intended product, Cyclopentenol, are c_A and c_B, under the assumptions of constant density and an optimum residence time distribution inside the reactor.

The following nonlinear differential equations, which are obtained from component balances for substances A and B as well as from energy balances for the reactor and cooling jacket, may be used to explain the dynamics of the reactor:

$$\left.\begin{aligned} \frac{dc_A}{dt} &= \frac{\dot{V}}{V_R}(c_{A0} - c_A) - k_1(\theta)c_A - k_3(\theta)c_A^2 \\ \frac{dc_B}{dt} &= -\frac{\dot{V}}{V_R}c_B + k_1(\theta)c_A - k_2(\theta)c_B \end{aligned}\right\} \tag{3.1}$$

Here, V_R stands for the reactor's volume and V for its volumetric flow. We can define the dilution rate as, $u = \frac{\dot{V}}{V_R}$. The following differential equation for the temperature (θ) of the reactor's interior is produced by the energy balance.

$$\begin{aligned} \frac{d\theta}{dt} = &-\frac{1}{\rho C_P}\left[k_1(\theta)C_A\Delta H_{R_{AB}} + k_2(\theta)C_B\Delta H_{R_{BC}} + k_3(\theta)c_A^2\Delta H_{R_{AD}}\right] + \frac{\dot{V}}{V_R}(\theta_0 - \theta) \\ &+ \frac{k_W A_R}{\rho C_P V_R}(\theta_K - \theta) \end{aligned} \tag{3.2}$$

Where, $\Delta H_{R_{ij}}$ are different reaction enthalpies (negative for exothermal reaction) and θ_0 is the temperature of the inlet stream. The temperature θ_K of the reactor coolant from which a certain amount of heat, Q_K, is removed by an external heat exchanger is given by –

$$\frac{d\theta_K}{dt} = \frac{1}{m_K C_{P_K}}\left[\dot{Q}_K - k_W A_R(\theta_K - \theta)\right] \tag{3.3}$$

Here, k_W stands for the heat transfer coefficient, A_R for the cooling jacket's surface area, and m_K for the coolant's mass. In this article, we analyze a scenario in which coolant dynamics (3.3) may be disregarded and the cooling rate continuously takes the value at the standard operation point. As a result, the model is simplified to an unstable third order nonlinear dynamical system, which is characterized by equations (3.l) and (3.2). In (3.2), we replace –

$$k_W A_R(\theta_K - \theta) = \overline{\dot{Q}_K}$$

And reduce it to –

$$\frac{d\theta}{dt} = -\frac{1}{\rho C_P}\left[k_1(\theta)C_A\Delta H_{R_{AB}} + k_2(\theta)C_B\Delta H_{R_{BC}} + k_3(\theta)c_A^2\Delta H_{R_{AD}} - \frac{\overline{\dot{Q}_K}}{V_R}\right] + \frac{\dot{V}}{V_R}(\theta_0 - \theta) \tag{3.4}$$

Now, according to Arrhenius' equation, the rate coefficients k_1, k_2 and k_3 are dependent on the reaction temperature as follows –

$$k(\theta) = k_0 * exp\left(\frac{-E_A}{R(\theta + 273.15)}\right) \tag{3.5}$$

Incremental approaches were used to obtain the reaction enthalpies [8] and the parameters k_0 and E_A from the literature that was accessible [7]. However, the precision of all parameters is only fairly determined. Table-1 below provides the parameters for standard operating circumstances.

Table 3.1: Model parameters and operating conditions

$k_{0_{AB}} = 1.287 * 10^{12}\ h^{-1}$	$k_{0_{BC}} = 1.287 * 10^{12}\ h^{-1}$
$k_{0_{AD}} = 9.043 * 10^{9}\ L.(mol.h)^{-1}$	$E_{A_{AB}}/R = -9758.3\ K$
$E_{A_{BC}}/R = -9758.3\ K$	$E_{A_{AD}}/R = -8560\ K$
$\Delta H_{R_{AB}} = 4.2\ kJ/mol$	$\Delta H_{R_{BC}} = -11\ kJ/mol$
$\Delta H_{R_{AD}} = -41.85\ kJ/mol$	$\rho = 0.9342\ kg.L^{-1}$
$C_P = 3.01\ kJ/(kg.K)$	$k_W = 4032\ kJ.(h.m^2.K)^{-1}$
$A_R = 0.215\ m^2$	$c_{A0} = 5\ mol.L^{-1}$
$\theta_0 = 403.15\ K$	

3.3 State-Space Representation

First, the nominal values for the essentials process variables are calculated around the equilibrium point and hence, tabulated as follows:

Table 3.2: Equilibrium point specifications

$\overline{k_1} = 50.2\ h^{-1}$	$\overline{k_2} = 50.2\ h^{-1}$
$\overline{k_3} = 6.693\ L.(mol.h)^{-1}$	$\overline{c_A} = 1.25\ mol.L^{-1}$
$\overline{c_B} = 0.9\ mol.L^{-1}$	$\bar{\theta} = 407.15\ K$
$\bar{u} = 19.5218\ h^{-1}$	

For control application to the CSTR, we shall proceed with the State-Space model of the entire system. Now, let us define the state-space variables as follows:

$$x_1 = c_A$$
$$x_2 = c_B$$
$$x_3 = \theta$$

Therefore, we can reformulate the differential equations (3.1) and (3.4) as follows:

$$\left.\begin{aligned} \dot{x_1} &= u.(c_{A0} - x_1) - k_1(x_3).x_1 - k_3(x_3).x_1^2 \\ \dot{x_2} &= -u.x_2 + k_1(x_3).x_1 - k_2(x_3).x_2 \\ \dot{x_3} &= -\frac{1}{\rho C_P}\left[k_1(x_3).\Delta H_{R_{AB}}.x_1 + k_2(x_3).\Delta H_{R_{BC}}.x_2 + k_3(x_3).\Delta H_{R_{AD}}.x_1^2 - \frac{\overline{\dot{Q}_K}}{V_R}\right] + u(\theta_0 - x_3) \end{aligned}\right\}$$

(3.6)

Applying Jacobian Linearization technique around a standard operating equilibrium point, we can simplify equation (3.6) as follows –

$$\dot{x_1} = \left(-\bar{u} - \overline{k_1} - 2\overline{k_3}\overline{x_1}\right)x_1 + \left(-\overline{\frac{\partial k_1}{\partial x_3}}\overline{x_1} - \overline{\frac{\partial k_3}{\partial x_3}}\overline{x_1}^2\right)x_3 + (\overline{c_{A0}} - \overline{x_1})u$$

$$\dot{x_2} = \overline{k_1}x_1 + \left(-\bar{u} - \overline{k_2}\right)x_2 + \left(\overline{\frac{\partial k_1}{\partial x_3}}\overline{x_1} - \overline{\frac{\partial k_2}{\partial x_3}\overline{x_2}}\right)x_3 + (-\overline{x_2})u$$

$$\begin{aligned} \dot{x_3} = -\frac{1}{\rho C_P}\Bigg[&.\left(\Delta H_{R_{AB}}\overline{k_1} + 2\overline{k_3}\Delta H_{R_{AD}}\overline{x_1}\right)x_1 + \overline{k_2}\Delta H_{R_{BC}}x_2 \\ &+ \left(\overline{\frac{\partial k_1}{\partial x_3}}\overline{x_1}\Delta H_{R_{AB}} + \overline{\frac{\partial k_2}{\partial x_3}}\overline{x_2}\Delta H_{R_{BC}} + \overline{\frac{\partial k_3}{\partial x_3}}\overline{x_1}^2\Delta H_{R_{AD}}\right)x_3\Bigg] - \bar{u}x_3 \\ &+ u(\theta_0 - \overline{x_3}) \end{aligned}$$

(3.7)

Now, putting all the nominal values into set of equations (3.6), we obtain the reduced state-space equations as:

$$\left.\begin{aligned} \dot{x_1} &= -86.4533x_1 - 4.23375x_3 + 3.75u \\ \dot{x_2} &= 50.199x_1 - 69.7208x_2 + 1.03425x_3 - 0.9u \\ \dot{x_3} &= 174.0375x_1 + 196.358x_2 - 6.599x_3 - 4u \end{aligned}\right\}$$

(3.7)

We have assumed that, the product concentration $c_B(= x_2)$ is to be controlled here. The inlet flow, normalized by the reactor volume, i.e. the dilution rate *u* is considered to be the only manipulated variable which can vary.

Hence, the State-Space representation of the system can be obtained as –

$$\begin{bmatrix}\dot{x_1}\\ \dot{x_2}\\ \dot{x_3}\end{bmatrix} = \begin{bmatrix}-86.4533 & 0 & -4.23375\\ 50.199 & -69.7208 & 1.03425\\ 174.0375 & 196.358 & -6.599\end{bmatrix}\begin{bmatrix}x_1\\ x_2\\ x_3\end{bmatrix} + \begin{bmatrix}3.75\\ -0.9\\ -4\end{bmatrix}u$$

(3.8)

And the output *y* is expressed in terms of state variables as –

$$y = [0 \quad 1 \quad 0]\begin{bmatrix}x_1\\ x_2\\ x_3\end{bmatrix}$$

(3.9)

Clearly, the A,B,C and D matrices of the state pace model for the system are –

$$A = \begin{bmatrix}-86.4533 & 0 & -4.23375\\ 50.199 & -69.7208 & 1.03425\\ 174.0375 & 196.358 & -6.599\end{bmatrix}, \quad B = \begin{bmatrix}3.75\\ -0.9\\ -4\end{bmatrix}$$

$$C = [0 \quad 1 \quad 0], \quad D = 0$$

(3.10)

3.4 Transfer function models

3.4.1 Continuous time model

Now, we can obtain the continuous-time transfer function model of the system from the state-space model by the relation -

$$G(s) = [C(sI - A)^{-1}B + D]$$

Therefore, putting the values from the relations in (3.10), we get,

$$G(s) = \frac{-0.9s^2 + 100.4s + 1233}{s^3 + 162.8s^2 + 7592s + 115323}$$

(3.11)

(3.11) represents the transfer function model of the system in continuous time domain. This, when represented in pole-zero form, yields –

$$G(s) = \frac{-0.9(s - 122.7)(s + 11.17)}{(s + 96.46)(s^2 + 66.31s + 1196)}$$

(3.12)

Clearly, it contains a Non-Minimum Phase zero at $s = 122.7$, which results in the initial negative kick in the step response, as shown in Fig. 3.3. The root locus (Fig. 3.2) for this as well as the step response (Fig. 3.3) are shown below:

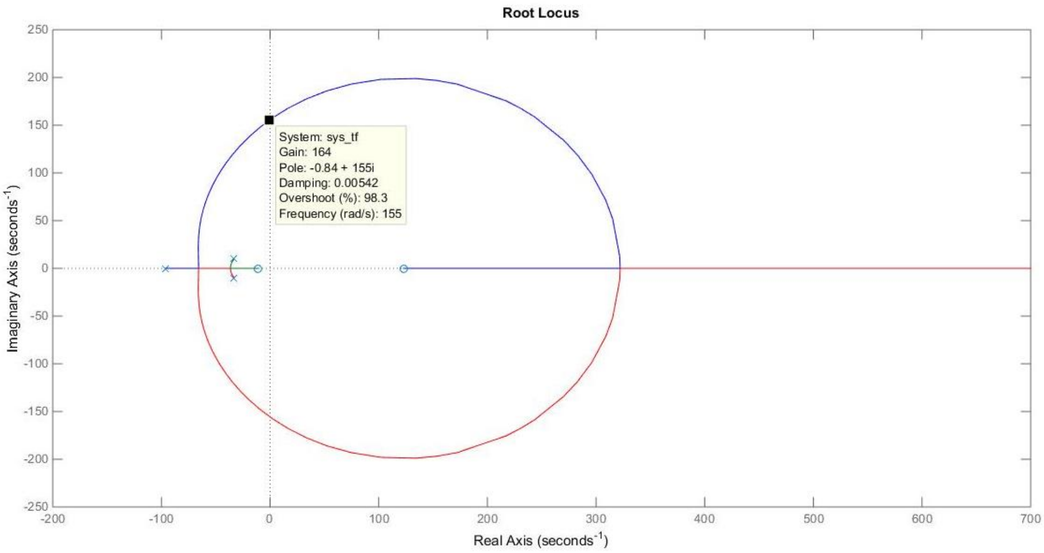

Fig. 3.2: Root locus of the continuous time model of CSTR

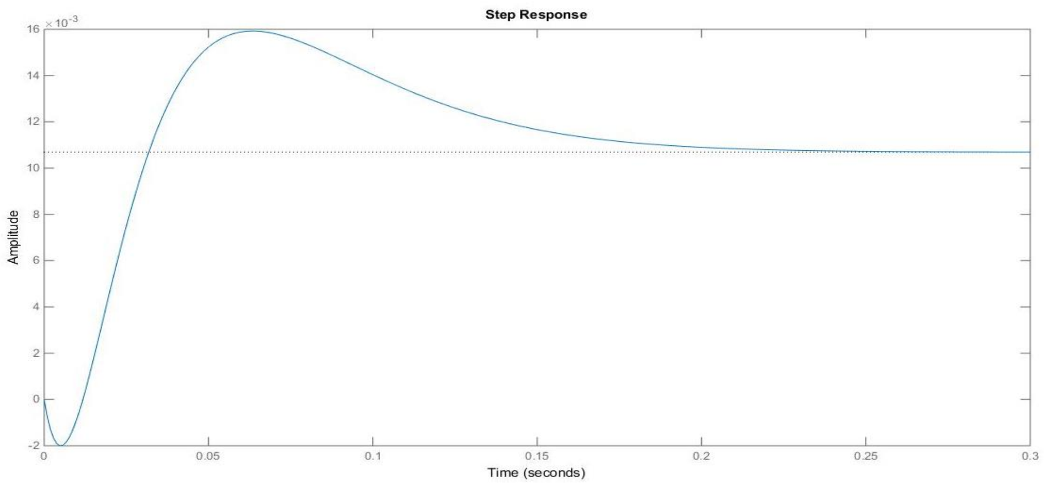

Fig. 3.3: Step response of the continuous time model of CSTR

3.4.2 Discrete time model

Since we are looking forward to apply the periodic control in discrete time domain only, hence we need to discretize the continuous time model of the CSTR. For continuous to discrete transformation, we shall proceed by Zero Order Hold method given as –

$$G(z) = (1 - z^{-1}).Z\left[\frac{G(s)}{s}\right]$$

For our system, we can note from the step response of continuous time model that, the peak of the non-minimum phase undershoot occurs at $t = 0.005\ s$. Hence, we shall consider the sampling time for discretization to be $T = 0.005\ s$. Applying this formula, we arrive at the discrete time transfer function or the Pulse Transfer Function model of the CSTR, with sampling time, $T = 0.005\ s$. as –

$$G(z) = \frac{-0.002002z^2 + 0.005808z - 0.003702}{z^3 - 2.31z^2 + 1.763z - 0.4431} \tag{3.13}$$

Similar to the case in continuous domain, the transfer function in pole-zero form is obtained as –

$$G(z) = \frac{-0.002002(z - 1.956)(z - 0.9457)}{(z - 0.6173)(z^2 - 1.692z + 0.7178)} \tag{3.14}$$

Here again, the NMP zero is found at $z = 1.956$, resulting in the initial negative kick in step response as shown in Fig. 3.5. The root locus and step response of the discrete time transfer function $G(z)$ are as follows –

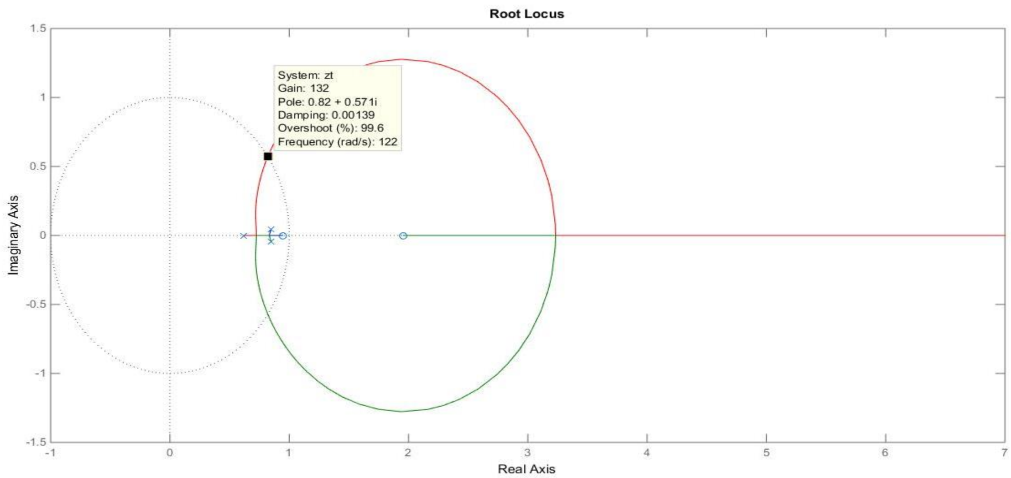

Fig. 3.4: Root locus of the discrete time model of CSTR

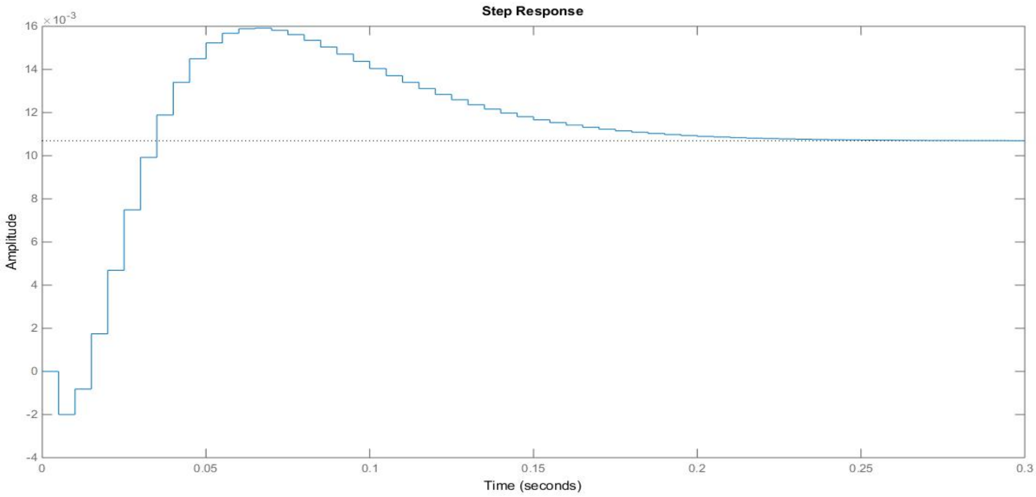

Fig. 3.5: Step response of the discrete time model of CSTR

Chapter 4

2-Periodic Controller for CSTR – Design, Simulation and Analysis

4.1 Drawbacks of LTI Control

4.1.1 LTI Deadbeat Controller

The CSTR model that we are dealing with has transfer function –

$$G(z) = \frac{-0.002002z^2 + 0.005808z - 0.003702}{z^3 - 2.31z^2 + 1.763z - 0.4431} \tag{4.1}$$

It has already been established in literature that LTI controller are not quite satisfactory for systems with Non-Minimum Phase zeros. However, we shall first examine this fact in our case. For that, we try to design an LTI Deadbeat controller. In order to design the LTI deadbeat controller, we must solve the famous Diophantine equation,

$$a(z)x(z) + b(z)y(z) = z^l$$

Subject to the constraints, $l \geq 2n - 1$ and $l = n + i$.

Where, $n =$ plant order, $i =$ controller $\left[C(z) = \frac{y(z)}{x(z)}\right]$ order.

In our case, $n = 3$. So, $l \geq 5$. Taking, $l = 5$, we get, $i = 2$.

Solving the Diophantine equation, we can find out the controller transfer function as –

$$C(z) = \frac{-92019.4z^2 + 128231z - 44194.8}{z^2 - 181.8838z + 369.2332} \tag{4.2}$$

The root locus for the controlled system is found as –

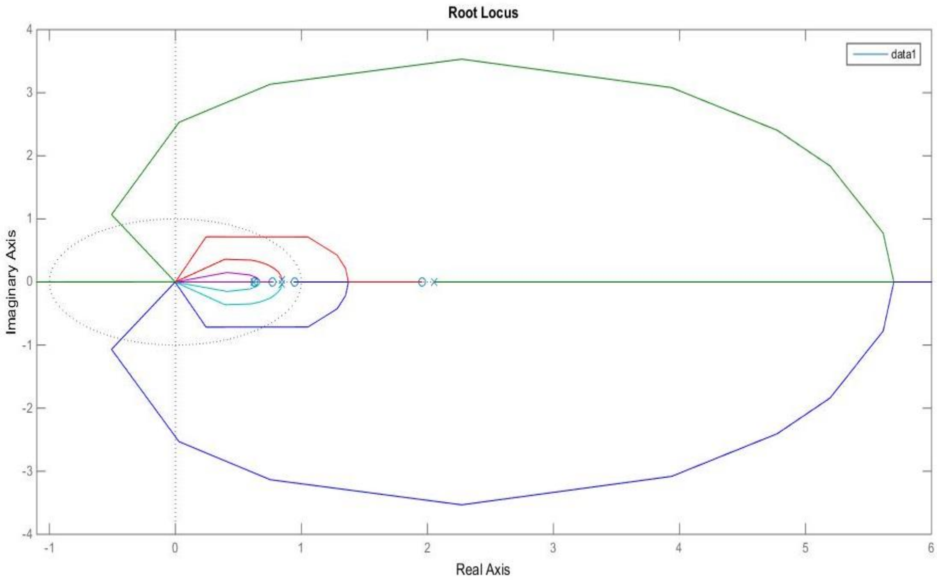

Fig. 4.1: Root locus of CSTR using discrete time LTI Deadbeat controller

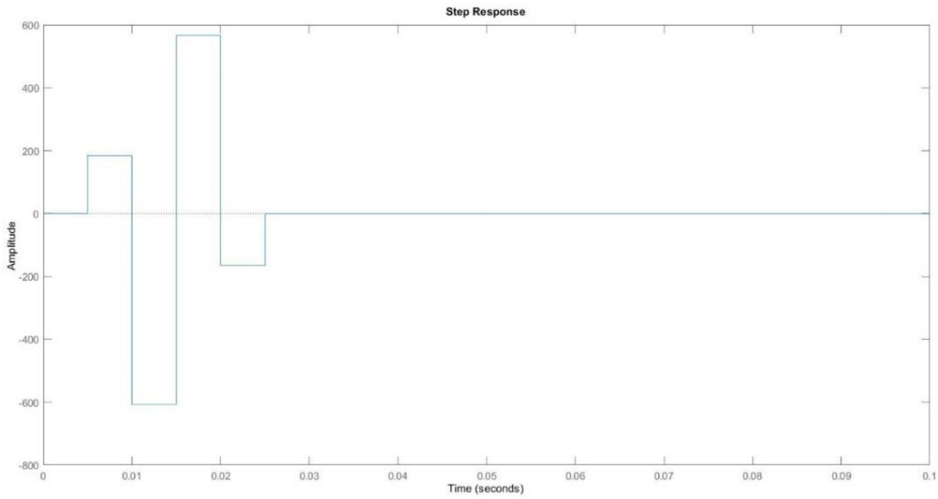

Fig. 4.2: Step response of CSTR using discrete time LTI Deadbeat controller

Although, the settling time is quite satisfactory (0.025 *s.*) here but the control effort and the overshoots are unacceptable. Hence, the LTI deadbeat controller is not practically realizable. Next, we shall examine the case of LTI Discrete PID controller for the CSTR. 2-periodic compensated deadbeat controller for the CSTR.

4.1.2 Discrete PID Controller

Here, we shall use pole placement method of PID controller design for our plant. The standard parallel form of PID controller is used here as follows –

$$C_{PID} = K_P + K_D \frac{z-1}{T} + K_I \frac{T}{z-1}$$

Where, sampling time, $T = 0.005\ s$.

Considering expected overshoot $\leq 20\%$ and settling time $\leq 0.3\ s$., upon calculation, we find the PID controller parameters as: $K_P = 26.47$, $K_D = 0.0835$ and $K_I = 2195$. Hence, the controller transfer function becomes –

$$C_{PID} = \frac{16.708(z^2 - 0.4157z + 0.0726)}{(z-1)} \tag{4.3}$$

The corresponding root locus and step response are as follows –

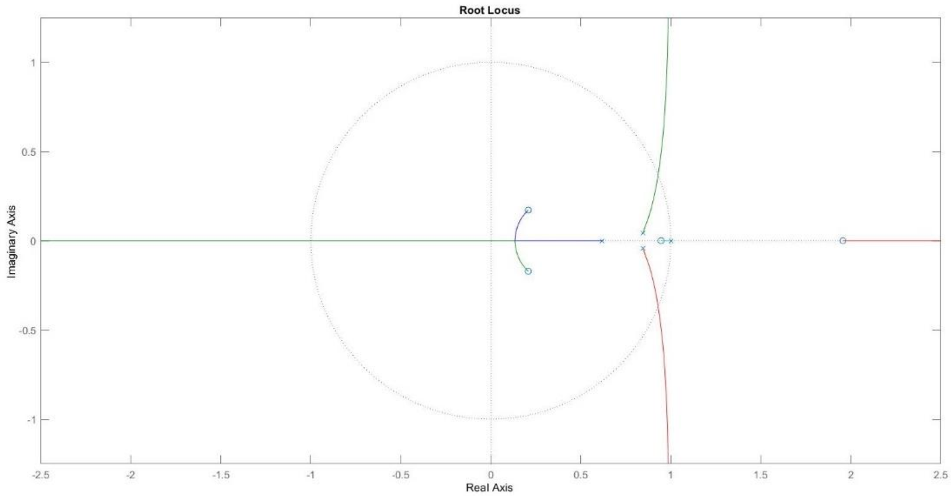

Fig. 4.3: Root locus of PID controlled CSTR plant.

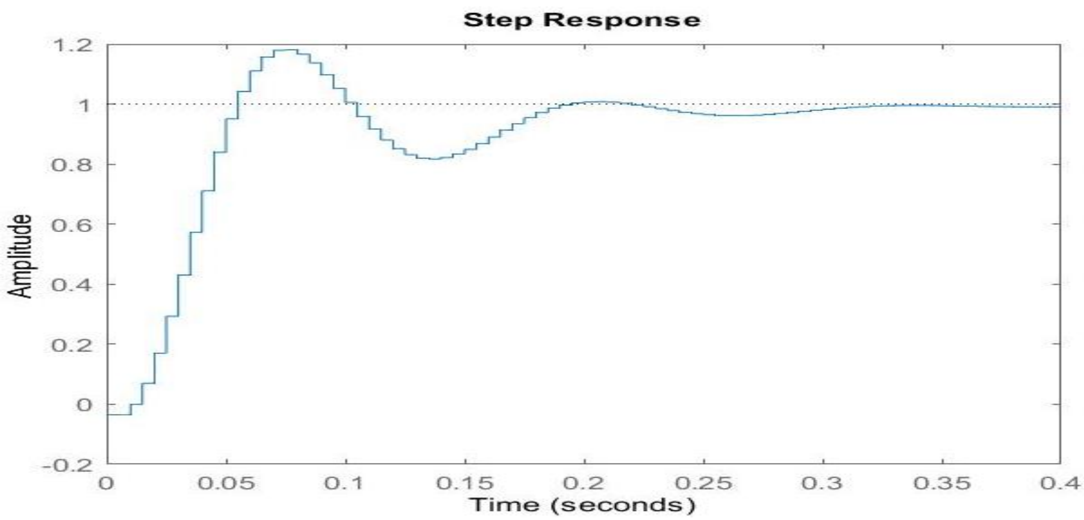

Fig. 4.4: Step response of PID controlled CSTR plant

We find that the overshoot and settling time are as expected. The Gain Margin is found to be $(k_{max}/k_{min}) = 2.83/.002 = 1415$. Henceforth, we shall consider this configuration to be our benchmark for comparative studies.

4.2 Design of 2-periodic Deadbeat Controller

4.2.1 Pole-Zero Placement

From the transfer function shown in (4.1), we can clearly write –

$$\left.\begin{array}{c} b(z) = -0.002002z^2 + 0.005808z - 0.003702 \\ a(z) = z^3 - 2.31z^2 + 1.763z - 0.4431 \end{array}\right\} \tag{4.4}$$

We shall now design a 2-periodic controller of the form as shown in Fig. 2.1. The order of the controller is decided by equation (2.17) as (since relative order of the plant is 1) –

$$m = (n-1) = (3-1) = 2$$

Referring to the characteristic equation (2.14), there would be 5 closed-loop poles and 4 loop zeros in the time-lifted domain. Besides placing all these poles at origin, we would now like to relocate the loop zeros as well (if possible, at the origin) to improve the loop robustness for deadbeat control. It would be convenient to effect as many stable pole-zero cancellation as possible while making these choices.

First, we choose 2 of the loop zeros and the 2 controller poles at the origin, thus ensuring 2 of the closed loop poles remain at origin. The other 2 loop zeros then would have to be placed at $z^2 = (0.2928 \pm 0.1509i)$ such that the 2 plant poles also end up at the origin in closed loop.

Then the corresponding pole and zero polynomials in the lifted domain becomes –

$$\left.\begin{array}{c} \hat{A}(z^2) = a^+a^- = -z^6 + 1.8098z^4 - 1.0598z^2 + 0.1964 \\ \hat{P}(z^2) = (-z^2).(-z^2) = z^4 \\ \hat{Z}(z^2) = z^4(-z^4 + 0.5856z^2 - 0.1085) \end{array}\right\} \tag{4.5}$$

Consequently, the effective loop transfer function becomes:

$$L(z^2) = \frac{k\hat{Z}(z^2)}{\hat{A}(z^2)\hat{P}(z^2)} = \frac{k(-z^4 + 0.5856z^2 - 0.1085)}{-z^6 + 1.8098z^4 - 1.0598z^2 + 0.1964} \tag{4.6}$$

The root locus for the loop transfer function is shown below:

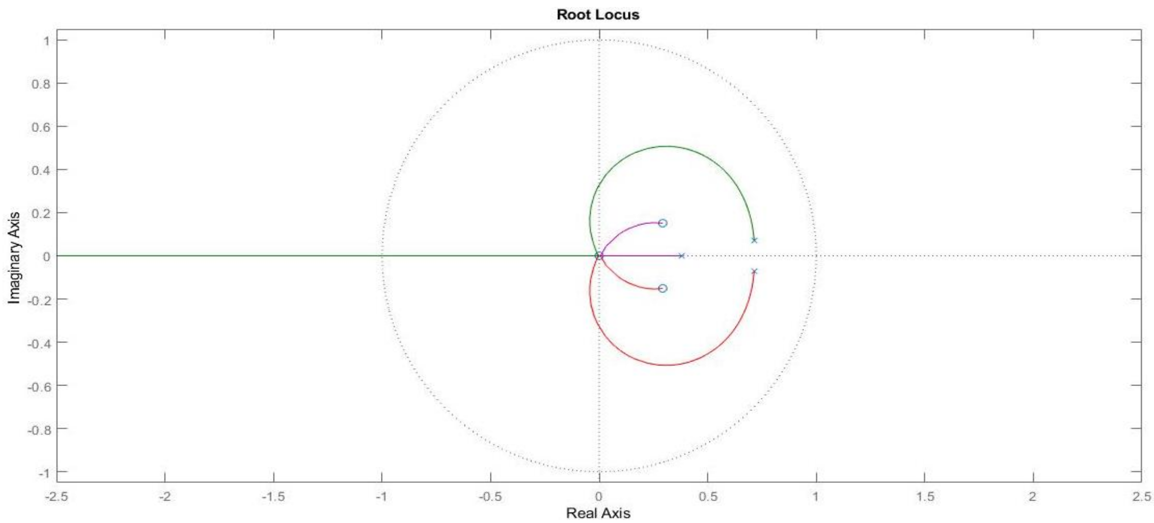

Fig. 4.5: Root locus of 2-periodically compensated deadbeat controlled CSTR

From the root locus, it follows that, the gain margin of the system for this configuration is 1220. Now, a loop-gain of $k = 1.8098$ would yield the closed loop characteristic equation to be:

$$\Delta_{CL} := -z^{10} = 0$$

Now, for the given system, following equation (2.18)

$$\begin{aligned}\hat{B}(z) \triangleq \boldsymbol{a}^{+}\boldsymbol{b}^{-} &= \left(z^3 - 2.31z^2 + 1.763z - 0.4431\right) \\ &\quad * \left(-0.002002z^2 - 0.005808z - 0.003702\right) \\ &= \left(-2.002z^5 - 1.1843z^4 + 6.1843z^3 - 0.7985z^2 - 3.9522z \right. \\ &\quad \left. + 1.6406\right) * 10^{-3}\end{aligned}$$

Hence,

$$\left.\begin{aligned}B_e(z^2) &= -1.1843z^4 - 0.7985z^2 + 1.6406 \\ B_d(z^2) &= -2.002z^4 + 6.1843z^2 - 3.9522\end{aligned}\right\} \tag{4.7}$$

Let us assume that, for $m = 2$,

$$\hat{L}(z) = \left[\hat{l}_0 + \hat{l}_1 z + \hat{l}_2 z^2 + \hat{l}_3 z^3 + \hat{l}_4 z^4\right]$$

So,

$$\left.\begin{aligned}L_e(z^2) &= \hat{l}_0 + \hat{l}_2 z^2 + \hat{l}_4 z^4 \\ L_d(z^2) &= \hat{l}_1 + \hat{l}_3 z^2\end{aligned}\right\} \tag{4.8}$$

By virtue of equation (2.20), we can form the Sylvester matrix as shown in (2.21) from (4.5), (4.7) and (4.8) by comparing the like powers of z^2 in both sides.

Therefore, we solve the Sylvester matrix (2.21) for the intermediate polynomial, $\hat{L}(z)$, which is obtained as –

$$\hat{L}(z) = -2483.48z^4 + 1719.21z^3 + 6114.37z^2 + 2538.24z$$

Or,

$$\hat{L}(z) = -2483.48z(z - 2.098)(z + 0.7857)(z + 0.6201) \tag{4.9}$$

4.2.2 Controller Parameters

Now, as discussed in the section 2.8.2, we shall calculate the 2-periodic controller parameters for each of the 4 cases.

4.2.2.1 Case I: $\boldsymbol{Q_0^+ = Q_1^-}$

From equation (4.9), we assume that,

$$\left.\begin{aligned} Q_0^- &\triangleq -2483.48z(z - 2.098) = -2483.48z^2 + 5210.29z \\ (P_0^+ - P_1^-) &\triangleq \Gamma(z) = (z + 0.7857)(z + 0.6201) = z^2 + 1.4057z + 0.4872 \end{aligned}\right\} \tag{4.10}$$

Therefore, solving the Sylvester matrix shown in (2.24) and following subsequent steps mentioned in section 2.8.2.1, we obtain the 2-periodic controller parameters as –

$\boldsymbol{Q_0(z)}$	$\boldsymbol{Q_1(z)}$	$\boldsymbol{P_0(z)}$	$\boldsymbol{P_1(z)}$
$d_{2,0} = -2483.48$	$d_{2,1} = -2483.48$	$c_{1,0} = 0.8761$	$c_{1,1} = 0.5296$
$d_{1,0} = -5210.29$	$d_{1,1} = 5210.29$	$c_{0,0} = 0.2436$	$c_{0,1} = -0.2436$
$d_{0,0} = 0$	$d_{0,1} = 0$		

Table 4.1: 2-periodic deadbeat controller parameters for Case – I

Hence, the 2-periodic controller transfer function is obtained as –

$$C(z, N) = \frac{(-2483.48z^2 - 5210.29z) + (-1)^N(-2483.48z^2 + 5210.29z)}{(z^2 + 0.8761z + 0.2436) + (-1)^N(0.5296z - 0.2436)} \tag{4.11}$$

The controller is realized using Controller Canonical Form as follows –

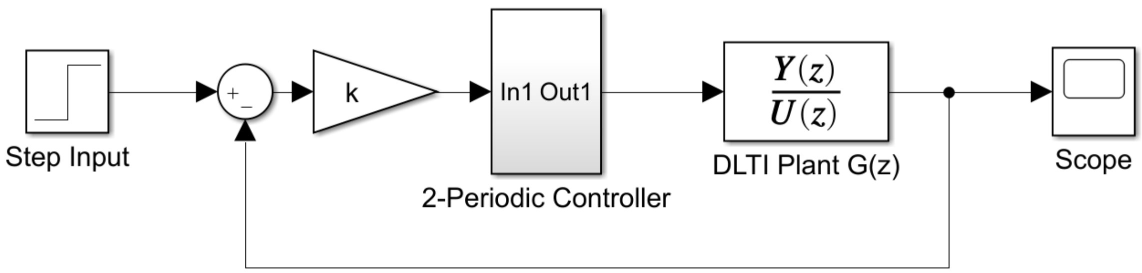

Fig. 4.6: Block diagram of the closed loop system

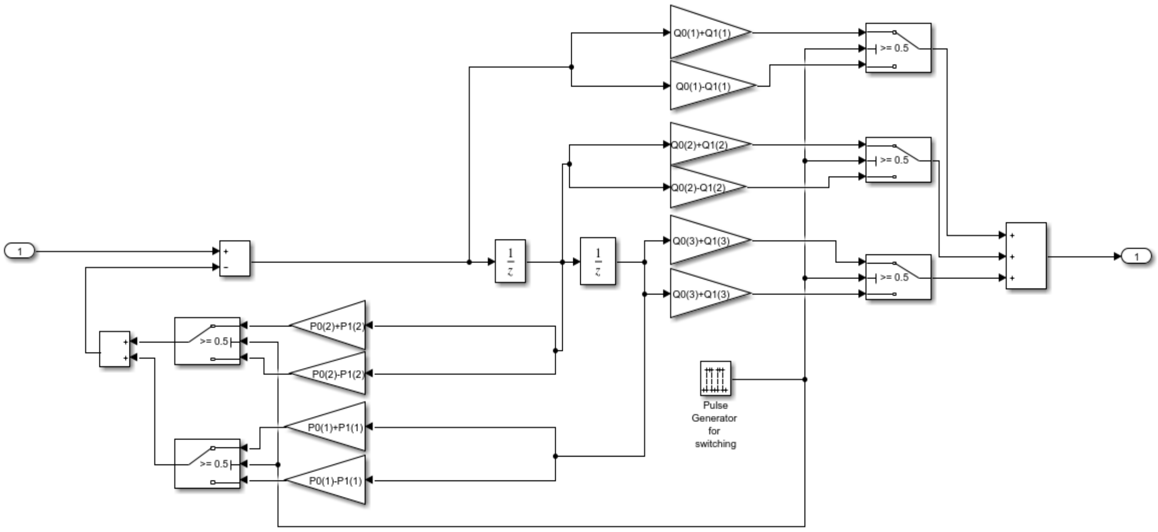

Fig. 4.7: 2-periodic controller in CCF with switching

The step response of the CSTR system with 2-periodically compensated deadbeat controller vide case-I is obtained as –

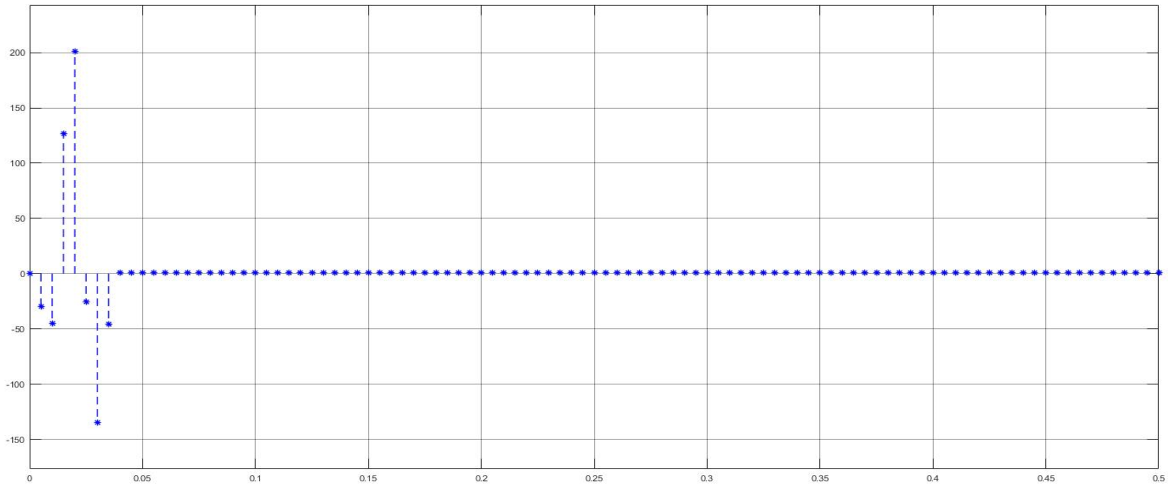

Fig. 4.8: Step response of 2-periodically compensated deadbeat controlled CSTR, Case – I

Clearly, the settling time is well within limit but the response has high overshoots and undershoots. However, the overshoots and undershoots have significantly improved compare to the LTI deadbeat controller case.

4.2.2.2 Case II: $\boldsymbol{Q_0^+ = -Q_1^-}$

From equation (4.9), we assume, by virtue of the discussion in section 2.8.2.2,

$$\left.\begin{array}{r} Q_0^- \triangleq -2483.48z(z-2.098) = -2483.48z^2 + 5210.29z \\ (P_0^+ + P_1^-) \triangleq \Gamma(z) = (z+0.7857)(z+0.6201) = z^2 + 1.4057z + 0.4872 \end{array}\right\} \tag{4.12}$$

Therefore, solving the Sylvester matrix shown in (2.24) and following subsequent steps mentioned in section 2.8.2.2, we obtain the 2-periodic controller parameters as –

$\boldsymbol{Q_0(z)}$	$\boldsymbol{Q_1(z)}$	$\boldsymbol{P_0(z)}$	$\boldsymbol{P_1(z)}$
$d_{2,0} = -2483.48$	$d_{2,1} = 2483.48$	$c_{1,0} = 0.8761$	$c_{1,1} = -0.5296$
$d_{1,0} = -5210.29$	$d_{1,1} = -5210.29$	$c_{0,0} = 0.2436$	$c_{0,1} = 0.2436$
$d_{0,0} = 0$	$d_{0,1} = 0$		

Table 4.2: 2-periodic deadbeat controller parameters for Case – II

The step response of the CSTR system with 2-periodically compensated deadbeat controller vide case-II is obtained as –

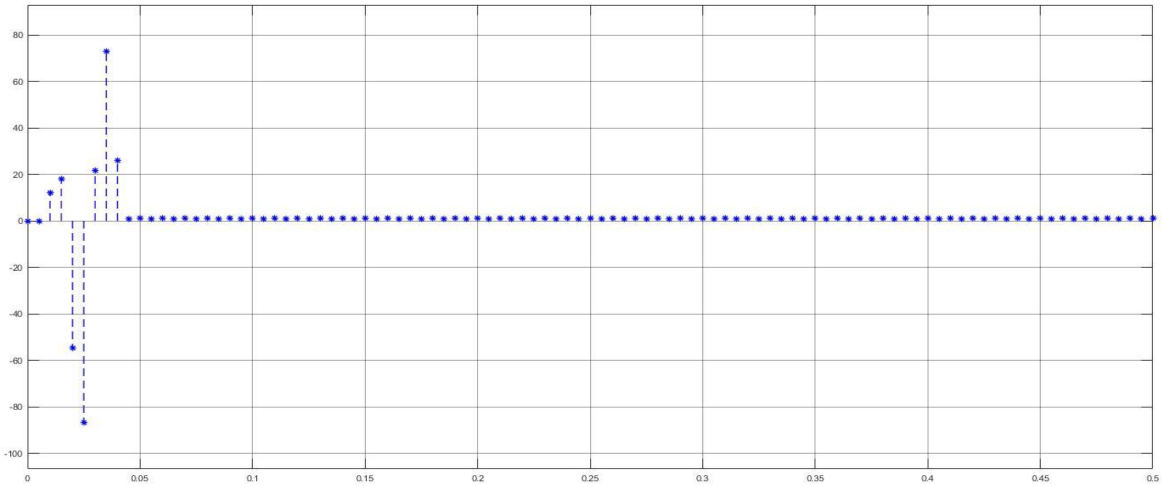

Fig. 4.9: Step response of 2-periodically compensated deadbeat controlled CSTR, Case – II

Similar to Case-I, the settling time is well within limit, but the response has high overshoots and undershoots. However, the overshoots and undershoots have significantly improved compared to Case-I.

4.2.2.3 Case III: $\boldsymbol{Q_0^+ = Q_1^+}$ & Case IV: $\boldsymbol{Q_0^+ = -Q_1^+}$

As discussed in the section 2.8.2.3 and 3.8.2.4, in order to design the controller for cases - III & IV, we need to satisfy the following condition, from equation (2.27),

$$Q_i^+ = (-1)^m Q_i^-, \quad \text{for } i = 0{,}1$$

Now, clearly in our case, this condition does not hold true. Hence, we cannot design the 2-periodic controller for cases - III & IV.

4.3 Design of generic 2-periodic controller

In the previous section, we have seen that, by deploying 2-periodic deadbeat controller, we can substantially improve the overshoots and undershoots with a well satisfactory settling time. Here, we shall try to improve on the transient overshoots further by the expense of settling time.

4.3.1 Pole-Zero Placement

Now, we shall place a total of 4 loop zeros and 2 controller poles at will to obtain satisfactory closed loop step response. This is done by trial-and-error method, keeping in mind to have as many pole-zero cancellation as possible in the closed loop.

Hence, we choose the lifted domain polynomials as follows –

$$\left.\begin{array}{c}\hat{A}(z^2) = a^+a^- = -z^6 + 1.8098z^4 - 1.0598z^2 + 0.1964 \\ \hat{P}(z^2) = z^4 - 1.66z^2 + 0.667 \\ \hat{Z}(z^2) = -0.0264z^8 + 0.0481z^6 - 0.0282z^4 + 0.0052z^2\end{array}\right\} \tag{4.13}$$

The root locus for the same is as shown:

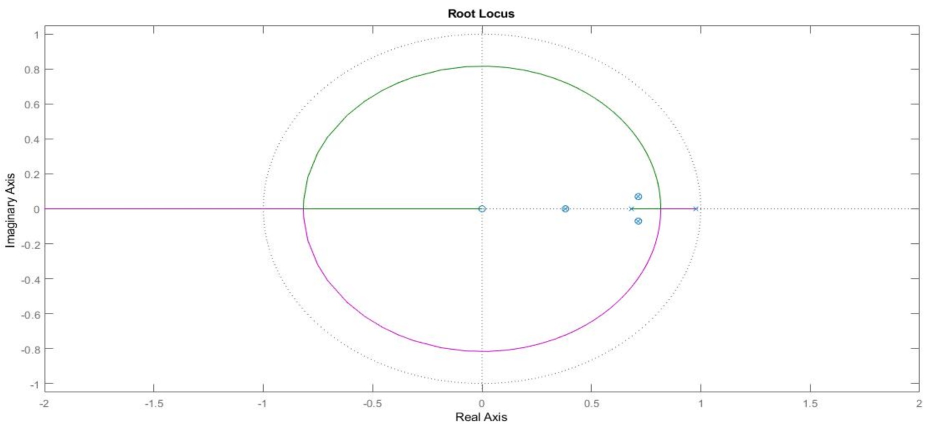

Fig. 4.10: Root locus of generic 2-periodically compensated CSTR

The loop GM for this case is found to be 1662. By virtue of equation (2.20), we can form the Sylvester matrix as shown in (2.21) from (4.13), (4.7) and (4.8) by comparing the like powers of z^2 in both sides. Therefore, we solve the Sylvester matrix (2.21) for the intermediate polynomial, $\hat{L}(z)$, which is obtained as –

$$\hat{L}(z) = 86.091z^4 + 198.8518z^3 + 151.7472z^2 + 38.1505z$$

Or,

$$\hat{L}(z) = 86.091z(z^2 + 1.6924z + 0.7178)(z + 0.6173) \tag{4.14}$$

4.3.2 Controller Parameters

Now, as discussed in the section 2.8.2, we shall calculate the 2-periodic controller parameters for each of the 4 cases.

4.3.2.1 Case I: $Q_0^+ = Q_1^-$

From equation (4.14), we assume that,

$$\left.\begin{aligned} Q_0^- &\triangleq 86.091z(z + 0.6173) = 86.091z^2 + 53.1481z \\ (P_0^+ - P_1^-) &\triangleq \Gamma(z) = (z^2 + 1.6924z + 0.7178) \end{aligned}\right\} \tag{4.15}$$

Therefore, solving the Sylvester matrix shown in (2.24) and following subsequent steps mentioned in section 2.8.2.1, we obtain the 2-periodic controller parameters as –

$\boldsymbol{Q_0(z)}$	$\boldsymbol{Q_1(z)}$	$\boldsymbol{P_0(z)}$	$\boldsymbol{P_1(z)}$
$d_{2,0} = 86.091$	$d_{2,1} = 86.091$	$c_{1,0} = 1.8232$	$c_{1,1} = -0.1308$
$d_{1,0} = -53.1481$	$d_{1,1} = 53.1481$	$c_{0,0} = 0.8235$	$c_{0,1} = 0.1057$
$d_{0,0} = 0$	$d_{0,1} = 0$		

Table 4.3: Generic 2-periodic controller parameters for Case – I

Hence, the 2-periodic controller transfer function is obtained as –

$$C(z, N) = \frac{(86.091z^2 - 53.1481z) + (-1)^N(86.091z^2 + 53.1481z)}{(z^2 + 1.8232z + 0.8235) + (-1)^N(-0.1308z + 0.1057)} \tag{4.16}$$

The step response of the CSTR system with 2-periodically compensated controller vide case-I is obtained as –

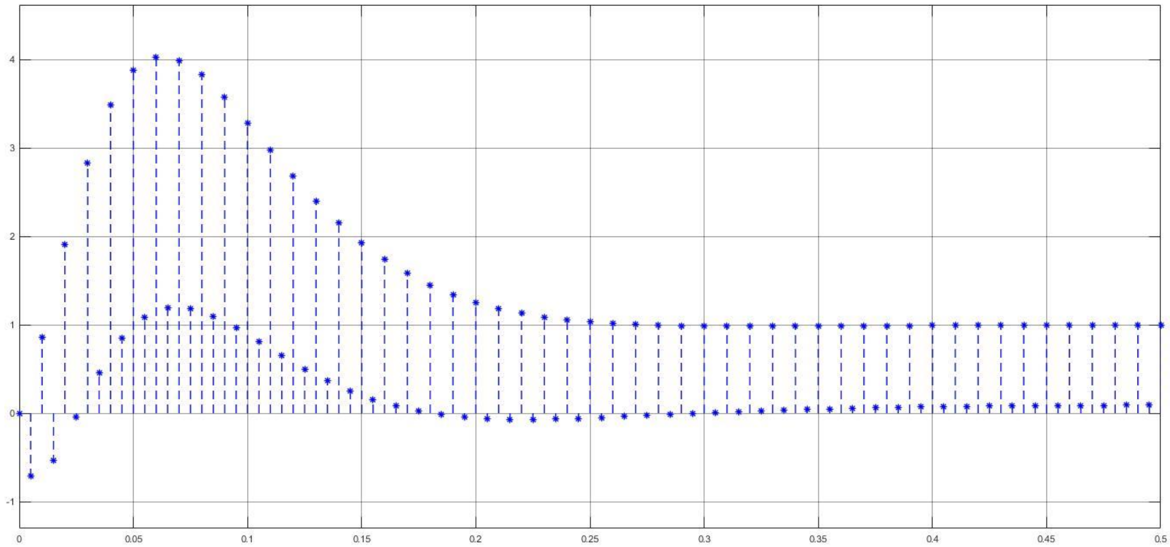

Fig. 4.11: Step response of generic 2-periodically controlled CSTR, Case – I

Clearly, here the step response shows that the overshoots and undershoots have gone down substantially compared to the deadbeat 2-periodic control. Although the settling time has been compromised a bit but it is not unacceptable.

4.3.2.2 Case II: $\boldsymbol{Q_0^+ = -Q_1^-}$

From equation (4.14), we assume that,

$$\left.\begin{array}{c} Q_0^- \triangleq 86.091z(z+0.6173) = 86.091z^2 + 53.1481z \\ (P_0^+ + P_1^-) \triangleq \Gamma(z) = (z^2 + 1.6924z + 0.7178) \end{array}\right\} \tag{4.17}$$

Therefore, solving the Sylvester matrix shown in (2.24) and following subsequent steps mentioned in section 2.8.2.1, we obtain the 2-periodic controller parameters as –

$\boldsymbol{Q_0(z)}$	$\boldsymbol{Q_1(z)}$	$\boldsymbol{P_0(z)}$	$\boldsymbol{P_1(z)}$
$d_{2,0} = 86.091$	$d_{2,1} = -86.091$	$c_{1,0} = 1.8232$	$c_{1,1} = 0.1308$
$d_{1,0} = -53.1481$	$d_{1,1} = -53.1481$	$c_{0,0} = 0.8235$	$c_{0,1} = -0.1057$
$d_{0,0} = 0$	$d_{0,1} = 0$		

Table 4.4: Generic 2-periodic controller parameters for Case – II

Hence, the 2-periodic controller transfer function is obtained as –

$$C(z,N) = \frac{(86.091z^2 - 53.1481z) + (-1)^N(-86.091z^2 - 53.1481z)}{(z^2 + 1.8232z + 0.8235) + (-1)^N(0.1308z - 0.1057)} \tag{4.18}$$

The step response of the CSTR system with 2-periodically compensated controller vide case-II is obtained as –

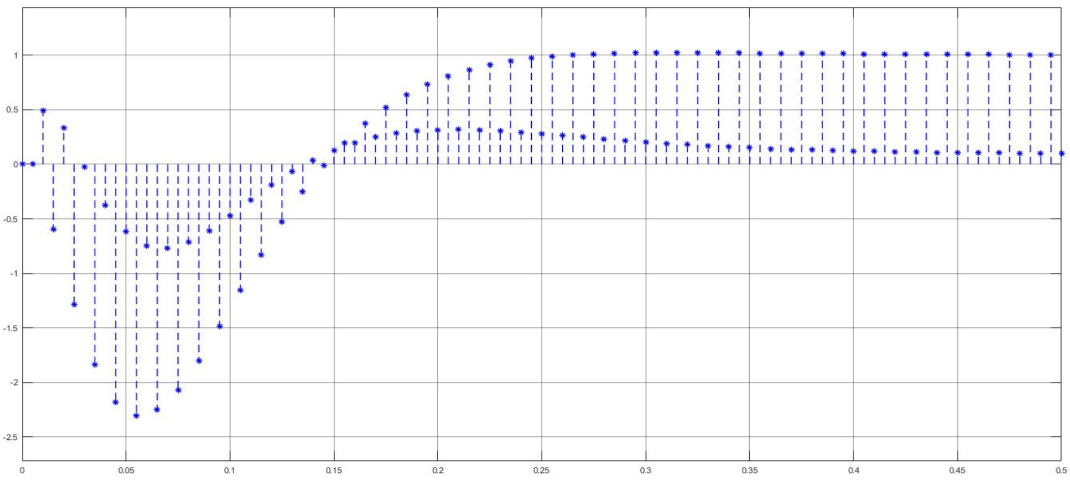

Fig. 4.12: Step response of generic 2-periodically controlled CSTR, Case – II

From Fig. 4.11 and 4.12, we can clearly see that, although the step responses are quite satisfactory, it contains steady-state ripples. To mitigate that, we shall employ the augmentations discussed in section 2.9.

4.4 2-Periodic Controller Design for Ripple-Free Steady-State Response

Since we have already established that, for the given system, only two types of controller configurations are possible, we shall check for each of the cases with the augmentations.

4.4.1 Augmentation with $(z+1)/z$

4.4.1.1 Pole-Zero Placement

With this augmentation, the plant transfer function becomes –

$$G(z) = \frac{b(z)}{a(z)} = \frac{-0.002002(z+1)(z-0.9457)(z-1.956)}{z(z-0.6173)(z^2-1.692z+0.7178)} \tag{4.19}$$

The controller order for this augmented plant will be $m = (n-1) = (4-1) = 3$. Hence, in the time-lifted domain, the no. of loop zeros will be 6 and closed loop poles will be 7. Out of this, we shall place 6 loop-zeros and 3 controller poles at will and check the responses. One such possible set of pole zero placement yields –

$$\left.\begin{array}{c}\hat{A}(z^2) = a^+a^- = z^8 - 1.8098z^6 + 1.0598z^4 - 0.1964z^2 \\ \hat{P}(z^2) = -(-z^2)^2(z^2 - 0.19) = -z^6 + 0.19z^4 \\ \hat{Z}(z^2) = -0.003(-z^2)^5(z^2 - 0.3811) = 0.003z^{12} - 0.0011z^{10}\end{array}\right\} \tag{4.20}$$

The root locus for the same is as shown below:

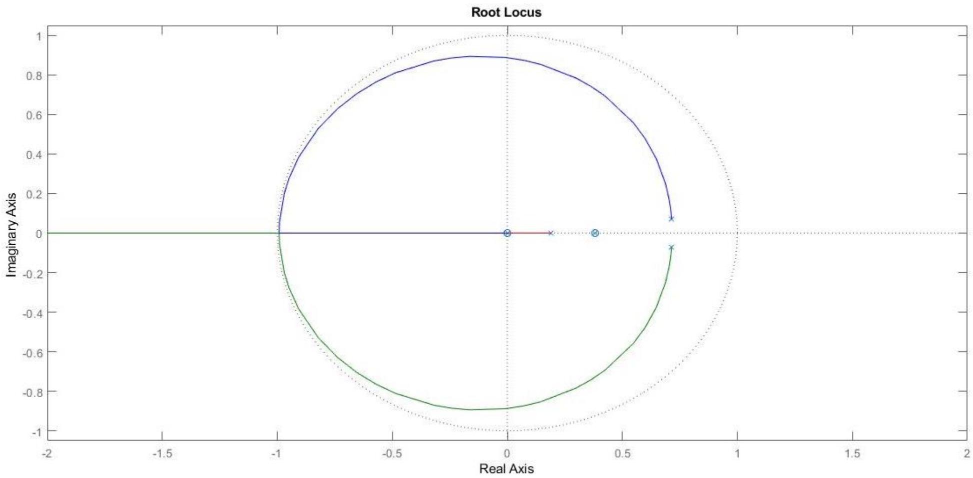

Fig. 4.13: Root locus of 2-periodic controller with Augmentation $(z+1)/z$ for CSTR

It is calculated from the root locus that, the loop GM for the augmented controller is 1750. By virtue of equation (2.20), upon solving the Sylvester matrix, we can find the intermediate polynomial as –

$$\hat{L}(z) = 89.5878z^6 + 37.3302z^5 - 245.3754z^4 - 275.5804z^3 - 80.8415z^2 \tag{4.21}$$

4.4.1.2 Controller Design: Case-I

From equation (4.21), we can segregate the roots of $\hat{L}(z)$ as follows –

$$\left.\begin{array}{c}Q_0^- \triangleq 89.5878z^3 + 55.3069z^2 \\ (P_0^+ - P_1^-) \triangleq \Gamma(z) = z^3 - 0.2007z^2 - 2.6151z - 1.4617\end{array}\right\} \tag{4.22}$$

Therefore, solving the Sylvester matrix shown in (2.24) and following subsequent steps mentioned in section 2.8.2.1, we obtain the 2-periodic controller parameters as –

$\boldsymbol{Q_0(z)}$	$\boldsymbol{Q_1(z)}$	$\boldsymbol{P_0(z)}$	$\boldsymbol{P_1(z)}$
$d_{3,0} = -89.5878$	$d_{3,1} = 89.5878$	$c_{2,0} = 1.7460$	$c_{2,1} = 1.9467$
$d_{2,0} = 55.3069$	$d_{1,1} = 55.3069$	$c_{1,0} = -0.2755$	$c_{1,1} = -2.3396$
$d_{1,0} = 0$	$d_{1,1} = 0$	$c_{0,0} = -0.7308$	$c_{0,1} = 0.7308$
$d_{0,0} = 0$	$d_{0,1} = 0$		

Table 4.5: 2-periodic controller parameters with Augmentation $(z+1)/z$ for Case – I

Hence, the 2-periodic controller transfer function is obtained as –

$$C(z,N) = \frac{(-89.5878z^3 + 55.3069z^2) + (-1)^N(89.5878z^3 + 55.3069z^2)}{(z^3 + 1.746z^2 - 0.2755z - 0.731) + (-1)^N(1.9467z^2 - 2.3396z + 0.731)} \tag{4.23}$$

The corresponding normalized step response of the CSTR system with 2-periodically compensated controller with Augmentation $(z+1)/z$ vide Case-I is obtained as –

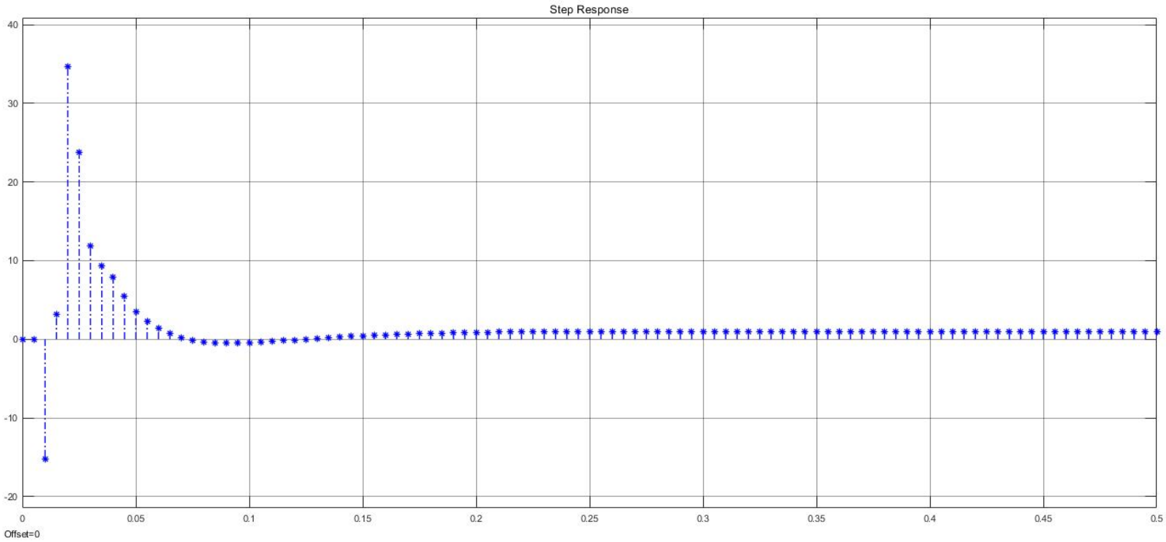

Fig. 4.14: Step response (normalized) of 2-periodic controlled CSTR with Augmentation $(z+1)/z$ for case-I

4.4.1.3 Controller Design: Case-II

From equation (4.21), we can segregate the roots of $\hat{L}(z)$ as follows –

$$\left.\begin{array}{r} Q_0^- \triangleq 89.5878z^3 + 55.3069z^2 \\ (P_0^+ + P_1^-) \triangleq \Gamma(z) = z^3 - 0.2007z^2 - 2.6151z - 1.4617 \end{array}\right\} \tag{4.24}$$

Therefore, solving the Sylvester matrix shown in (2.24) and following subsequent steps mentioned in section 2.8.2.1, we obtain the 2-periodic controller parameters as –

$\boldsymbol{Q_0(z)}$	$\boldsymbol{Q_1(z)}$	$\boldsymbol{P_0(z)}$	$\boldsymbol{P_1(z)}$
$d_{3,0} = -89.5878$	$d_{3,1} = -89.5878$	$c_{2,0} = 1.7460$	$c_{2,1} = -1.9467$
$d_{2,0} = 55.3069$	$d_{1,1} = -55.3069$	$c_{1,0} = -0.2755$	$c_{1,1} = 2.3396$
$d_{1,0} = 0$	$d_{1,1} = 0$	$c_{0,0} = -0.7308$	$c_{0,1} = -0.7308$
$d_{0,0} = 0$	$d_{0,1} = 0$		

Table 4.6: 2-periodic controller parameters with Augmentation $(z+1)/z$ for Case –II

Hence, the 2-periodic controller transfer function is obtained as –

$$C(z,N) = \frac{(-89.5878z^3 + 55.3069z^2) + (-1)^N(-89.5878z^3 - 55.3069z^2)}{(z^3 + 1.746z^2 - 0.275z - 0.731) + (-1)^N(-1.9467z^2 + 2.3396z - 0.731)} \tag{4.25}$$

The corresponding normalized step response of the CSTR system with 2-periodically compensated controller with Augmentation $(z + 1)/z$ vide Case-II is obtained as –

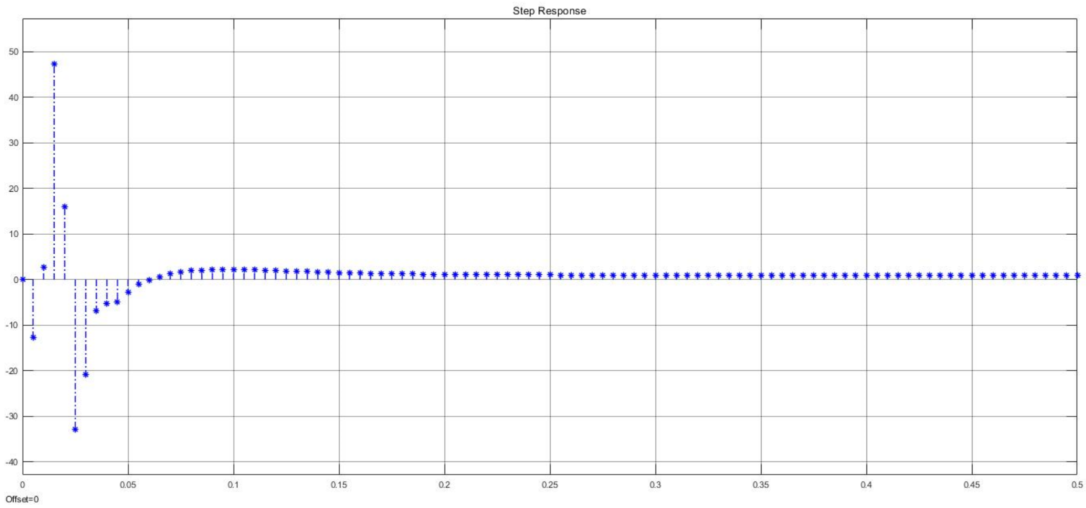

Fig. 4.15: Step response (normalized) of 2-periodic controlled CSTR with Augmentation $(z + 1)/z$ for Case-II

From Fig. 4.14 and 4.15, we can infer that, the steady-state ripples have been taken care of successfully. However, transient overshoot and undershoot have increased but settling time hasn't been affected much.

4.4.2 Augmentation with $z/(z-1)$

4.4.2.1 Pole-Zero Placement

With this augmentation, the plant transfer function becomes –

$$G(z) = \frac{b(z)}{a(z)} = \frac{-0.002002z(z - 0.9457)(z - 1.956)}{(z - 1)(z - 0.6173)(z^2 - 1.692z + 0.7178)} \tag{4.26}$$

The controller order for this augmented plant will be $m = (n - 1) = (4 - 1) = 3$. Hence, in the time-lifted domain, the no. of loop zeros will be 6 and closed loop poles will be 7. Out of this, we shall place 6 loop-zeros and 3 controller poles at will and check the responses. One such possible set of pole zero placement yields –

$$\left.\begin{aligned} \hat{A}(z^2) &= a^+a^- = z^8 - 1.8098z^6 + 1.0598z^4 - 0.1964z^2 \\ \hat{P}(z^2) &= -z^2(z^2 + 0.25)(z^2 - 0.8) = -z^6 + 0.55z^4 + 0.2z^2 \\ \hat{Z}(z^2) &= -0.08(-z^2)^2(z^2 + 0.25)(z^2 - 0.3811)(z^2 - 1.43z + 0.515) \end{aligned}\right\} \tag{4.27}$$

The root locus for the same is as shown below:

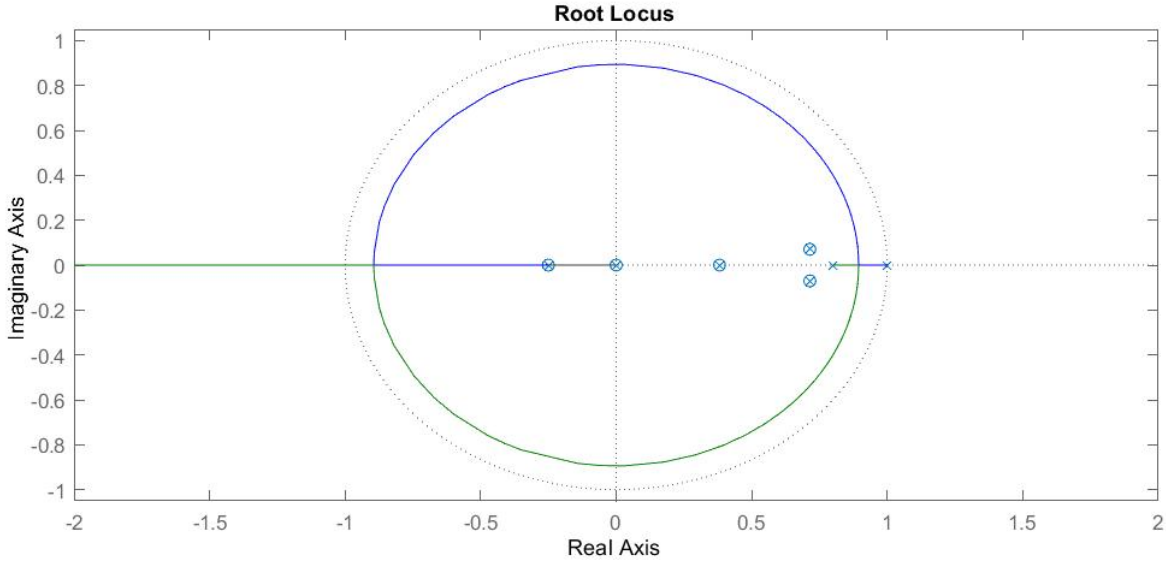

Fig. 4.16: Root locus of 2-periodic controller with Augmentation $z/(z-1)$ for CSTR

It is calculated from the root locus that, the loop GM for the augmented controller is 1800. By virtue of equation (2.20), upon solving the Sylvester matrix, we can find the intermediate polynomial as –

$$\hat{L}(z) = 172.8715z^6 + 90.5707z^5 - 408.3814z^4 - 467.566z^3 - 136.8094z^2 \tag{4.28}$$

4.4.2.2 Controller Design: Case-I

From equation (4.28), we can segregate the roots of $\hat{L}(z)$ as follows –

$$\left.\begin{array}{r} Q_0^- \triangleq 172.8715z^3 + 106.722z^2 \\ (P_0^+ - P_1^-) \triangleq \Gamma(z) = z^3 - 0.0934z^2 - 2.3047z - 1.2819 \end{array}\right\} \tag{4.29}$$

Therefore, solving the Sylvester matrix shown in (2.24) and following subsequent steps mentioned in section 2.8.2.1, we obtain the 2-periodic controller parameters as –

$\boldsymbol{Q_0(z)}$	$\boldsymbol{Q_1(z)}$	$\boldsymbol{P_0(z)}$	$\boldsymbol{P_1(z)}$
$d_{3,0} = -172.8715$	$d_{3,1} = 172.8715$	$c_{2,0} = 2.2171$	$c_{2,1} = 2.3105$
$d_{2,0} = 106.722$	$d_{1,1} = 106.722$	$c_{1,0} = 0.0635$	$c_{1,1} = -2.3682$
$d_{1,0} = 0$	$d_{1,1} = 0$	$c_{0,0} = -0.6410$	$c_{0,1} = 0.6410$
$d_{0,0} = 0$	$d_{0,1} = 0$		

Table 4.7: 2-periodic controller parameters with Augmentation $z/(z-1)$ for Case – I

Hence, the 2-periodic controller transfer function is obtained as –

$$C(z,N) = \frac{(-172.8715z^3 + 106.722z^2) + (-1)^N(172.8715z^3 + 106.722z^2)}{(z^3 + 2.217z^2 + 0.0635z - 0.641) + (-1)^N(2.3105z^2 - 2.3682z + 0.641)}$$

(4.30)

The corresponding step response of the CSTR system with 2-periodically compensated controller with Augmentation $z/(z-1)$ vide Case-I is obtained as –

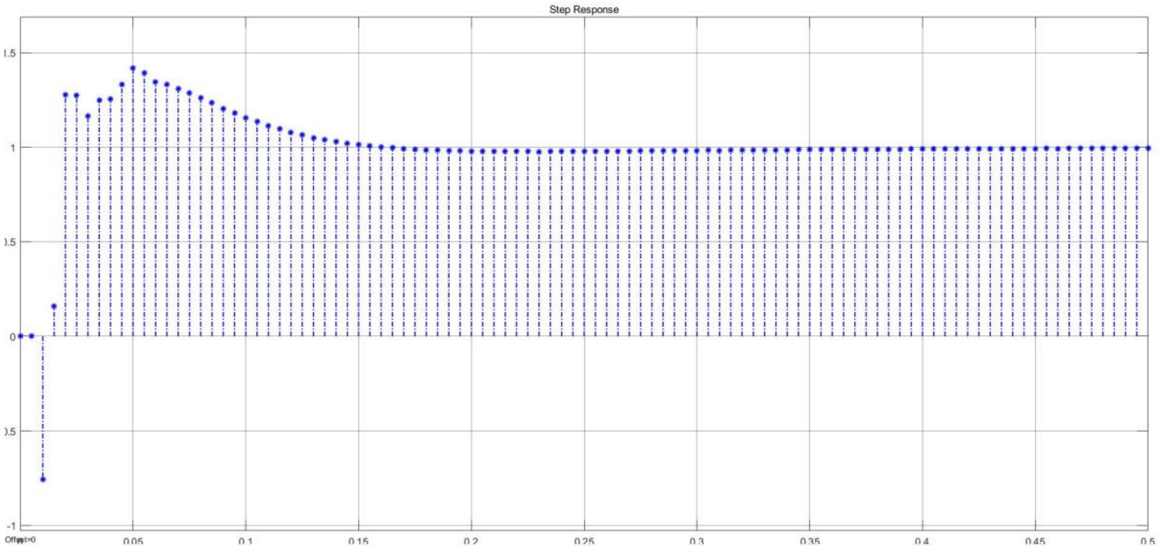

Fig. 4.17 Step response of 2-periodic controlled CSTR with Augmentation $z/(z-1)$ for case-I

4.4.2.3 Controller Design: Case-II

From equation (4.28), we can segregate the roots of $\hat{L}(z)$ as follows –

$$\left.\begin{array}{r} Q_0^- \triangleq 172.8715z^3 + 106.722z^2 \\ (P_0^+ + P_1^-) \triangleq \Gamma(z) = z^3 - 0.066z^2 - 2.2582z - 1.2622 \end{array}\right\}$$

(4.31)

Therefore, solving the Sylvester matrix shown in (2.24) and following subsequent steps mentioned in section 2.8.2.1, we obtain the 2-periodic controller parameters as –

$\boldsymbol{Q_0(z)}$	$\boldsymbol{Q_1(z)}$	$\boldsymbol{P_0(z)}$	$\boldsymbol{P_1(z)}$
$d_{3,0} = -172.8715$	$d_{3,1} = -172.8715$	$c_{2,0} = 2.2171$	$c_{2,1} = -2.3105$
$d_{2,0} = 106.722$	$d_{1,1} = -106.722$	$c_{1,0} = 0.0635$	$c_{1,1} = 2.3682$
$d_{1,0} = 0$	$d_{1,1} = 0$	$c_{0,0} = -0.6410$	$c_{0,1} = -0.6410$
$d_{0,0} = 0$	$d_{0,1} = 0$		

Table 4.8: 2-periodic controller parameters with Augmentation $z/(z-1)$, Case – II

Hence, the 2-periodic controller transfer function is obtained as –

$$C(z,N) = \frac{(-172.8715z^3 + 106.722z^2) + (-1)^N(-172.8715z^3 - 106.722z^2)}{(z^3 + 2.217z^2 + 0.0635z - 0.641) + (-1)^N(-2.3105z^2 + 2.368z - 0.641)}$$

(4.32)

The corresponding step response of the CSTR system with 2-periodically compensated controller with Augmentation $z/(z-1)$ vide Case-II is obtained as –

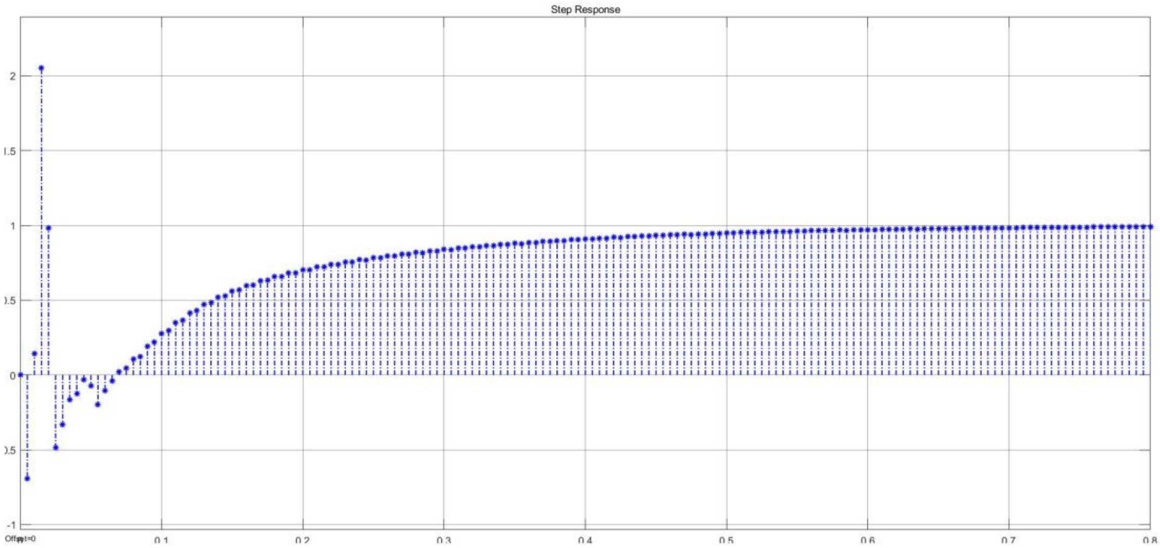

Fig. 4.18: Step response of 2-periodic controlled CSTR with Augmentation $z/(z-1)$ for Case-II

From Fig. 4.17 and 4.18, we can infer that, the steady-state ripples have been taken care of successfully just as in previous augmentation. However, transient overshoot and undershoot have decreased to an acceptable level with slight rise in the settling time. Therefore, it can be concluded that, augmentation with $z/(z-1)$ gives an overall better response in terms of transient and steady-state behavior, especially for controller configuration in Case-I.

4.5 Robustness Analysis and Comparative Study

In this section, we shall study the robustness of the designed controllers, i.e., Discrete-LTI PID controller and 2-Peridoic controller case-I with augmentation $z/(z-1)$ and deduce a comparison between them.

In the CSTR, parameter variation may arise due to several factors which will be reflected in the Steric factors $k_{0_{AB}}$, $k_{0_{BC}}$ and k_{AD}. Also, disturbances may occur in inflow concentration c_{A0} and its temperature θ_0. Hence, we shall see how robust the 2-Periodic controller is against these variations in comparison with the PID controller. Note that, the acceptable range criteria for the reaction constants as well as the inflow parameters are considered when the corresponding step response yields overshoot $\leq 70\%$ and settling time $\leq 0.5\ s$.

4.5.1 Variation in $k_{0_{AB}}$(Steric Factor for reaction $A \rightarrow B$)

Type of Controller	PID		2-Periodic	
	Min	Max	Min	Max
Stable	-55%	+404%	-64%	+765%
Acceptable	-13%	+125%	-15%	+150%

Table 4.9: Stable & Acceptable limits of $k_{0_{AB}}$ variation for PID and 2-Periodic controllers

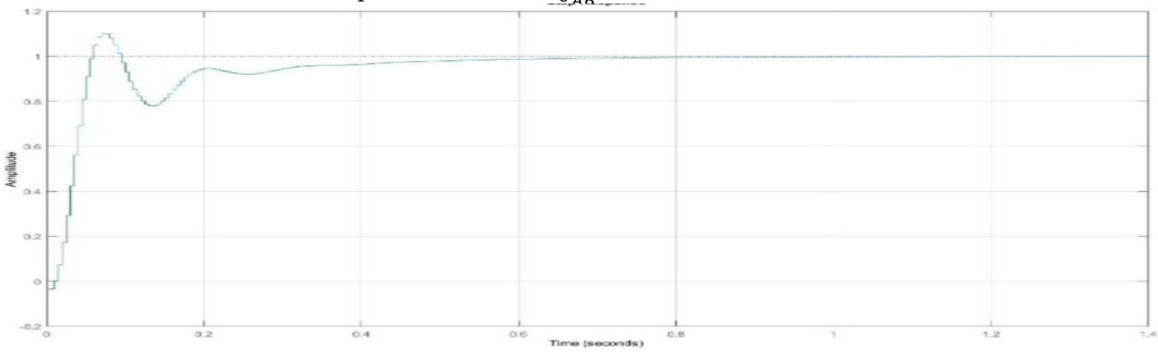

Fig. 4.19(a): Step response at the min. acceptable limit of $k_{0_{AB}}$ variation using PID controller

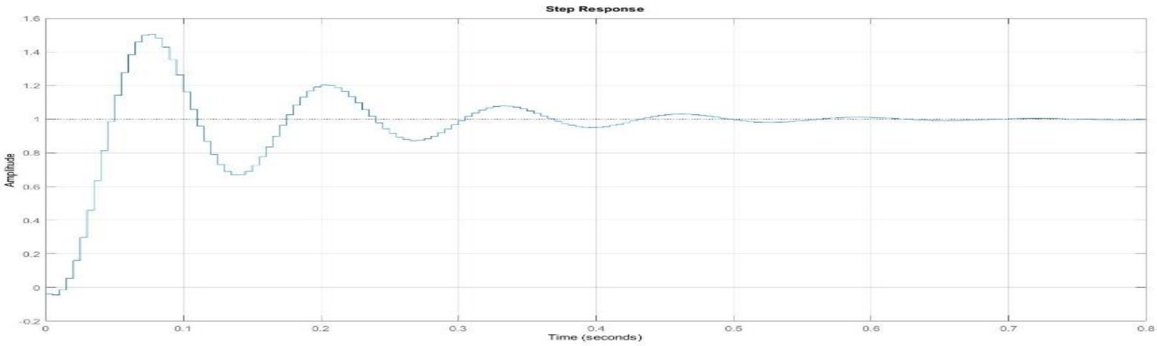

Fig. 4.19(b): Step response at the max. acceptable limit of $k_{0_{AB}}$ variation using PID controller

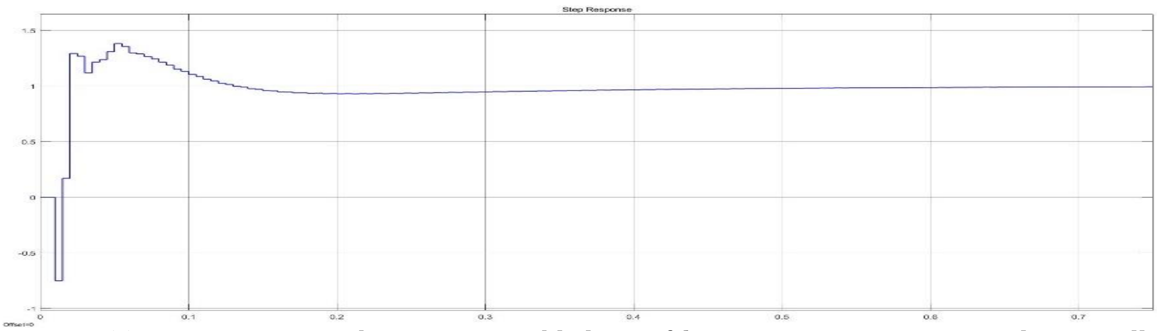

Fig. 4.19(c): Step response at the min. acceptable limit of $k_{0_{AB}}$ variation using 2-Periodic controller

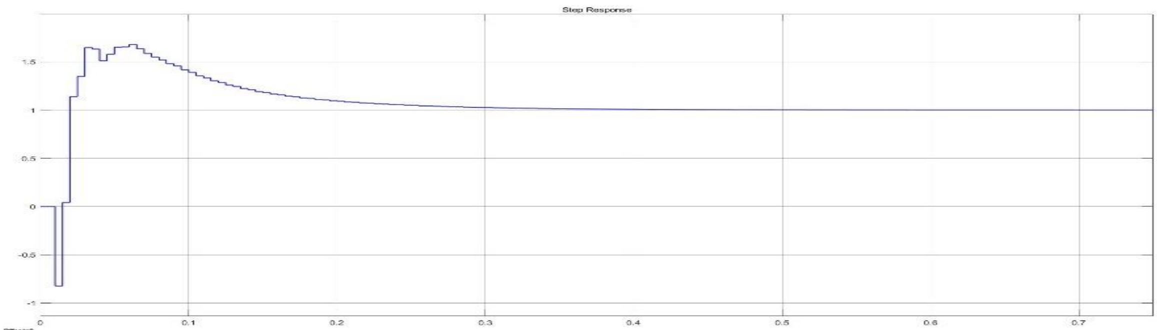

Fig. 4.19(d): Step response at the max. acceptable limit of $k_{0_{AB}}$ variation using 2-Periodic controller

4.5.2 Variation in $k_{0_{BC}}$(Steric Factor for reaction $B \rightarrow C$)

Type of Controller	PID		2-Periodic	
	Min	Max	Min	Max
Stable	-100%	+62%	-100%	+62.5%
Acceptable	-100%	+11.5%	-100%	+12%

Table 4.10: Stable & Acceptable limits of $k_{0_{BC}}$ variation for PID and 2-Periodic controllers

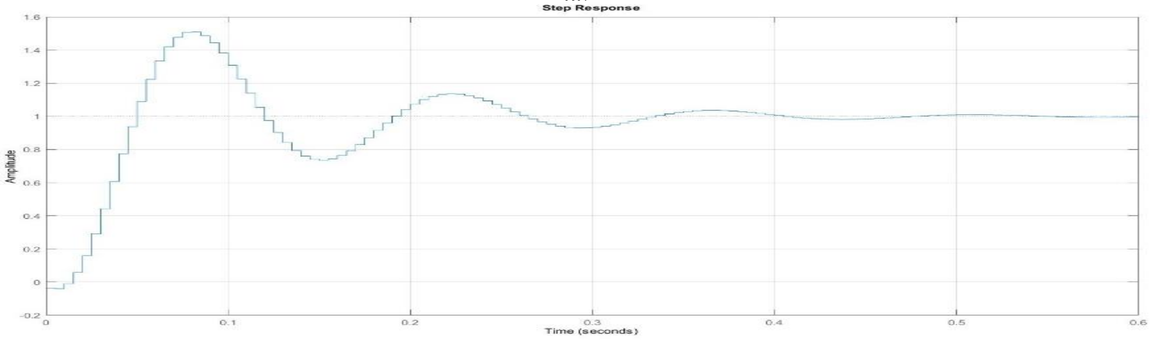

Fig. 4.20(a): Step response at the min. acceptable limit of $k_{0_{BC}}$ variation using PID controller

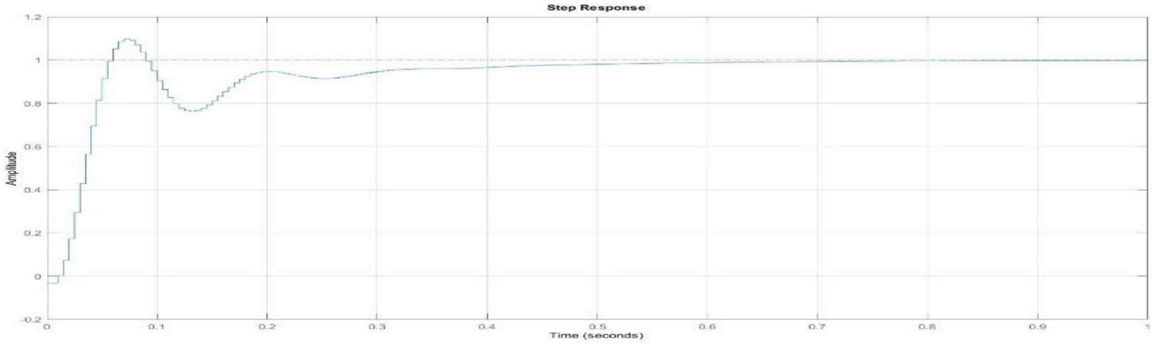

Fig. 4.20(b): Step response at the max. acceptable limit of $k_{0_{BC}}$ variation using PID controller

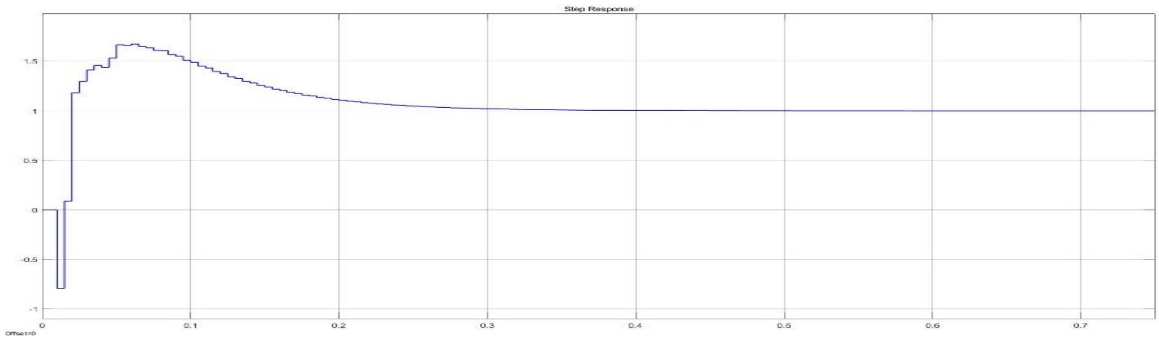

Fig. 4.20(c): Step response at the min. acceptable limit of $k_{0_{BC}}$ variation using 2-Periodic controller

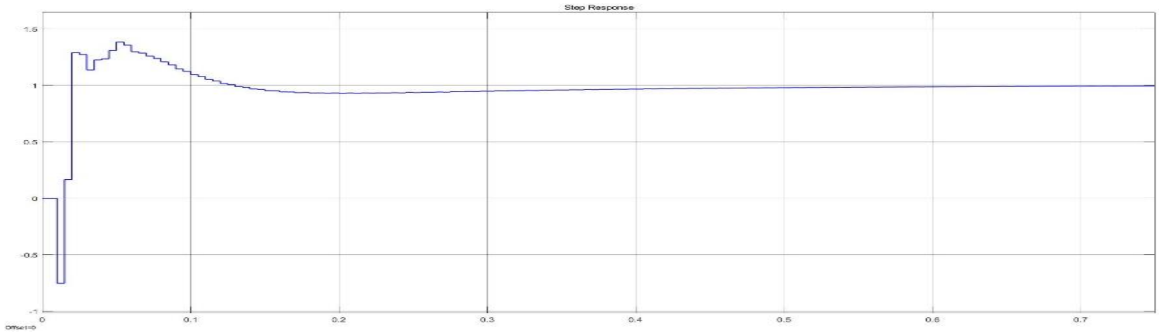

Fig. 4.20(d): Step response at the max. acceptable limit of $k_{0_{BC}}$ variation using 2-Periodic controller

4.5.3 Variation in $k_{0_{AD}}$(Steric Factor for reaction $A \rightarrow D$)

Type of Controller	PID		2-Periodic	
	Min	Max	Min	Max
Stable	-100%	+138%	-100%	+142%
Acceptable	-100%	+36%	-100%	+37%

Table 4.11: Stable & Acceptable limits of $k_{0_{AD}}$ variation for PID and 2-Periodic controllers

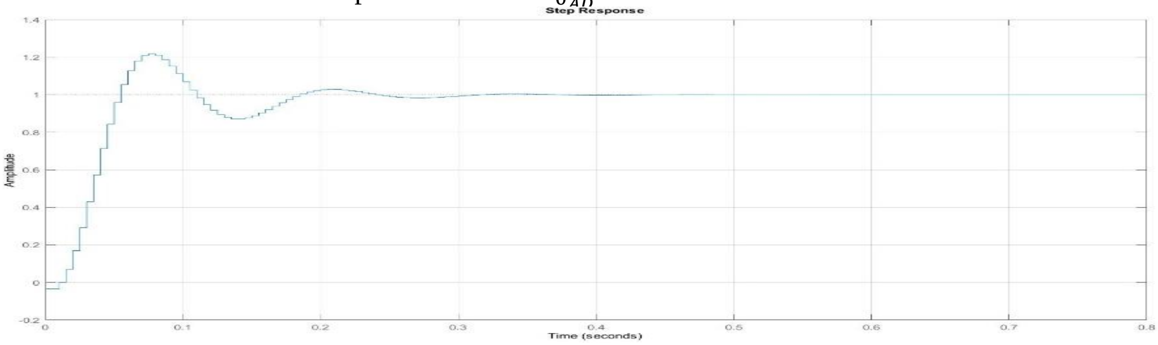

Fig. 4.21(a): Step response at the min. acceptable limit of $k_{0_{AD}}$ variation using PID controller

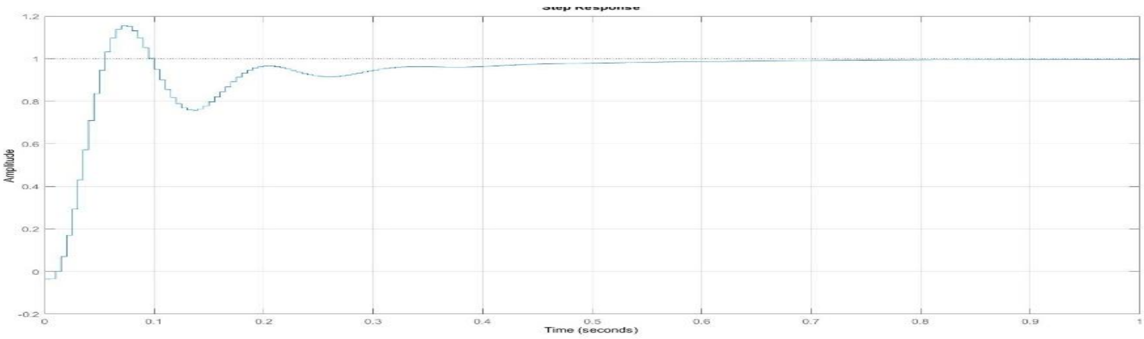

Fig. 4.21(b): Step response at the max. acceptable limit of $k_{0_{AD}}$ variation using PID controller

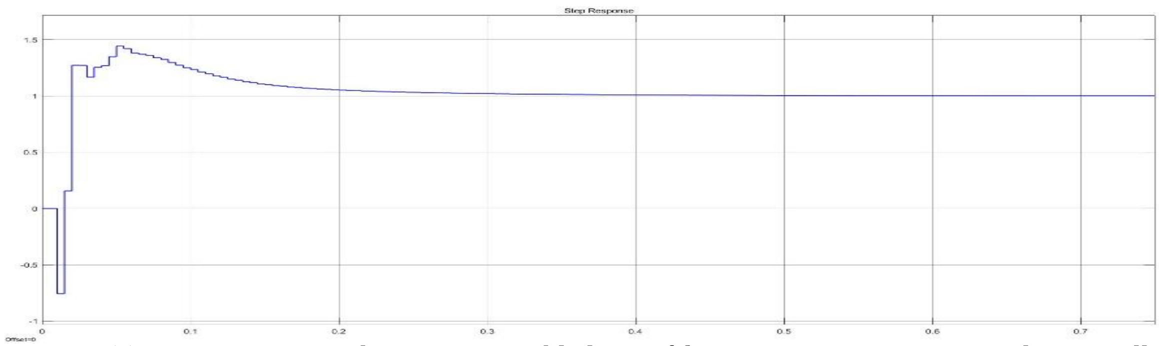

Fig. 4.21(c): Step response at the min. acceptable limit of $k_{0_{AD}}$ variation using 2-Periodic controller

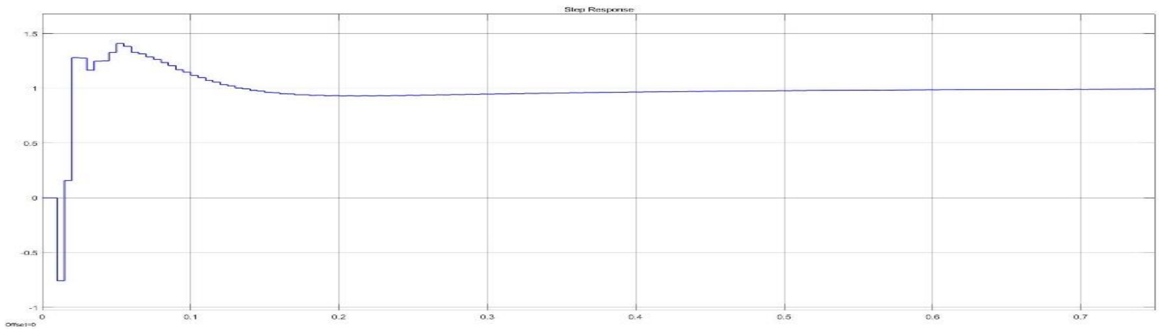

Fig. 4.21(d): Step response at the max. acceptable limit of $k_{0_{AD}}$ variation using 2-Periodic controller

4.5.4 Variation in c_{A0}(Inflow concentration)

Type of Controller	PID		2-Periodic	
	Min	Max	Min	Max
Stable	-45.4%	+27.5%	-48.2%	+29.5%
Acceptable	-15.2%	+15.8%	-16%	+17%

Table 4.12: Stable & Acceptable limits of c_{A0} variation for PID and 2-Periodic controllers

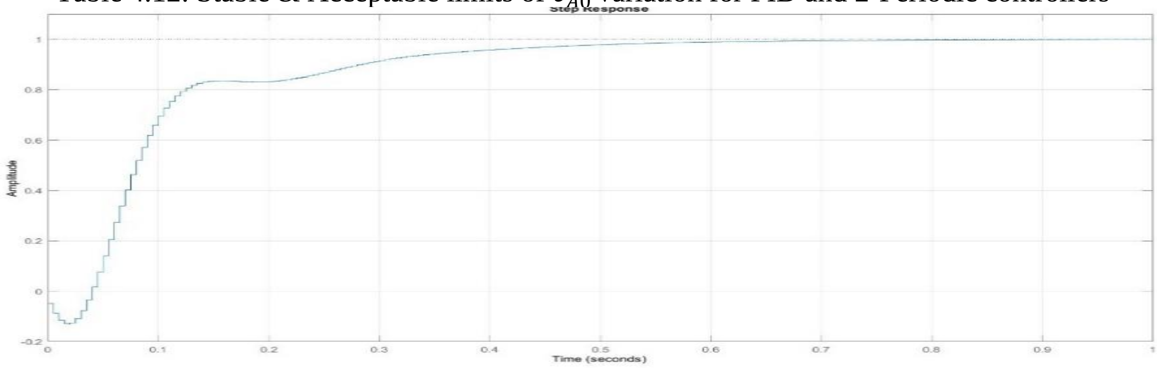

Fig. 4.22(a): Step response at the min. acceptable limit of c_{A0} variation using PID controller

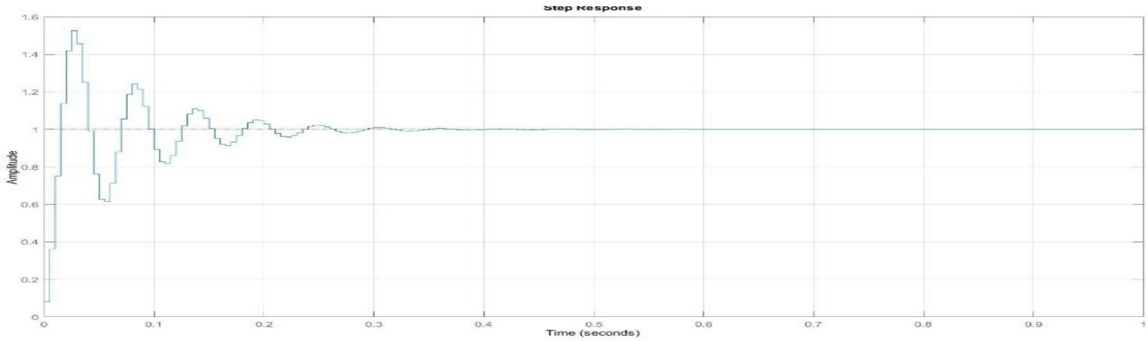

Fig. 4.22(b): Step response at the max. acceptable limit of c_{A0} variation using PID controller

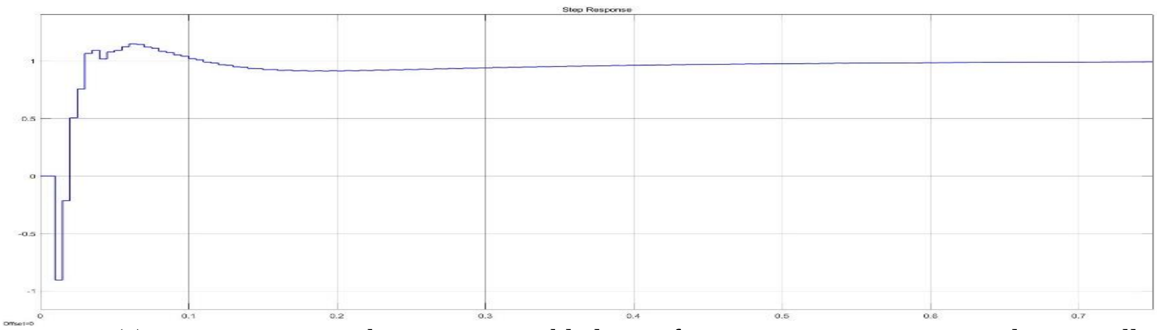

Fig. 4.22(c): Step response at the min. acceptable limit of c_{A0} variation using 2-Periodic controller

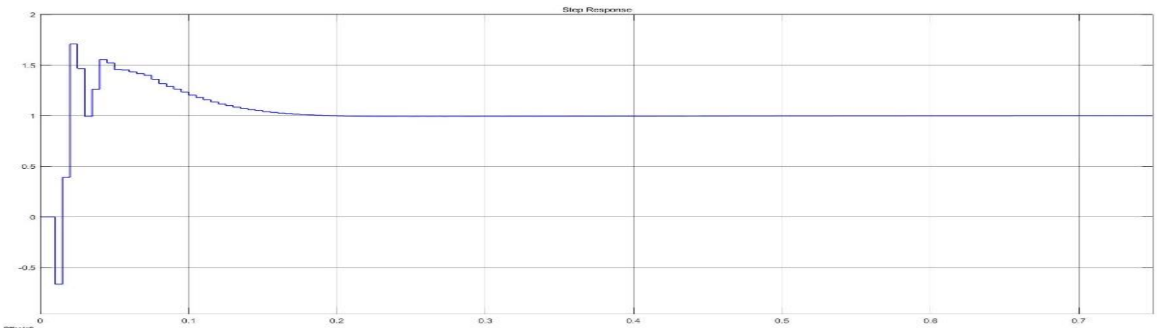

Fig. 4.22(d): Step response at the max. acceptable limit of c_{A0} variation using 2-Periodic controller

4.5.5 Variation in θ_0(Inflow temperature)

Type of Controller	PID		2-Periodic	
	Min	Max	Min	Max
Stable	-7.2%	+2.46%	-25.1%	+2.5%
Acceptable	-3.5%	+0.86%	-6.7%	+0.89%

Table 4.13: Stable & Acceptable limits of θ_0 variation for PID and 2-Periodic controllers

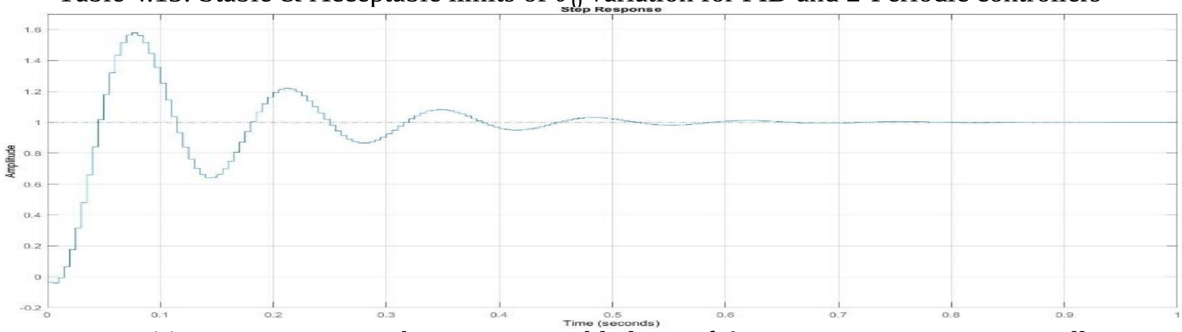

Fig. 4.23(a): Step response at the min. acceptable limit of θ_0 variation using PID controller

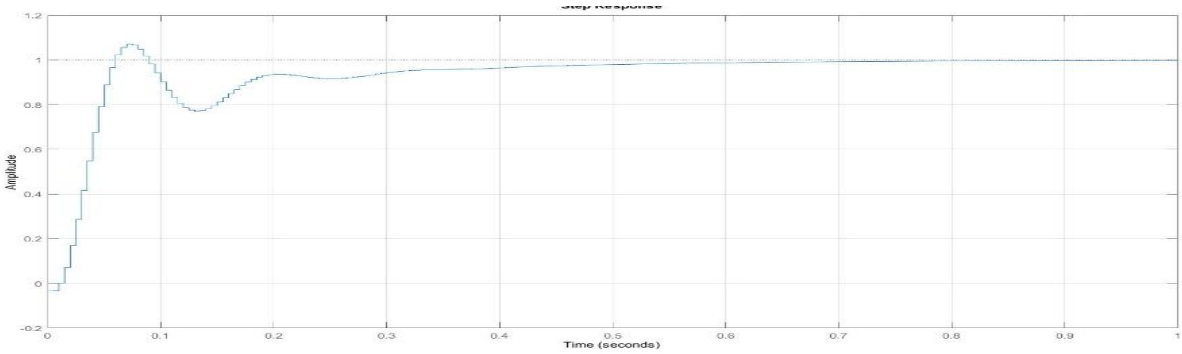

Fig. 4.23(b): Step response at the max. acceptable limit of θ_0 variation using PID controller

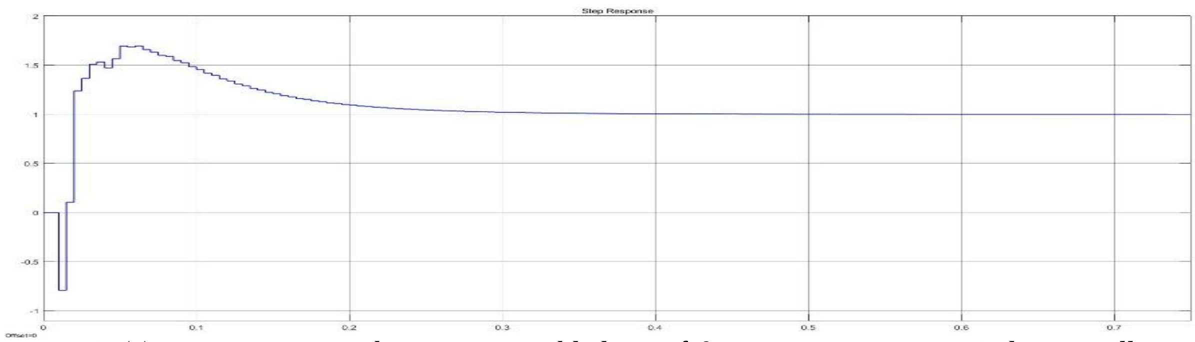

Fig. 4.23(c): Step response at the min. acceptable limit of θ_0 variation using 2-Periodic controller

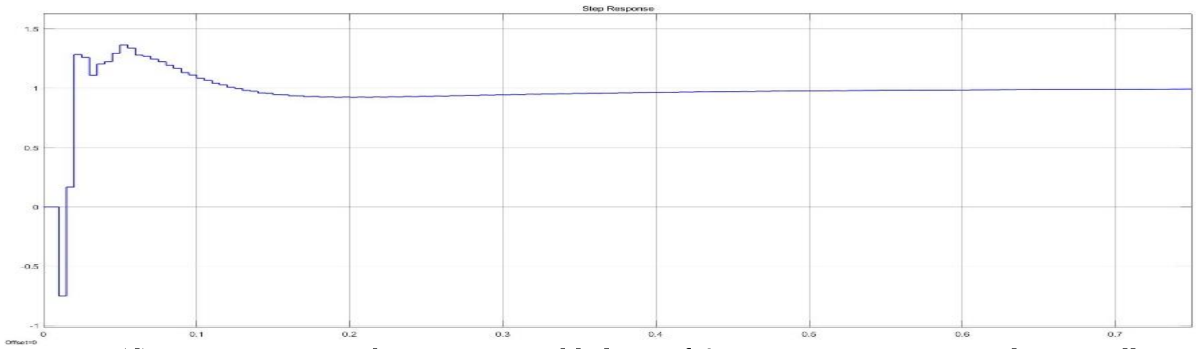

Fig. 4.23(d): Step response at the max. acceptable limit of θ_0 variation using 2-Periodic controller

4.5.6 Observations

From the step responses, root loci and the comparative analysis done in this chapter, we can note down the following observations –

- 2-periodic control provides much better Gain Margin compared to the discrete-LTI PID control in general.

- For variation in reaction rate constant $k_{0_{AB}}$ which corresponds to the primary desired reaction occurring in the CSTR, we find 2-periodic controller to be far more robust compared to the LTI counterpart.

- On the other hand, for the rate constants $k_{0_{AC}}$ and $k_{0_{AD}}$, which correspond to the side reactions, both the controller provide similar robustness. However, the PID controller has an edge over the 2-periodic controller in terms of overshoot. Note that, the stable range for these two parameters in both the controllers goes down to -100%. This is owing to the fact that, both of these two reactions are unsolicited in the Van de Vusse CSTR [4,24]. Hence, without these reactions, the controllers work just fine.

- For variation in inflow concentration c_{A0}, the 2-periodic controller is proven to have provided slightly better robustness compared to the LTI controller. Moreover, 2-periodic controller has much less oscillation in the transient response than PID controller.

- In case of disturbance in the inflow temperature θ_0, not much difference is observed for the upper limit of disturbance between the two controllers but for the lower limit, 2-periodic controller performs significantly better than the other.

Chapter 5

Conclusion

5.1 Contribution of the thesis

i. Compensation of LDTI plants using 1-DOF 2-periodic controller has been studied in details and the controller synthesis steps are demonstrated with the help of a synthetic example.

ii. A non-isothermal Van de Vusse Continuous Stirred Tank Reactor (CSTR) has been mathematically modelled step by step from the chemical reaction rate equations, Arrhenius equation and thermodynamic equations. Thereafter, its State-Space model is developed, followed by deducing continuous-time amd discrete-time transfer functions.

iii. 2-periodic controller is synthesized for CSTR considering every possible configuration. Augmentation is performed on the plant and then higher order 2-periodic controller is designed in order to nullify steady-state ripples in the output step responses.

iv. A comparative study is done between a discrete LTI PID controller and the best configured 2-periodic controller in light of model parameter variations and input disturbances.

5.2 Scope of future work

i. The proposed 2-periodic controller has been developed and tested in simulation environment only. It needs to be implemented on a real-time Continuous Stirred Tank Reactor to study the possible merits and demerits of such controllers from a practical point of view.

ii. The desired pole and loop-zero placements have been carried out by trial and error except for the deadbeat case. A suitable algorithm may be developed for the same.

iii. The coolant dynamics in the CSTR has been neglected for the synthesis. Hence, this complexity may be incorporated into the study and check on stability and robustness by implementing the 2-periodic compensation technique.

REFERENCES

[1] S. Chakraborty, “2-periodic/2-rate compensation of discrete-time plants”, Ph.D. dissertation, Indian Institute of Technology, Kharagpur, India, 2015.

[2] G. Nayak, S. Chakraborty and S. K. Das, “2-Periodic compensation of SISO discrete - linear - time-invariant plants”, Indian Control Conference (ICC), Guwahati, pp. 289-294, 2017.

[3] S. K. Das and P. K. Rajagopalan, “Techniques of analysis and robust control via zero placement of periodically compensated discrete-time plants”, Control and Dynamic Systems, Advances in Theory and Applications: Academic, Vol.74, 1996.

[4] Engell, S. and K. U. Klatt; “Nonlinear Control of a Non Minimum Phase CSTR”, Proceedings of the 1993 American Control Conference, pp. 2341–2945, San Fransico, U.S.A. (1993).

[5] Chyi-Tsong Chen & Shih-Tien. Peng (2006); “A Sliding Mode Control Scheme for Uncertain Non-Minimum Phase CSTRs”, Journal of Chemical Engineering of Japan - J CHEM ENG JPN. 39. 181-196. 10.1252/jcej.39.181.

[6] S. K. Das, S. Chakraborty, “Robust Compensation of Discrete-time Plant using 2-Periodic Controller”, 7th IFAC Symposium on Robust Control Design (ROCOND 2012), June 20-22, 2012.

[7] S. Das, S. Chakraborty and M. Maitra, “Performance Evaluation of 2-Degrees-of-Freedom 2- Periodic Controller: Stabilization of Cart-Inverted Pendulum System”, 2018 IEEE Applied Signal Processing Conference (ASPCON), 2018, pp. 273-278.

[8] S. Lee, S. Meerkov and T. Runolfsson, “Vibrational feedback control: Zeros placement capabilities”, IEEE Transactions on Automatic Control, vol. 32, no. 7, pp. 604-611, Jul 1987.

[9] S. K. Das and P. K. Rajagopalan, “Periodic discrete-time system: stability analysis and robust control using zero placement”, IEEE Trans. Automatic Control, Vol.37, pp. 374-378, Mar. 1992.

[10] O. A. Sebakhy, M. I. El Singaby and I. F. El Arabawy, "Shaping of the output response in a class of linear multivariable systems," in *IEEE Transactions on Automatic Control*, vol. 33, no. 5, pp. 457-458, May 1988, doi: 10.1109/9.1224.

[11] W. A. Wolovich, Automatic Control System. Philadelphia, PA: Saunders,1994.

[12] J. C. Doyle, B. A. Francis, and A. R. Tannenbaum, Feedback Control theory. Macmillan Publishing Company, New York, 1993.

[13] S. Lee, S. M. Meerkov, and T. Runolfson, “Vibrational feedback control: Zeros placement capabilities”, IEEE Trans. on Automatic Control, Vol. 32, No. 7, pp. 604-611, July, 1987.

[14] F. Allgöwer; “Approximate Input–Output Linearization of Non-Minimum Phase Nonlinear Systems”, Technical Report 1996, Swiss Federal Institute of Technology, Berne, Switzerland (1996).

[15] J. Alvarez-Ramirez and A. Morales; “PI Control of Continuously Stirred Tank Reactors: Stability and Performance”, Chem. Eng. Sci., 55, 5497–5507 (2000).

[16] C. T. Chen and C. S. Dai; “Robust Controller Design for a Class of Nonlinear Uncertain Chemical Processes”, J. Process Control, 11, 469–482 (2001).

[17] N. M. Iyer and A. E. Farell; “Adaptive Input–Output Linearizing Control of a Continuous Stirred Tank Reactor”, Comput. Chem. Eng., 19, 575–579 (1995).

[18] N. H. Jo, J. Byun, H. Shim and J. H. Seo; “Robust Stabilization of Nonminimum Phase Nonlinear Systems”, Proceedings of the American Control Conference, pp. 3359–3363, Philadelphia, U.S.A. (1998).

[19] C. Kravaris, M. Niemiec, R. Berber and C. B. Brosilow; “Nonlinear Model-Based Control of Nonminimum-Phase Processes”, Nonlinear Model Based Process Control, R. Berber and C. Kravaris eds., pp. 115–141, Kluwer, Dordrecht, the Netherlands (1998).

[20] R. A. Wright and C. Kravaris; “Non-Minimum Phase Compensation for Nonlinear Processes”, AIChE J., 38, 26–40 (1992).

[21] C. Kravaris, P. Daoutidis and R. A. Wright; “Output Feedback Control of Nonminimum Phase Nonlinear Processes,” Chem. Eng. Sci., 49, 2107–2122 (1994).

[22] C. Kravaris and P. Daoutidis; “Nonlinear State Feedback Control of Second-Order Nonminimum-Phase Nonlinear Systems,” Comput. Chem. Eng., 14, 439–449 (1990).

[23] P. T. Kabamba, “Control of Linear Systems using Generalized Sampled-Data Hold Functions”, IEEE Trans. Automatic Control, Vol. 32, No. 9, pp. 772-783, Sept. 1987.

[24] J. C. Kantor; “Stability of State Feedback Transformations for Nonlinear Systems—Some Practical Considerations,” Proceedings of 1986 American Control Conference, pp. 1014–1016, Seattle, U.S.A. (1986).

[25] A. Aoyama, F. J. Doyle, III and V. Venkatasubramanian; “ControlAffine Neural Network Approach for Nonminimum-Phase Nonlinear Process Control,” J. Process Control, 6, 17–26 (1996).

[26] G. M. Kranc, “Input-output analysis of multirate feedback systems”, IRE Trans. Automatic Control, Vol. AC-3, pp. 21-28, Nov. 1957.

[27] J. Hauser, S. Sastry and G. Meyer; “Nonlinear Control Design for Slightly Non-minimum Phase Systems: Application to V/STOL Aircraft,” Automatica, 28, 665–679 (1992).

[28] I. P. Greschak and G. C. Verghese, “Periodically varying compensation of time-invariant systems”, Syst. Contr. Lett., Vol. 2, pp. 88-93, August 1982.

[29] I. A. Shkolnikov and Y. B. Shtessel; “Tracking in a Class of Nonminimum-Phase Systems with Nonlinear Internal Dynamics via Sliding Mode Control Using Method of System Center,” Automatica, 38, 837–842 (2002).

[30] M. Bakosova, D. Puna and A. Meszaros, "Control of a Continuous-time Stirred Tank Reactor via Robust Static Output Feedback," 2006 14th Mediterranean Conference on Control and Automation, 2006, pp. 1-6.

[31] T. Wonghong, "Real-time PID controller tuning via unfalsified control," 2012 9th International Conference on Electrical Engineering/Electronics, Computer, Telecommunications and Information Technology, 2012, pp. 1-4.

[32] E. A. N. Idris and S. Engell, "Gain-scheduled state estimation and optimizing nmpc applied to a non-minimum phase CSTR," 2012 IEEE International Conference on Control Applications, 2012, pp. 482-487.

[33] A. Singh, S. Yadav and N. Singh, "Enhancement of Continuous-Stirred Tank Reactor System Using Jaya Algorithm," 2018 2nd International Conference on Electronics, Materials Engineering & Nano-Technology (IEMENTech), 2018.

[34] B. A. Francis and T. T. Georgiou, “Stability theory for linear time-invariant plants with periodic digital controllers,” IEEE Trans. Automatic Control, Vol. 33, No. 9, pp. 820-832, Sept. 1988.

[35] C. I. Byrnes and A. Isidori, "Steady state response, separation principle and the output regulation of nonlinear systems," Proceedings of the 28th IEEE Conference on Decision and Control, 1989, pp. 2247-2251 vol.3.

[36] S. Bittanti and P. Colaneri; “Periodic Systems: Filtering and Control”, Springer Verlag, 2009.

[37] S. Bittanti and P. Colaneri “Invariant representations of discrete-time periodic systems”, Automatica, Vol. 47, Issue 12, pp. 1777-1793, Dec. 2000.

[38] R. A. Meyer and C. S. Burrus, “A unified analysis of multirate and periodically time-varying digital filters”, IEEE Trans. Circuits Systems, Vol. 22, pp. 162-167, March 1975.

[39] T. Saha, N. Murmu, S. Chakraborty and M. Maitra, "Stabilization of Cart Inverted Pendulum System by 2-rate controllers based on PSO technique," 2020 IEEE Applied Signal Processing Conference (ASPCON), 2020, pp. 104-108.

[40] S. K. Das and J. Dey, “Periodic Compensation of Continuous-Time Plants”, IEEE Trans. on Automatic Control, Vol. 52, No. 5, pp. 898-904, May 2007.

[41] S. K. Das and K.K. Paul, “Robust Compensation of a Cart-Inverted Pendulum system using Periodic Controller: Experimental Results”, Automatica, Vol. 47, Issue 11, pp. 2543-2547, Nov. 2011.

[42] S. K. Das, “Simultaneous stabilization of two discrete-time plants using a 2-periodic controller”, IEEE Trans. Automatic Control, Vol.46, pp. 125-130, Jan. 2001.

[43] S. K. Das and P. K. Kar, “Simultaneous Pole Placement of M Discrete-Time Plants Using a M-Periodic Controller”, IEEE Trans. Automatic Control, Vol.48, No. 11, pp. 2045-2050, Nov. 2003.

[44] A. Chakraborty and J. Dey, "Performance comparison between sliding mode control and periodic controller for cart-inverted pendulum system," *2015 IEEE International Conference on Industrial Technology (ICIT)*, 2015, pp. 405-410, doi: 10.1109/ICIT.2015.7125132.

[45] A. Chakraborty and J. Dey, "Real-time study of robustness aspects of periodic controller for cart-inverted pendulum system," *2013 IEEE International Conference on Industrial Technology (ICIT)*, 2013, pp. 169-174.

[46] P. P. Khargonekar, K. Poolla and A. Tannenbaum, “Robust control of linear time invariant plants using periodic compensation”, IEEE Trans. Automatic Control, Vol. 30, pp. 1088-1096, Nov. 1985.

[47] K. J. Astrom, P. Hagander and J. Sternby, “Zeros of sampled systems”, Automatica, Vol. 20, Issue 1, pp. 31-38, January 1984.

[48] S. Engell, K. U. Klatt; “Benchmark Problem: Continuous Stirred Tank Reactor with Consecutive and Parallel Reaction”, German Society for Maurement and Automation (GMA), 1992.

[49] Carlos E. García, David M. Prett, Manfred Morari, “Model predictive control: Theory and practice - A survey”, Automatica, Volume 25, Issue 3, 1989, Pages 335-348.

[50] T. Kaczorek, “Pole placement for linear discrete-time systems by periodic output feedbacks”, Systems & Control Letters, Vol. 6, Issue 4, pp. 267269, October 1985.

[51] P. Bolzern, P. Colaneri and R. Scattolini, “Zeros of discrete-time linear periodic systems”, IEEE Trans. Automatic Control, Vol. 31, pp. 1057-1058, Dec. 1986.

[52] A. Feuer and G. C. Goodwin, “Generalized sample hold functions-frequency domain analysis of robustness, sensitivity, and intersample difficulties”, IEEE Trans. Automatic Control,”, Vol. 39, No. 5, pp. 1042 - 1047, May 1994.

[53] S. Bittanti and P. Colaneri, “Analysis of discrete-time linear periodic systems”, C.T. Leondes Control and dynamic systems, Academic Press, New York, 1996, Vol. 78.

[54] S. Bittanti and P. Colaneri, “Periodic control”, Encyclopaedia of Electrical Engineering, J.G.Webster Ed., John Wiley and Sons, Inc., New York, 1999.

[55] B. W. Bequette; “Nonlinear Control of Chemical Processes: A Review,” Ind. Eng. Chem. Res., 30, 1391–1413 (1991).

[56] W. L. Luyben; “Process Modelling, Simulation, and Control for Chemical Engineers”, 2nd ed., McGraw-Hill, New York, U.S.A. (1990).